Investigating the Physiological Role of Glucokinase in Central Glucose Sensing

A thesis submitted for the degree of Doctor of Philosophy, Imperial College London

Christopher Mark James Holton

2015

Imperial College London

Section of Investigative Medicine

Division of Diabetes, Endocrinology and Metabolism

Department of Medicine

Abstract

The brain is dependent on a constant supply of glucose as its primary fuel. Consequently, the brain has developed ways to tightly control intake of glucose, via glucose sensing neurones containing the enzyme glucokinase (GK). This thesis identifies a role for a subset of glucose sensing neurones in the arcuate nucleus (ARC) of the hypothalamus to promote glucose intake. These neurones form part of a pathway separate to the control of peripheral glucose homeostasis.

Direct injection of a GK activator into the ARC increases glucose intake. Stereotactic injection of recombinant adeno-associated virus containing GK antisense (rAAV-GKAS) into the ARC of rats chronically decreases GK activity compared to controls. Knockdown of ARC GK reduces glucose intake in an acute and long-term setting. Direct injection of an ATP-sensitive potassium (K_{ATP}) channel inhibitor into the ARC increases glucose intake in a similar manner to that of a GK activator. In addition, pre-treatment with a K_{ATP} channel activator attenuates the orexigenic effect of a GK activator. ARC glucose sensing neurones are likely mediated by neuropeptide Y (NPY) as both activation of GK and inhibition of K_{ATP} channels stimulate NPY release in hypothalamic explants. Also, pharmacological inhibition of Y1 and Y5 receptors, and P/Q type voltage gated calcium channels, attenuate the orexigenic effect of GK activators.

ARC glucose sensing neurones represent a novel pathway that may be part of a mechanism to ensure adequate glucose is constantly available to the brain. This work suggests that ARC GK has a physiological role in the homeostatic regulation of glucose intake. ARC GK responds to periods of fasting and may contribute to an increased preference for glucose. Thus, ARC glucose sensing may drive dietary sugar intake, which may be a contributing factor in obesity.

Declaration of Contributors

The majority of the work in this thesis was performed by the author. All collaboration and assistance is described below.

Recombinant AAV was prepared by Dr James Gardiner. GK-pTR-CGW plasmid was prepared by Dr James Gardiner, Dr Errol Richardson and Dr Sufyan Hussain. *In vitro* testing of rAAV-GKAS was conducted by Dr Errol Richardson.

Assistance with the molecular cloning, preparation of probes and the glucokinase activity assay was provided by Dr David Ma.

Feeding studies and stereotactic injections were performed in collaboration with Dr Sufyan Hussain, Dr David Ma and Mr Ivan De Backer.

Hypothalamic explants were performed with assistance from Prof. Waljit Dhillo and Dr James Kinsey-Jones.

Radioimmunoassays were performed under supervision of Prof. Mohammed Ghatei. Alpha MSH antibody and label was prepared by Prof. Mohammed Ghatei.

Declaration of Copyright

The copyright of this thesis rests with the author and is made available under a Creative Commons Attribution Non-Commercial No Derivatives licence. Researchers are free to copy, distribute or transmit the thesis on the condition that they attribute it, that they do not use it for commercial purposes and that they do not alter, transform or build upon it. For any reuse or redistribution, researchers must make clear to others the licence terms of this work.

Acknowledgements

I would like to thank my supervisor James Gardiner for his guidance and coaching throughout my research.

I am very grateful to be part of the “dream team” with David Ma, Sufyan Hussain and Ivan De Backer. Thank you for your mentorship and assistance during many experiments.

Thank you to everyone within the Bloom group for providing continual support: in particular from Lucy Brooks and Kat Banks in the form of new ways to make me laugh.

I would also like to thank the Biotechnology and Biological Sciences Research Council (BBSRC) for my funding.

Finally, many thanks go to my family and friends, especially Amy, Mum and Dad. Your support during my many years of student life is much appreciated.

Abbreviations

2DG	2-Deoxyglucose
3OMG	3-O-methyl-N-acetylglucosamine
5TG	5-thio-d-glucose-6-phosphate
AAV	Adeno-associated virus
ACC	Acetyl-coenzyme A carboxylase
aCSF	Artificial cerebrospinal fluid
ADP	Adenosine diphosphate
AgRP	Agouti related peptide
Amp	Ampicillin resistance gene
AMPK	Adenosine monophosphate activated protein kinase
α-MSH	Alpha melanocyte stimulating hormone
ANOVA	Analysis of variance
ARC	Arcuate nucleus
AP	Area postrema
AS	Antisense
ATP	Adenosine triphosphate
BBB	Blood brain barrier
BLAST	Basic local alignment search tool
Bp	Base pairs
CART	Cocaine-and amphetamine-related transcript
cDNA	Copy DNA
CFTR	Cystic fibrosis transmembrane regulator
CNS	Central nervous system
CRR	Counterregulatory response

CSF	Cerebrospinal fluid
DMN	Dorso medial nucleus
DMNX	Dorsal motor nucleus of the vagus
DNA	Deoxyribonucleic acid
dNTP	Deoxynucleotide triphosphate
DREADD	Designer receptors exclusively activated by designer drugs
DTT	Dithiothreitol
DVC	Dorsal vagal complex
EDTA	Ethylenediaminetetraacetic acid
ELISA	Enzyme-linked immune-sorbent assay
GABA	Gamma-aminobutyric acid
GDW	Glass distilled water
GE	Glucose-excited
GEE	General estimating equation
GFP	Enhanced green fluorescent protein
GI	Glucose-inhibited
GK	Glucokinase
GKAS	GK antisense
GKRP	GK regulatory protein
GKS	GK sense
GLP-1	Glucagon-like peptide-1
GLUT	Transmembrane glucose transporters
G-6-P	Glucose-6-phosphate
GTE	Glucose-Tris-EDTA
HEK	Human embryonic kidney
HFD	High fat diet

ICV	Intracerebroventricular
IP	Intraperitoneal
ITR	Inverted terminal repeats
ITT	Insulin tolerance test
JAK	Janus kinase
K_{ATP}	ATP-sensitive potassium channel
kcal	Kilo calorie
kDa	Kilo dalton
K_{ir}	Inward-rectifier potassium ion channel
kJ	Kilo joule
K_m	Michaelis constant
KO	Knock out
LH	Lateral hypothalamus
MCH	Melanin-concentrating hormone
ME	Median eminence
mM	Milli Molar
mRNA	Messenger ribonucleic acid
MSH	Melanocyte stimulating hormone
mw	Molecular weight
NADPH	Nicotinamide adenine dinucleotide phosphate
NBD	Nucleotide binding site
NO	Nitric oxide
NPY	Neuropeptide Y
NTS	Nucleus of the solitary tract
p	Probability
PBS	Phosphate buffered saline

PCR	Polymerase chain reaction
POMC	Pro-opiomelanocortin
PVN	Paraventricular nucleus
rAAV	Recombinant adeno associated virus
rAAV-GFP	rAAV enhanced green fluorescent protein
rAAV-GKAS	rAAV glucokinase antisense
rAAV-GKS	rAAV glucokinase sense
rpm	Revolutions per minute
RNA	Ribonucleic acid
RT-PCR	Real-time PCR
SAP	Shrimp alkaline phosphatase
SDS	Sodium dodecyl sulfate
SEM	Standard error of the mean
SGLT-1	Sodium-dependant glucose transporter 1
SSC	Saline sodium citrate
SUR1	Sulfonylurea receptor 1
TAE	Tris-acetate EDTA
TE	Tris EDTA
tRNA	Transfer ribonucleic acid
VMH	Ventromedial hypothalamus
VMN	Ventromedial hypothalamic nucleus
WPRE	Woodchuck hepatitis virus post-transcriptional regulatory element

Table of Contents

CHAPTER ONE: GENERAL INTRODUCTION 14

1.1 THE OBESITY PANDEMIC 15
1.2 THE CENTRAL CONTROL OF ENERGY HOMEOSTASIS 16
1.2.1 Ventromedial hypothalamus 16
1.2.2 Lateral hypothalamus 17
1.2.3 Paraventricular and dorsomedial nuclei 18
1.2.4 Dorsal vagal complex of the brainstem 18
1.3 THE IMPORTANCE OF GLUCOSE HOMEOSTASIS 19
1.3.1 Pancreatic glucose sensing 20
1.3.2 Brain glucose sensing 20
1.3.3 The reward value of glucose 21
1.3.4 Glucose-sensing neurones 22
1.3.4.1 GE neurone glucose sensing 22
1.3.4.2 GI neurone glucose sensing 24
1.3.5 Glucose sensing neurones in the CNS 26
1.3.5.1 VMN glucose sensing 26
1.3.5.2 ARC glucose sensing 27
1.3.5.3 Brainstem glucose sensing 28
1.4 MECHANISM OF GLUCOSE SENSING 29
1.4.1 Glucokinase 29
1.4.2 Transmembrane glucose transporters 30
1.4.3 ATP-sensitive potassium channels 31
1.4.4 The multiple roles of glucose sensing cells 34
1.5 APPROACHES FOR INVESTIGATING THE NEURONAL CIRCUITS CONTROLLING ENERGY HOMEOSTASIS IN RODENTS 35
1.5.1 Direct cannulation 35
1.5.2 Genetic modification by global mutation 36
1.5.3 Selective genetic modification 37
1.5.4 Vectors used for gene transfer 37
1.5.4.1 Retroviral vectors 38
1.5.4.2 Adenoviral vectors 39
1.5.4.3 Adeno-associated viral vectors 39
1.6 SUMMARY 40

CHAPTER TWO: MATERIALS AND METHODS 41

2.1. METHODS USED TO PRODUCE PLASMIDS CONTAINING GK AND TO PRODUCE RAAV 42
2.1.1 Production of rAAV 42
2.1.2 Digestion of PCR products 42
2.1.3 Electroelution of DNA fragments 43
2.1.4 Ligation of PCR product into pTR-CGW 44
2.1.5 Transformation of competent bacteria by heat shock 45
2.1.6 DNA sequencing 46
2.1.7 Large scale preparation of plasmid 46
2.1.8 Caesium chloride gradient purification 47
2.1.9 Plasmid digestion for dot blot and in situ hybridisation 49

2.1.10 Quantification of total virus titre by dot-blot analysis *50*
2.1.11 In vitro transfection of GKAS pTR-CGW into cultured cells *52*
2.2 METHODS USED FOR PHYSIOLOGICAL AND PHARMACOLOGICAL MEASUREMENT OF GLUCOSE SENSING IN VIVO 54
2.2.1 Animal maintenance *54*
2.2.2 Optimisation of successful stereotactic injection *54*
2.2.3 Stereotactic injection of rAAV-GK antisense into the arcuate nucleus of rats *55*
2.2.4 Stereotactic cannulation of the left arcuate nucleus in rats *56*
2.2.5 Feeding studies with genetically altered animals *57*
2.2.6 Twenty four hour feeding studies with intra-ARC injections *57*
2.2.7 Collection of tissue samples *58*
2.3 METHODS USED FOR EX VIVO MEASUREMENT OF GLUCOSE SENSING 59
2.3.1 Glucokinase activity assay *59*
2.3.2 Production of radiolabelled RNA probes for in situ hybridisation *61*
2.3.3 In situ hybridisation for glucokinase and WPRE mRNA *62*
2.3.5 Hypothalamic explant static incubation system *64*
2.3.6 Measurement of NPY and α-MSH in aCSF samples *65*
2.3.6.1 α-MSH radioimmunoassay *66*
2.3.6.2 NPY radioimmunoassay *67*
2.3.7 Cresyl violet staining of ink injected rat brains *67*
2.4 STATISTICAL ANALYSIS 68

CHAPTER 3: THE EFFECT OF ALTERED ARC GLUCOKINASE ACTIVITY ON GLUCOSE INTAKE 69

3.1 INTRODUCTION 70
3.1.1 The glucostatic control of food intake *70*
3.1.2 Glucokinase and food intake *70*
3.1.3 Techniques used to alter glucokinase in vivo *71*
3.2 HYPOTHESIS AND AIMS 73
3.2.1 Hypothesis *73*
3.2.2 Aims *73*
3.3 RESULTS 74
3.3.1 Localisation of GK expression in the hypothalamus *74*
3.3.2 Effect of pharmacologically increasing ARC GK activity on chow and glucose intake *75*
3.3.3 Visualisation of accurate ARC injection *79*
3.3.4 Measurement of total viral titre by dot blot analysis *80*
3.3.5 Quantification of GK knockdown in vitro *80*
3.3.6 Quantification of knockdown of ARC GK in vivo *81*
3.3.7 Effect of ARC GK knockdown on body weight *82*
3.3.8 Effect of ARC GK knockdown on food intake *83*
3.3.9 Effect of ARC GK knockdown on acute glucose intake *84*
3.3.10 Effect of ARC GK knockdown on cumulative glucose intake *85*
3.4 DISCUSSION 89
3.4.1 Endogenous expression of GK in the rat hypothalamus *89*
3.4.2 Increasing arcuate glucokinase activity increases glucose intake *89*
3.4.3 Accurate injection of substances into the ARC *90*
3.4.4 Methods and measurements of altered glucokinase activity *90*
3.4.5 Decreasing arcuate glucokinase activity decreases glucose intake *91*
3.4.6 ARC glucokinase and the control of overall calorie intake *92*
3.4.7 Two separate physiological roles for hypothalamic glucokinase *92*
3.4.8 The physiological relevance of ARC GK in the regulation of food intake *95*

3.4.9 Conclusion *95*

CHAPTER 4: PHARMACOLOGICAL MANIPULATION OF ARCUATE NUCLEUS GLUCOSE SENSING 96

4.1 Introduction 97
4.1.1 The role of ATP-sensitive potassium channels *97*
4.1.2 The role of voltage-gated calcium channels in ARC GK-regulated glucose intake *98*
4.1.3 The neurotransmitters involved in ARC GK-regulated increase in glucose intake *100*
4.2 Hypothesis and Aims 102
4.2.1 Hypothesis *102*
4.2.2 Aims *102*
4.3 Results 104
4.3.1 Effect of pharmacologically inhibiting ARC K_{ATP} channels on chow and glucose intake *104*
4.3.2 Effect of pharmacologically activating ARC K_{ATP} channels on chow and glucose intake *108*
4.3.3 Effect of pharmacologically activating ARC GK and K_{ATP} channels on NPY and α-MSH release from hypothalamic neurones *112*
4.3.4 Effect of pharmacologically activating K_{ATP} channels on the ARC GK-regulated increase in glucose intake *114*
4.3.5 Effect of simultaneously activating ARC GK and K_{ATP} channels on hypothalamic NPY release *116*
4.3.6 Role of voltage-gated calcium channels in the ARC GK-regulated increase in glucose intake *118*
4.3.7 Effect of NPY receptor inhibition on the ARC GK-regulated increase in glucose intake *120*
4.4 Discussion 122
4.4.1 The link between GK and K_{ATP} channels in ARC glucose sensing neurones *122*
4.4.2 ARC GK neurones release NPY *122*
4.4.3 ARC GK-induced increase of glucose intake is mediated via P/Q-type VGCC *123*
4.4.4 ARC GK-regulated increase in glucose intake is mediated by Y1 and Y5 receptors *124*
4.4.5 Other mechanisms of glucose sensing *126*
4.5 Conclusions 127

CHAPTER 5: GENERAL DISCUSSION 128

5.1 Introduction 129
5.2 Previous investigation of glucose sensing 129
5.3 Investigating the role of ARC GK in appetite 130
5.4 Investigating the mechanisms of ARC glucose sensing 131
5.5 The significance of this work for obesity and diabetes research 134
5.6 Limitations and unresolved questions 135
5.7 Future directions 137
5.8 Conclusion 138

6. REFERENCES 139

7. APPENDIX 153

7.1 Appendix I – Solutions 153
7.2 Coronal section of the rat brain 159
7.3 Appendix II – Nutritional Information for RM1 standard chow diet 160
7.4 Appendix III – DNA sequencing of plasmid for in situ hybrisidation 161
7.5 Appendix IV – List of suppliers 162

List of Figures and Tables

Figure 1.1 Glucose excited neurone 23
Figure 1.2 Glucose inhibited neurone 25
Figure 1.3 Protein structures and modulators of SUR1 and K_{ir}6.2 subunits of K_{ATP} channels 33
Figure 2.1 Schematic of the two step reaction in the GK activity assay 59
Figure 3.1 Endogenous GK mRNA expression in the rat hypothalamus 74
Figure 3.2 Effect of increasing ARC GK activity on food intake 76
Figure 3.3 Effect of increasing ARC GK activity on 2% glucose intake 77
Figure 3.4 Effect of increasing ARC GK activity on chow and 2% glucose intake 78
Figure 3.5 Confirmation of cannula placement in rats cannulated into the ARC 79
Figure 3.6 Effect of in vitro GKAS-pTR-CGW plasmid transfection on GK activity 80
Figure 3.7 Confirmation of GK knockdown by activity assay 81
Figure 3.8 Effect of decreasing ARC GK on body weight 82
Figure 3.9 Effect of decreasing ARC GK on food intake 83
Figure 3.10 Effect of decreasing ARC GK on acute glucose and chow intake 84
Figure 3.11 Effect of decreasing ARC GK on glucose intake 85
Figure 3.12 Effect of decreasing ARC GK on food intake 86
Figure 3.13 Effect of decreasing ARC GK on energy intake 87
Figure 3.14 Effect of decreasing ARC GK on body weight 88
Figure 4.1 Effect of inhibiting K_{ATP} channels on food intake 105
Figure 4.2 Effect of inhibiting K_{ATP} channels on glucose intake 106
Figure 4.3 Effect of inhibiting K_{ATP} channels on chow and glucose intake 107
Figure 4.4 Effect of K_{ATP} channel activation on food intake 109
Figure 4.5 Effect of K_{ATP} channel activation on glucose intake 110
Figure 4.6 Effect of K_{ATP} channel activation on chow and glucose intake 111
Figure 4.7 Effect of pharmacological agents on neuropeptide release from hypothalamic neurones 113
Figure 4.8 Effect of K_{ATP} channel activation on the ARC GK-regulated increase in glucose intake 115
Figure 4.9 Effect of increased ARC GK and K_{ATP} channel activities on hypothalamic NPY release 117
Figure 4.10 Effect of VGCC inhibition on the ARC GK-regulated increase in glucose intake 119
Figure 4.11 Effects of NPY receptor inhibition on the ARC GK-mediated increase in glucose consumption 121
Figure 5.1 Proposed mechanism of ARC glucose sensing 133
Figure 7.1 Schematic of a coronal section of the rat brain 159
Figure 7.2 Nutritional information for RM1 standard chow diet 160
Figure 7.3 Sequence of GK-pTR-CGW-plasmid 161

Chapter one: General introduction

1.1 The obesity pandemic

Obesity is a leading cause of preventable death worldwide. The prevalence of obesity is increasing; more than 24% of UK adults are currently obese compared with less than 15% in 1993, according to data collected by the Health & Social Care Information Centre (2014). A rise in the prevalence of obesity is detrimental for the long-term health of the population as it increases the risk of diabetes, cardiovascular diseases, cancers and many other diseases (Stevens, Singh et al. 2012). Regular exercise and a reduction in energy-dense foods are the most efficient and cost effective ways to treat obesity, but weight loss is rarely maintained over the long term. Unfortunately, pharmacological treatments have fared little better in promoting weight loss, and there is not yet an effective non-surgical treatment for obesity (Viktoria, Matthias et al. 2013).

Obesity arises from an imbalance in energy homeostasis with more energy consumed than energy used. Excess energy is stored as adipose tissue, as a reserve for times when food is scarce. However, there does not seem to be a mechanism to prevent excess storage when food is in abundance. Historically, an excess of dietary fat intake was thought to be the main contributor to obesity. This premise initiated the production of many low-fat foods in an attempt to create healthier diets. Unfortunately, sugars were added as a substitute to fat. Foods with high sugar content are now considered a major contributor of obesity and it is likely that the high quantity of both fat and sugar as energy sources in Western-type diets is a major cause of the obesity pandemic.

Key questions to be answered are why the homeostatic mechanisms within the body still allow continuous intake of high energy food; and why, in many people, there does not seem to be an adiposity threshold to limit food intake. Understanding the mechanisms behind energy homeostasis is crucial for treating the obesity pandemic.

1.2 The central control of energy homeostasis

Maintenance of a stable supply of nutrients to all cells in the body is governed by homeostatic processes. Energy homeostasis regulates the balance between food intake, energy expenditure and body adiposity.

The brain plays a pivotal role in integrating signals governing energy homeostasis from several parts of the body including the liver, pancreas and gastrointestinal tract. Signals pass to the hypothalamus in many different ways, including in the blood and via sensory neurones in the vagus nerve. Much of the information is integrated by the hypothalamus; a relatively small region of the brain, recognised as a key junction for much of the information regarding energy homeostasis (Thorens 2011). The hypothalamus consists of several nuclei, which have discrete populations of neurones and are thought to control specific aspects of energy homeostasis. Neuronal connectivity studies show that there are more neuronal outputs from the hypothalamus than inputs; supporting the view that the hypothalamus coordinates responses from many circuits (Oh, Harris et al. 2014).

1.2.1 Ventromedial hypothalamus

Specific ablation of the ventromedial hypothalamus (VMH) in rats provided the first evidence that the pathways of hunger and satiety can be separated (Hetherington and Ranson 1940). Lesions of the VMH produce profound hyperphagia, leading to the hypothesis that specific areas of the hypothalamus control food intake. The VMH is subdivided into the ventromedial nucleus (VMN) and the arcuate nucleus (ARC) to separate the different functions and populations of neurones in these nuclei.

The VMN is historically considered the satiety centre. In early lesion studies, hyperphagia was most pronounced in animals with lesions ablating the entire VMN (Hetherington and Ranson 1940, King 2006). Interestingly, most VMN ablated animals continue over eating until a certain level of adiposity is achieved, individual to each animal; after which eating levels return to relatively normal levels (Brooks and Lambert 1946). This phenomenon suggests that the VMN sets a threshold, around which energy homeostasis is regulated (King 2006). The mechanism for VMN-mediated control of food intake is likely via the vagus

nerve, as vagotomy considerably blunts the VMN ablation phenotype (Cox and Powley 1981).

The ARC is located in the basal part of the VMH closest to the median eminence and basal part of the third ventricle. This is a specialised location in the hypothalamus for monitoring hormones and nutrients from both the blood and cerebral spinal fluid (CSF). The median eminence is highly fenestrated to allow more blood-borne constituents to pass through it, compared to other areas of the brain where the blood brain barrier (BBB) is intact (Langlet, Levin et al. 2013). The median eminence facilitates diffusion of circulating hormones and nutrients to the ARC in concentrations that are closer to blood concentrations, compared with other parts of the central nervous system. The ARC also receives tanycyte projections from the lining of the third ventricle to facilitate the transport of CSF constituents (Langlet, Mullier et al. 2013).

There are two well characterised populations of neurones in the ARC that regulate energy homeostasis. Anorexigenic neurons express pro-opiomelanocortin (POMC) and cocaine- and amphetamine-regulated transcript (CART). These neurones are activated by leptin and insulin to reduce feeding (Cone, Cowley et al. 2001). An important result of leptin activation is the increased expression of POMC; the precursor for many peptides. One peptide in particular is alpha-melanocyte stimulating hormone (α-MSH), which acts as an anorexigenic neurotransmitter at melanocortin receptors within the hypothalamus. Another well characterised population of ARC neurones co-express neuropeptide Y (NPY) and agouti-related peptide (AgRP) (Gropp, Shanabrough et al. 2005, Tong, Ye et al. 2008). NPY/AgRP neurones are powerful drivers of food intake. Optogenetic stimulation of just 800 AgRP neurones are sufficient to produce intense feeding (Aponte, Atasoy et al. 2011). NPY/AgRP neurones are activated by the hunger-stimulating peptide ghrelin, and are inhibited by leptin (Cone, Cowley et al. 2001).

1.2.2 Lateral hypothalamus

Early studies suggested that the lateral hypothalamus (LH) was the 'hunger centre' (Anand and Brobeck 1951). The LH contains populations of neurones involved in the regulation of reward, motivation and arousal. Reward behaviours are in part regulated by orexin-

containing neurones in the LH that project to the cortex, limbic system and other hypothalamic nuclei (Horvath, Diano et al. 1999, Harris, Wimmer et al. 2005). The LH also contains populations of neurones that express the powerful orexigenic peptide melanin concentrating hormone (MCH). Ablating MCH neurones in mice decreases their preference for sucrose over non-caloric sweeteners and reduces striatal dopamine release (Domingos, Sordillo et al. 2013). Both orexin and MCH neurones in the LH are inhibited by anorexigenic NPY projections from the ARC to reduce food intake (Mercer, Chee et al. 2011).

1.2.3 Paraventricular and dorsomedial nuclei

Neurones in the anterior part of the paraventricular nucleus (PVN) release hormones into the blood at the median eminence and posterior pituitary (Tasker and Dudek 1991). These include thyrotropin-releasing hormone, which regulates release of thyroid hormones in the thyroid-hypothalamic-pituitary axis. Neurones in the posterior PVN project to autonomic neurones in the brainstem, which control peripheral tissues via the vagus nerve, and also receive information from several neuroendocrine pathways involved in energy homeostasis. For example, GLP-1 infusion decreases neuronal activation within the PVN as shown by manganese-enhanced magnetic resonance imaging (Parkinson, Chaudhri et al. 2009). In addition, NPY and orexin-A injection into the PVN stimulates food intake, indicating that the PVN plays an important role in integrating the information regarding food intake (Stanley, Chin et al. 1985, Edwards, Abusnana et al. 1999).

Neurones within the dorsomedial nucleus (DMN) communicate with the nearby ARC in relation to energy balance. CART and NPY colocalise in DMN neurones of diet-induced obese mice (Lee, Verma et al. 2013). DMN NPY expression significantly increases in rodent models of obesity (Guan, Yu et al. 1998, Bi, Ladenheim et al. 2001) and it is hypothesised that DMN neurones modulate ARC feeding signals (Dhillo, Small et al. 2002).

1.2.4 Dorsal vagal complex of the brainstem

The dorsal vagal complex (DVC) comprises nuclei that regulate the autonomic response to energy homeostasis: the nucleus of the solitary tract (NTS), area postrema (AP) and dorsal

motor nucleus of the vagus (DMNX). DMNX and NTS neurones receive input from several peripheral tissues regarding energy balance including the gastrointestinal tract, pancreas and liver (Grill 2006). The information from these sensory afferents merges with central pathways regulating energy homeostasis. Feedback is also provided by parasympathetic projections from the CNS to peripheral organs (Shapiro and Miselis 1985, Rinaman 2010). The DMNX plays an important role in determining meal size (Grill 2006).

The AP is a circumventricular organ with highly fenestrated capillaries, similar to the median eminence. The AP resides beneath the fourth ventricle to allow access to blood and CSF nutrients at similar concentrations to that in the median eminence. Ablation of the AP results in an increase in food intake in rodents (Adachi, Kobashi et al. 1995). A similar effect is observed with leptin receptor knockdown in the AP and medial NTS (Hayes, Skibicka et al. 2010).

In conclusion, several regions of the CNS are involved in regulating energy homeostasis. Many of these are interconnected to form neuronal networks that control specific physiological processes.

1.3 The importance of glucose homeostasis

Glucose is used as the primary fuel in humans and other mammals. Blood glucose levels are tightly regulated by the coordinated actions of several tissues. In non-diabetic humans pre-prandial glucose levels are typically 4.0-5.9mM and 2 hour post-prandial levels rise up to 8.0mM (Diabetes Diabetes 2014). Similar levels are observed in rodents (Wynne, Stanley et al. 2005). Hypoglycaemia triggers a counterregulatory response that activates neuroendocrine pathways to increase glucagon and adrenaline release (Evans, McCrimmon et al. 2004). Liver and kidney glucose production increases, while muscle and adipose tissue glucose uptake decreases. Hyperglycaemia triggers an increase in insulin release and glucose uptake. Blood glucose levels also influence food intake. Intravenous injection of glucose decreases feeding in several mammal species (Woods, Stein et al. 1984, Burggraf,

Willing et al. 1997). Conversely, injection of insulin to induce hypoglycaemia rapidly increases food intake (Biggers, Myers et al. 1989, Dunn-Meynell, Sanders et al. 2009).

1.3.1 Pancreatic glucose sensing

Blood and extracellular glucose concentrations are monitored by specific glucose sensors. In pancreatic β-cells the intracellular glucose concentration is correlated with the release of insulin. The enzyme glucokinase (GK) catalyses the first step in glycolysis and is the critical component of glucose sensing (Matschinsky and Ellerman 1968, Liang, Najafi et al. 1990, Schuit, Huypens et al. 2001, Levin, Routh et al. 2004).

Glucose sensing in β-cells occurs when glucose enters the cell via GLUT2 transporters and is phosphorylated into glucose-6-phosphate (G6P) by GK. G6P undergoes further metabolism in glycolysis and the tri-carboxylic acid cycle leading to the production of adenosine triphosphate (ATP). An increase in the ratio of ATP to adenosine diphosphate (ADP) blocks ATP-sensitive potassium (K_{ATP}) channels, resulting in an increase in intracellular cations. If sufficient K_{ATP} channels are blocked, the β-cell membrane potential exceeds a threshold and the membrane depolarises to stimulate opening of voltage-gated calcium channels and insulin release (Ashcroft, Proks et al. 1994).

1.3.2 Brain glucose sensing

While glucose sensing in β-cells is important for glucose homeostasis, the brain is central to coordination of the complete response to altered glucose concentrations. More than 60 years ago Jean Mayer hypothesised that a central glucostatic mechanism controls food intake, in an alternative pathway to energy homeostasis (Mayer 1953). It was previously established that small variations in food intake regulate long term adiposity and energy expenditure. Mayer argued that glucose is the primary signal to provide this regulation (Mayer 1955). He recognised that peripheral signals such as insulin must be integrated by a specific regulatory network, but the main signalling molecule should be a metabolite that can affect hunger and satiety. Therefore Mayer hypothesised that a fall in blood glucose

would trigger hunger for foods high in glucose. Similarly, George Bray describes glucose as having a dynamic role in homeostasis by initiating food intake (Bray 1996).

1.3.3 The reward value of glucose

Mayer's theory is in accord with current investigation into the physiological role of hypothalamic glucose sensing in conveying the reward value of sugar (Mayer 1953). Glucose is the preferred energy source over other types of food (Sclafani 2004, Johnson and Kenny 2010). During food restriction in mice, the reward value of sucrose (glucose and fructose combined) was found to be more powerful than optogenetic stimulation of limbic dopaminergic neurones (Domingos, Vaynshteyn et al. 2011). Magnetic resonance imaging in humans suggest that ingestion of glucose, but not fructose; increases connectivity between the hypothalamus and striatum (Page, Chan et al. 2013). It is likely that there is an innate mechanism to ensure that available glucose is consumed, possibly via reward processes. As the brain is reliant on glucose as a fuel, it is possible that the mechanism is in place to ensure that there is a constant supply of glucose.

1.3.4 Glucose-sensing neurones

CNS glucose sensing occurs in specific glucose-sensing neurones, which are classed into two groups depending on their electrophysiological properties. Those that respond to increasing concentrations of glucose by increasing frequency of their action potentials are named glucose-excited (GE); those that decrease the frequency of their action potentials are glucose-inhibited (GI), (Spanswick, Smith et al. 1997, Song, Levin et al. 2001).

1.3.4.1 GE neurone glucose sensing

Analogous to β-cells, glucokinase is expressed in most GE and GI neurones in the CNS (Dunn-Meynell, Routh et al. 2002, Kang, Routh et al. 2004) and has been identified as a major regulator in neuronal glucose sensing (Levin, Routh et al. 2004). GE neurones and pancreatic β-cells share the same mechanism for detecting an increase in glucose levels (Levin, Routh et al. 2004). GK activity is dependent upon the prevailing glucose concentration. Metabolism of glucose results in an increase in ATP that is thought to close K_{ATP} channels and increase the intracellular cation concentration. Closure of enough K_{ATP} cannels results in depolarisation and neuronal firing (figure 1.1).

Some GE neurones have been shown to express sodium-dependent glucose transporters (SGLT) (O'Malley, Reimann et al. 2006). The SGLT1 activator α-methylglucopyranosid activates GE neurones in primary cultures of rat hypothalamic neurones independent of K_{ATP} channel sensitivity. Intracerebroventricular (ICV) injection of the SGLT1 antagonist phloridzin stimulates feeding in rats (Tsujii and Bray 1990), thus may describe an alternative mechanism for GE neurone glucose sensing. However the roles of SGLT1-expressing neurones in glucose sensing are unclear. A similar transporter has been identified in *Drosophila*, which detects sugar intake (Dus, Ai et al. 2013).

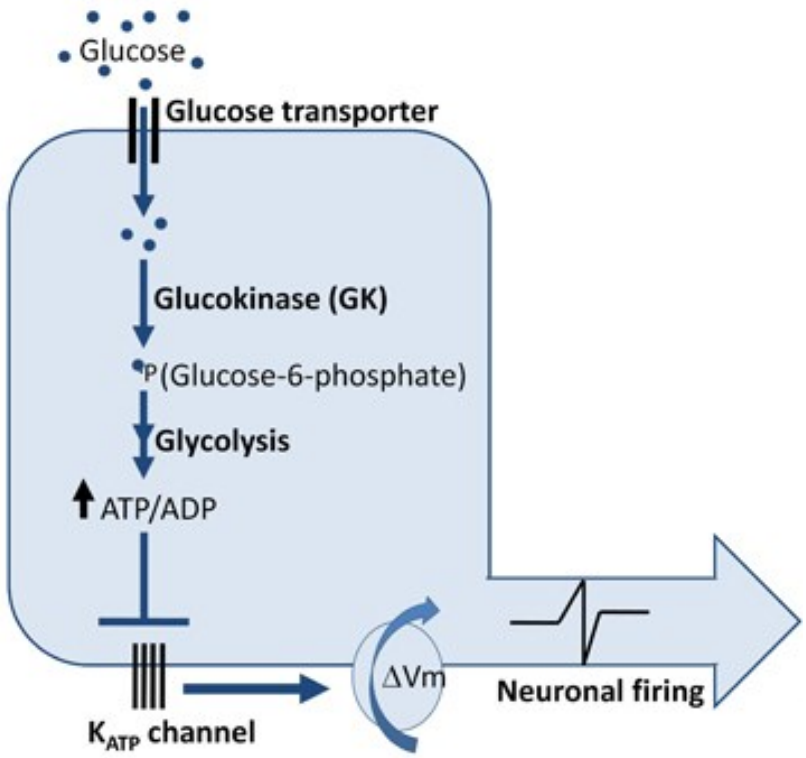


Figure 1.1 Glucose excited neurone: Mechanism for glucose sensing in GE neurones. Glucokinase phosphorylates glucose at a rate proportional to glucose influx. Local ATP levels affect K^+ permeability via K_{ATP} channels therefore affecting neuronal firing and neurotransmitter release. ΔVm, change in membrane potential, membrane depolarisation. Adapted from Diggs-Andrews, Silverstein et al. (2009).

1.3.4.2 GI neurone glucose sensing

GI neurones may utilise several different molecular mechanisms for glucose sensing (Thorens 2012). GK is expressed in most GI neurones (Kang, Dunn-Meynell et al. 2006), but an increase in glucose concentration results in membrane hyperpolarisation, therefore it is likely that a different intracellular mechanism to K_{ATP} channels is involved. Calcium imaging studies reveal that over 70% of GI neurones in the VMN are affected by GK inhibitors (Dunn-Meynell, Routh et al. 2002), indicating that GK is an important regulator in most GI neurones. AMP-activated kinase (AMPK), nitric oxide (NO) synthase and cystic fibrosis transmembrane regulator (CFTR) channels are also implicated in the mechanism of GI glucose sensing (figure 1.2).

Insulin and low glucose concentrations increase the ratio of AMP to ATP, which alters AMPK activity and NO signalling in GI neurones (Fioramonti, Lorsignol et al. 2004, Canabal, Potian et al. 2007). Reduced ATP concentrations may close CFTR channels and depolarise the cell membrane during low glucose levels (Gadsby, Vergani et al. 2006). CFTR channels regulate chloride ion flow and likely control membrane potential in GI neurones (Sheppard and Robinson 1997). However, much of the mechanism of GI neurones has only been shown *in vitro*. Some evidence for a role of AMPK in GI neurones has been demonstrated *in vivo*. Leptin activates AMPK and NO synthase in VMH GI neurones (Murphy, Fakira et al. 2009). Also, knockout of the α2 subunit for AMPK specifically in POMC or AgRP neurones impairs glucose sensing. Therefore AMPK may be an important regulator of glucose sensing in some neurones (Claret, Smith et al. 2007).

Glucose-inhibited neurone

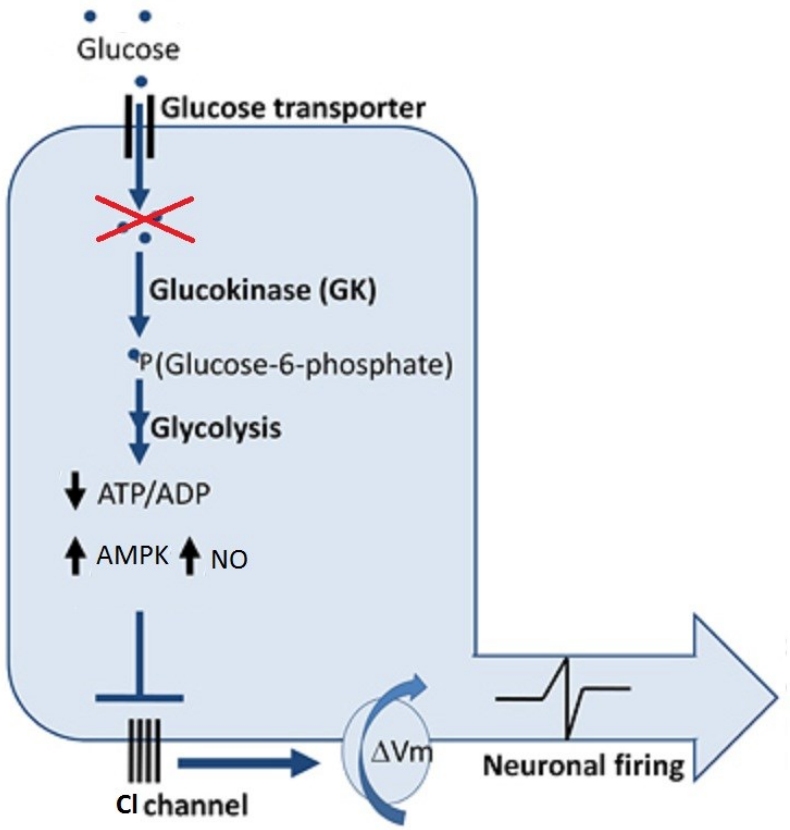


Figure 1.2 Glucose inhibited neurone: Mechanism for glucose sensing in GI neurones. Glucokinase phosphorylates glucose at a rate proportional to glucose influx. Neuronal firing is dependent upon Cl^- permeability, possibly controlled by AMPK and NO synthase. A decrease in glucose phosphorylation results in an increase in neuronal firing (Claret, Smith et al. 2007). ΔVm, change in membrane potential, membrane depolarisation. Adapted from Diggs-Andrews, Silverstein et al. (2009).

1.3.5 Glucose sensing neurones in the CNS

Intravenous glucose and insulin injections have been shown to alter neuronal activity during electrophysiological studies performed as many as 50 years ago (Anand, Chhina et al. 1964). The physiological importance of this response has since been investigated. ICV injection of glucose reduces food intake in rats (Tsujii and Bray 1990). Conversely, injection of 2-deoxyglucose (2-DG), an analogue of glucose that cannot undergo glycolysis and inhibits ATP production, results in an increase in food intake (Tsujii and Bray 1990). Injection of 2-DG into the VMH also increases blood glucose concentrations (Borg, Sherwin et al. 1995). Further investigation is required to understand the physiological roles of specific hypothalamic nuclei in glucose homeostasis.

1.3.5.1 VMN glucose sensing

Electrophysiological recordings in rats reveal that 14-19% of VMN neurones are glucose-excited and 3-14% are glucose-inhibited (Song, Levin et al. 2001, Dunn-Meynell, Routh et al. 2002). Of these, 64% of GE and 43% of GI neurones express GK (Kang, Routh et al. 2004). The main role of VMN GK neurones is mediating the counterregulatory response (CRR) to hypoglycaemia (Borg, Sherwin et al. 1995). VMN glucose sensing neurones detect acute drops in blood glucose and respond by sending signals to the pancreas and adrenal glands for stimulating hormone secretion and raising blood glucose concentrations (Levin, Becker et al. 2008). Increasing GK activity *in vivo* decreases the release of several peripheral hormones including adrenaline, noradrenaline and glucagon. In contrast, reducing the expression or activity of VMN GK elicits the opposite response by stimulating adrenalin release and increasing glucose availability (Levin, Becker et al. 2008). Glucagon and adrenalin levels are also elevated when VMN neurones are hyperpolarised by K_{ATP} channel openers (McCrimmon, Evans et al. 2005, Chan, Lawson et al. 2007). Hyperpolarisation mimics the effects of decreased GK activity in GE neurones, therefore reduced GE (and increased GI) firing likely drives the CRR to hypoglycaemia. Consistent with this, activation of NO signalling in GI neurones also induces adrenaline release (Fioramonti, Marsollier et al. 2010).

Lactate, a source of energy provided by astrocytes during periods of hypoglycaemia, further demonstrates the physiological role of GI neurones in the CRR to hypoglycaemia. Lactate increases firing in VMN GE neurones, similar to glucose (Song and Routh 2005). However, lactate does not affect the CRR to hypoglycaemia via GI neurones during hypoglycaemia, indicating that glucose concentrations are the primary regulators of this pathway. The neurotransmitters involved in VMN glucose signalling have not been fully elucidated, but may include a short feedback loop via inhibitory GABA in the VMN (Chan, Lawson et al. 2007).

1.3.5.2 ARC glucose sensing

Electrophysiological recordings from ARC neurones reveal that there are two distinct regions of glucose sensing neurones. In the medial portion of the ARC, 14% of neurones are GI and 3% are GE; in the lateral portion of the ARC, 13% of neurones are GE and 1% are GI (Wang, Liu et al. 2004). However, high levels of GK mRNA are observed in both parts of the ARC: as high as that expressed in the VMN (Lynch, Tompkins et al. 2000). GK is expressed in POMC and NPY neurones. Whole cell patch clamp recordings from mouse brain slices show that most POMC neurones have GE properties (Ibrahim, Bosch et al. 2003). Selective knockout of K_{ATP} channels in POMC neurones impairs glucose-induced depolarisation (Parton, Ye et al. 2007). In contrast, almost all GI responses found in one study were from NPY neurones (Muroya, Yada et al. 1999). In addition, many AgRP expressing neurones have a reduced expression of AMPK in response to glucose (Lee, Li et al. 2005, Mountjoy, Bailey et al. 2007). This reveals that POMC and NPY neurones resemble to some extent GE and GI neurones respectively. However, the independent roles of the ARC and VMN in glucose homeostasis have not been investigated (Levin, Routh et al. 2004, McCrimmon, Evans et al. 2005, Levin, Becker et al. 2008). As expression of POMC, CART, NPY and AgRP are different in ARC and VMN neurones, differences in GE and GI neurone signalling may be altered.

The extracellular glucose concentration throughout most of the brain remains relatively stable, even when blood glucose levels fluctuate (Wang, Liu et al. 2004). In non-glucose sensing neurones, transporters carry glucose across the BBB and into cells to make use of all available glucose (Vannucci, Maher et al. 1997). However, extracellular glucose

concentrations are more similar to the blood in brain regions near the 3rd and 4th ventricles than other regions of the CNS (Silver and Erecinska 1994, de Vries, Arseneau et al. 2003, Langlet, Levin et al. 2013). Extracellular VMH glucose concentrations vary between 0.5 and 2.5mM, whereas concentrations remain around 0.5mM in other regions of the CNS (de Vries, Arseneau et al. 2003, Wang, Liu et al. 2004). In parallel, the neuroendocrine form of GK is most sensitive to glucose within 0.5 and 2.5mM, identifying the VMH as ideal for glucose sensing (Kang, Dunn-Meynell et al. 2006).

To further enhance neuronal glucose sensitivity, areas where the lining of the BBB is discontinuous can expose regions of the CNS to glucose concentrations more closely mirroring blood levels. Tanycyctes project extensively from the median eminence to the ARC as shown by GLUT1 immunoreactivity: allowing ARC neurones to be exposed to higher levels of glucose than the VMN (Peruzzo, Pastor et al. 2000). Recently, the structural organisation of the BBB in the ME has been shown to change during hypoglycaemia (Langlet, Levin et al. 2013). Both fasting and administration of 2-DG increases the permeability of ARC cells to improve their access to nutrients. In addition, some ARC GE neurones are responsive to high extracellular glucose concentrations (above 5mM) via an AMPK pathway (Fioramonti, Lorsignol et al. 2004). There is no evidence that GLUT1 tanycytes project to the VMN. Therefore, it is likely that glucose sensing within the VMN and ARC differ, however the physiological role of this difference has not been identified.

1.3.5.3 Brainstem glucose sensing

Brainstem neurones integrate hypothalamic pathways with vagal efferent signalling to the pancreas and other peripheral tissues to control glucose homeostasis. Insulin secretion is partly controlled by orexinergic projections from the LH to the brainstem (Buijs, Chun et al. 2001). Detection of hypoglycaemia by the CNS activates vagal projections to the pancreas via the DMNX and NTS (Wu, Gao et al. 2004).

The brainstem also contains neurones for glucose and amino acid sensing, similar to the hypothalamus (Adachi, Kobashi et al. 1995, Blouet and Schwartz 2012). Some neurones express GK and K_{ATP} channels, indicating that the brainstem may have an important role in glucose sensing (Balfour, Hansen et al. 2006). Similar to the ARC, GK has been detected in

cells surrounding the 4th ventricle that have direct access to CSF. Immunoreactivity for both GLUT2 and K_{ATP} channels are observed in NTS and AP neurones nearest the 4th ventricle (Maekawa, Toyoda et al. 2000). The functions of these glucose sensors, and to what extent they modulate the hypothalamic signals, are not yet known. However, recent evidence indicates that tanycytes in the AP closely resemble those in the median eminence (Langlet, Mullier et al. 2013). Therefore ambient glucose concentrations surrounding the AP might more closely resemble that of glucose in the blood, compared with other regions of the CNS.

1.4 Mechanism of glucose sensing

The intracellular machinery involved in glucose sensing, which was originally modelled in β-cells, utilises GK as an intracellular regulator. A similar mechanism appears to occur in most GE neurones as GK remains the most specific marker of glucose sensing neurones.

1.4.1 Glucokinase

GK is part of the hexokinase family of enzymes that convert intracellular glucose to G6P in all mammalian cells. Of the four types of hexokinase identified within eukaryotic cells, GK (also called hexokinase IV) plays a distinct role. Unlike other hexokinases, GK phosphorylates glucose at a rate proportional to the intracellular glucose concentration (Printz, Magnuson et al. 1993). GK has a higher Michaelis constant (K_m) for glucose than the other hexokinases therefore it is less easily saturated by increasing intracellular glucose concentrations. This is considered to play a role in glucose sensing.

It is important to note that in cells expressing GK, other hexokinases are also present to maintain a constant supply of G6P regardless of fluctuations in extracellular glucose concentrations. It is possible that glucose sensing involving GK is a compartmentalised reaction within cells as not to interfere with normal ATP production. In support of compartmentalisation, glucose transporters and K_{ATP} channels are located proximal to each other on the cell membrane (Arkhammar, Nilsson et al. 1987).

In humans and rodents, GK is expressed in the liver, β-cells and CNS (Grossbard and Schimke 1966, Matschinsky and Ellerman 1968, De Vos, Heimberg et al. 1995). In the CNS, GK is expressed in the VMN, ARC, PVN, DMN, LH, medial amygdala nucleus, NTS, AP and parts of the thalamus (Lynch, Tompkins et al. 2000, Hawrylycz, Ng et al. 2014). The role of GK in the hypothalamus and brainstem has been investigated previously to some extent; the role of GK in the thalamus and medial amygdala is mostly unknown. In the medial amygdala nucleus, a subset of GK neurones have been shown to project to the VMN and influence the CRR to hypoglycaemia (Zhou, Podolsky et al. 2010).

Hepatic GK and neuroendocrine GK are the two major functional isoforms of GK. Neuroendocrine GK, a 465 amino acid peptide, is expressed in β-cells and the CNS (Roncero, Alvarez et al. 2000). The neuroendocrine isoform of GK is 15 amino acids longer than the hepatic isoform (Magnuson and Shelton 1989). Both catalyse the same reaction but hepatic GK is regulated by insulin and has a role in glucose clearance after feeding (Massa, Gagliardino et al. 2011), whereas neuroendocrine GK functions as a direct glucose sensor. Post-transcriptional processing of neuroendocrine GK produces a minor form of GK in β-cells with a lower affinity for glucose (Magnuson and Shelton 1989). However, this alternate isoform is not thought to participate in glucose sensing. GK activity is controlled by GK regulatory protein (GKRP) in some regions of the CNS, but the physiological function of this regulation is unknown (Alvarez, Roncero et al. 2002).

1.4.2 Transmembrane glucose transporters

Glucose transporters (GLUT) control the entry and exit of glucose, allowing rapid cellular uptake of glucose. Fourteen isoforms of GLUT have currently been identified, many of which are expressed in the human brain. GLUT1 is expressed in astrocytes and endothelial cells and plays an integral role in transporting glucose across the BBB (Simpson, Vannucci et al. 2001, Mueckler and Thorens 2013). GLUT6, 8 and 10 are also expressed in the brain but their specific roles in glucose homeostasis, if any, remain unclear. GLUT3 is the main transporter for facilitating glucose uptake in neurones (Leino, Gerhart et al. 1997). GLUT3 has a high apparent affinity for glucose (around 3mM) therefore is suited for low extracellular concentrations in the brain (Uldry, Ibberson et al. 2002). GLUT2 is important in

pancreatic β-cells for controlling insulin secretion, so it is likely to be an integral part of glucose sensing in the CNS as well (Navarro, De Fonseca et al. 1996, Schuit, Huypens et al. 2001, Uldry, Ibberson et al. 2002). Despite GLUT2 having a low apparent affinity for glucose (17-20mM), the uptake of glucose into β-cells is still significantly higher than the rate of glucose phosphorylation by GK (Mueckler and Thorens 2013). While GLUT3 is highly expressed in glucose sensing neurones, GLUT2 co-localises with GK (Navarro, De Fonseca et al. 1996, Kang, Routh et al. 2004). GLUT2 is also expressed in tanycytes lining the floor of the third ventricle (Garcia, Millan et al. 2003). The proximity of tanycytes to higher levels of glucose in CSF and blood may explain why a high affinity for glucose is not required for uptake in glucose sensing neurones. GLUT2 knockout mice have an impaired regulation of NPY expression in response to fasting and re-feeding that is not due to impaired β-cell function (Bady, Marty et al. 2006). Furthermore, ICV injection of 2-DG does not promote feeding in GLUT2 knockout mice. Selective knockdown of GLUT2 in the ARC inhibits glucose sensing and insulin secretion (Leloup, Orosco et al. 1998).

While GLUT2 and 3 are important for glucose sensing, the regulation of glucose entry is not considered the regulatory step in most of types of glucose sensitive neurones during physiological conditions. This is partly because GLUT isoforms are also involved in the maintenance of a stable intracellular glucose concentration as a fuel for all intracellular processes. Therefore even during periods of hypoglycaemia there are mechanisms in place to take up any available glucose from the blood and extracellular space to maintain these processes.

1.4.3 ATP-sensitive potassium channels

Glucose sensing in β-cells is regulated by GK but an intracellular mediator triggers insulin release. K_{ATP} channels are thought to couple GK with cell membrane depolarisation. K_{ATP} channels control movement of K^+ ions across the cell membrane and are abundantly expressed in many different cell types that can depolarise such as cardiac, skeletal and vascular smooth muscle (Seino and Miki 2003). K_{ATP} is an octameric protein consisting of two subunits (figure 1.3). Different cell types express specific K_{ATP} subunits that have slight variations in electrophysiological properties for different functions (Seino and Miki 2003). In

β-cells, $K_{ir}6.2$ make up the pore and SUR1 the regulatory subunit in the form of two homomeric tetramers (Inagaki, Gonoi et al. 1997). The ratio of ATP to ADP ultimately determines closing of the channel pore. ATP is a negative allosteric regulator of K_{ATP} channels and binds primarily to $K_{ir}6.2$ (Tucker, Gribble et al. 1998), which closes the pore and prevents K^+ ions exiting the cell. Other adenosine nucleotides, namely ADP, stimulate K_{ATP} channels by binding to SUR1 in the presence of Mg^{2+} (Gribble, Tucker et al. 1997). This interaction is disrupted by sulfonylureas such as glibenclamide, thus enabling ATP to have a more potent effect at $K_{ir}6.2$ and reducing K^+ conductance further (Hambrock, Löffler-Walz et al. 2002). In diabetic patients sulfonylureas are used as a treatment to stimulate insulin secretion (U. K. Prospective Diabetes Study U. K. Prospective Diabetes Study Group 1998).

$K_{ir}6.2$ and SUR1 are expressed throughout the CNS, including in the hypothalamus and brainstem (Karschin, Ecke et al. 1997). K_{ATP} channels are expressed in both POMC and NPY neurones in the ARC as 70% of neurones within the ARC respond to the potassium channel blocker tolbutamide (van den Top, Lyons et al. 2007). Global $K_{ir}6.2$ knockout markedly impairs the response to glucose in hypothalamic neurones (Park, Choi et al. 2011). When $K_{ir}6.2$ knockout is restricted to POMC neurones there are global impairments in glucose tolerance and glucose-stimulated α-MSH release (Parton, Ye et al. 2007). On the other hand, injection of diazoxide in the VMN to stimulate K_{ATP} channel opening and hyperpolarise affected neurones amplifies the CRR to hypoglycaemia (McCrimmon, Evans et al. 2005). Therefore K_{ATP} channels likely play an important role in hypothalamic glucose sensing.

Interestingly, ATP binds to both CFTR and K_{ATP} channels to trigger depolarisation as they share similar homology (figure 1.3), but they control depolarisation in GI and GE neurones respectively.

ATP-sensitive potassium channel

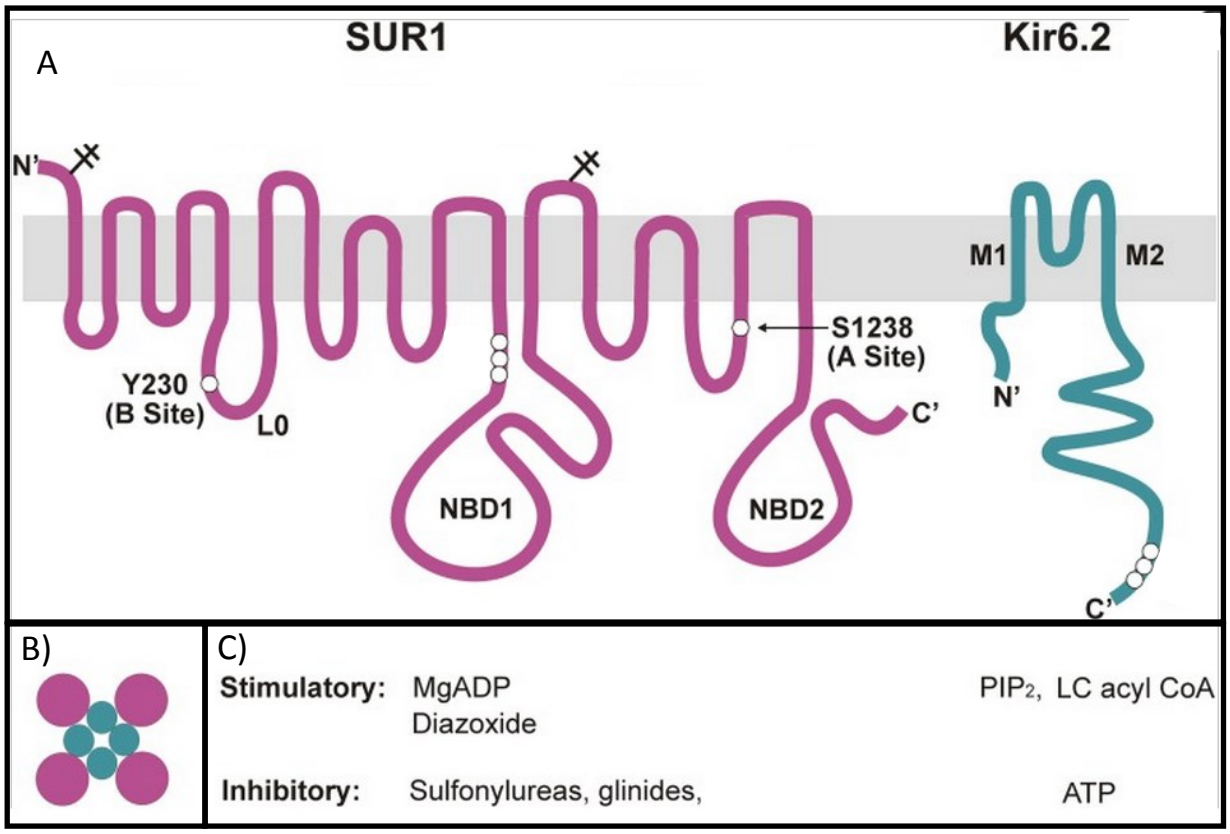


Figure 1.3 Protein structures and modulators of SUR1 and K_{ir}6.2 subunits of K_{ATP} channels: (A) Schematic of SUR1 and K_{ir}6.2 subunits. SUR1 has two cytoplasmic nucleotide binding domains (NBD1 and NBD2) and K_{ir}6.2 has two transmembrane helices that form the pore (M1 and M2). The cytoplasmic linker L0 binds the protein-specific N-terminal domain to the subunit's core structure, which is present in similar receptors such as CFTR. (B) Schematic of the quaternary structure of K_{ATP} channels. (C) Ligands of K_{ATP} channels. Sulfonylureas such as glibenclamide bind to SUR1 at site A and B, whereas Mg-nucleotides bind to the NBDs. ATP binds to K_{ir}6.2. Adapted from Martin, Chen et al. (2013).

1.4.4 The multiple roles of glucose sensing cells

The multiple mechanisms that have been described within glucose sensing cells illustrate that not all glucose sensors are part of the same neuronal circuits. While some hypothalamic glucose sensing neurones have been shown to control the CRR to hypoglycaemia, some glucose sensing neurones might have different roles. Therefore it is likely that glucose sensing neurones that express different glucose transporters, enzymes and ion channels exert many different physiological effects. Many glucose sensing neurones are responsive to other metabolic signals and may be communicating a more general representation of energy homeostasis rather than glucose specifically. Intracellular mediators such as AMPK and K_{ATP} channels are involved in glucose, leptin and insulin signalling (Spanswick, Smith et al. 2000, Claret, Smith et al. 2007). As GK is not expressed in all glucose sensing neurones, it is likely that some neurones respond to a variety of metabolic signals involving other mechanisms. For example, glucose sensing via phosphorylation of AMPK has been described in both GE and GI neurones, but it is unclear whether AMPK regulates glucose sensing or cellular energy homeostasis in these neurones (Claret, Smith et al. 2007, Murphy, Fakira et al. 2009).

Insulin and leptin are amongst other metabolic signals that induce changes in energy homeostasis via similar machinery to that used in glucose sensing neurones. Leptin and insulin can both open K_{ATP} channels resulting in a decrease in membrane potential and the inhibition of action potentials (Spanswick, Smith et al. 1997, Spanswick, Smith et al. 2000). However, leptin and insulin also act via alternate signalling pathways, namely PIP3-mediated signals, in POMC neurones (Plum, Ma et al. 2006). Similarly, in fatty acid sensing pathways, oleic acid depolarises POMC neurones by blocking K_{ATP} channels (Jo, Su et al. 2009). Esterification of long chain fatty acids to fatty acyl-CoAs enables ATP production via β-oxidation and thus inhibition of K_{ATP} channels (Lam, Schwartz et al. 2005). As fatty acid sensing neurones have been identified in the hypothalamus, it is possible that integration of fatty acid and glucose sensing signals occurs within some neurones (Migrenne, Cruciani-Guglielmacci et al. 2006).

A lactate-facilitated mechanism of glucose sensing has been investigated (Song and Routh 2005). Lactate is integral to neuronal metabolism as it is provided as a substitute fuel by

astrocytes, and converted to acetyl-CoA in neurones (Pellerin and Magistretti 1994, Pellerin, Bouzier-Sore et al. 2007). Blocking the monocarboxylate transporter desensitises orexin neurones in the LH to changes in glucose (Parsons and Hirasawa 2010). Whether release of lactate by astrocytes is proportional to glucose concentrations during euglycaemia remains to be investigated, but this pathway further demonstrates other mechanisms of glucose sensing. The contribution of the multiple pathways and metabolic signals therefore requires further investigation.

1.5 Approaches for investigating the neuronal circuits controlling energy homeostasis in rodents

1.5.1 Direct cannulation

Investigating the mechanisms involved in glucose sensing is important for understanding the pathophysiology of obesity and diabetes. To achieve this, several techniques are utilised to elucidate the specific roles of molecules *in vivo*. Acute changes in specific enzyme or receptor activity within the CNS can be investigated by direct administration of compounds. ICV injections have proven useful for studying the effects of peptides regulating food intake such as NPY, AgRP and α-MSH in the brain (Zarjevski, Cusin et al. 1993, Rossi, Kim et al. 1998). Injection of compounds into specific nuclei by cannulation enables the investigation of the physiological role of specific nuclei involved in energy homeostasis. This has been performed in rodents to identify endogenous peptides involved in feeding (Edwards, Abusnana et al. 1999, Batterham, Cowley et al. 2002). However, direct cannulation is not suitable for looking at the chronic effects of compounds. The pharmacological activity of most compounds only last for a short time, but direct injections can only be repeated a limited number of times before local inflammation and tissue damage occurs around the injection site.

1.5.2 Genetic modification by global mutation

Chronic investigation of the mechanisms regulating energy homeostasis can be achieved by generating genetic modifications of specific genes *in vivo*. Null mutations and gain of function mutations can be introduced into the mouse gene to create a permanent global alteration in that gene. Measuring the alterations due to a genetic knockout can identify important genes involved in food intake such as those that encode leptin (Halaas, Gajiwala et al. 1995) but there are a few drawbacks to this approach. Compensatory mechanisms can result in up-regulation of similar genes during development to correct for the effects of the deleted gene (Picciotto 1998). Additionally, global knockout of a gene may produce unwanted side effects due to expression in other areas of the body. An example of compensation can be observed in NPY knockout mice. Despite NPY knockout not resulting in any changes in food intake or energy homeostasis, postnatal knockdown ablation of NPY produces irreversible starvation (Erickson, Clegg et al. 1996, Luquet, Perez et al. 2005, Mercer, Chee et al. 2011).

Global homozygous knockout of the glucokinase gene results in neonatal lethality (Remedi, Koster et al. 2005). This highlights the physiological importance of the enzyme to development, and shows that other hexokinases are not able to compensate in order to adequately control glucose metabolism. By disrupting a neuroendocrine-specific exon, targeted knockout of neuroendocrine GK aims to retain normal liver functionality and only reduce GK in the CNS and pancreas (Terauchi, Sakura et al. 1995). These mice are still significantly insulin resistant and develop severe diabetes and die within a week. In contrast, heterozygous GK knockout produces a milder phenotype yet still results in partially reduced global GK expression. These animals can be made hyperglycaemic on high fat diet (Baker, Atkinson et al. 2014). However the precise role of CNS GK in the contribution of the hyperglycaemic phenotype cannot be quantified with the heterozygous knockout. Therefore a knockout of GK in specific tissue subtypes would produce a more selective model but this is technically challenging as no differences between hypothalamic and pancreatic GK genes have been identified.

1.5.3 Selective genetic modification

Site specific recombinase technology allows selective expression of a transgene in specific tissues or brain regions. Cre-Lox recombination relies upon the inversion or removal of DNA by Cre-recombinase (Cre) at a specific binding site flanked by short target sequences named Lox-P. Insertion of both Cre and Lox-P genes can be linked to a tissue-specific endogenous promoter to restrict the extent of Cre activation and transgene expression. Cre-Lox recombination has been used to investigate the effects of specific alterations in hypothalamic feeding circuits; for example, the development of mice with leptin receptor knockout exclusively in POMC expressing neurones (Balthasar, Coppari et al. 2004). Mice expressing Cre under the POMC promoter were crossed with mice with LoxP sites flanking the Janus kinase (JAK) docking site of the leptin receptor allele. As the only functional leptin receptors in POMC expressing cells are in ARC neurones this creates a model for studying the effects of leptin knockdown in ARC POMC neurones. A limitation of this technique is that developmental compensation can still occur. For example, knockout of AgRP/NPY expressing neurones in neonates does not affect feeding, but selective ablation of the same neurones using diphtheria toxin in adult mice, does (Luquet, Perez et al. 2005).

A disadvantage of Cre-Lox recombination is that investigation is restricted to transgenic mice only. Transgenic modifications in wild-type rats can be achieved by direct injection of foreign DNA encoding for a particular protein. A transgenic alteration in the brain requires stereotactic injection under general anaesthesia to ensure accurate and specific expression of the gene. An advantage of direct injection is that it eliminates developmental changes caused by expression during development. Also, location-specific injection provides the benefit of genetic alteration in a specific area to avoid side effects of global alterations.

1.5.4 Vectors used for gene transfer

As injection of naked DNA is not able to efficiently infect host cells *in vivo*, the gene of interest is packaged into a vector. The most efficient vectors are based on wild-type viruses that can efficiently infect mammalian cells. Other non-viral vectors have been used but they have not made much success in clinical and preclinical experiments (Lam and Dean 2010). Use of virus-mediated transfection is a powerful and efficient way to provide selective

genetic modification *in vivo*. However, any immune response and replication of the virus needs to be eliminated. Depending on the severity of the host's immune response, destruction of a foreign body by proteasome degradation, production of antibodies or fever can occur. The immune response can affect transduction of the gene of interest and the host's physiological response to the treatment. To circumvent the immune response, wild-type viruses are re-engineered by removal of as much endogenous viral DNA as possible. Removal of the genes required for self-replication also eliminates the ability for the virus to multiply. The virus is therefore safer to work with and cannot spread to other areas of the host once after the initial infection.

A limitation of stereotactic injection of vectors is that the extent of expression is dependent upon the skill of the surgeon. In addition, sufficient time should be allowed for maximal gene expression, which can be up to four weeks.

1.5.4.1 Retroviral vectors

Retroviral vectors are able to integrate into the host's chromosomes to increase their effectiveness, unlike many viral vectors that are present in the nucleus as an episome. However, depending on where the vector integrates in the chromosome, disruption of an endogenous gene can occur due to insertional mutagenesis. With the exception of the lentivirus, retroviral vectors only have the ability to transfect dividing cells. These are therefore useful as a treatment for cancer but are not ideal when introducing a gene into quiescent adult neurons. Also many retroviral-based vectors have a low transfection efficiency and a low titre (Gardlik, Palffy et al. 2005). Lentiviruses overcome many of these limitations and are ideal for *in vivo* transfection as they do not produce a significant immune response (Quinonez and Sutton 2002). They also allow large therapeutic genes to be inserted at over 18kb (Kumar, Keller et al. 2001). However, as they are based on human immunodeficiency virus, they pose a potential safety risk during production, as a replication-competent virus can potentially be generated. Also, lentivirus vectors spread further than the intended injection site, which is a concern when injecting into specific brain areas (Blömer, Naldini et al. 1997).

1.5.4.2 Adenoviral vectors

Recombinant adenoviruses can be produced at a high titre and can transfect a high ratio of cells making them useful for altering gene expression in large tissues like the liver (Brunetti-Pierri, Stapleton et al. 2007). The double stranded DNA of an adenovirus is enclosed in a large capsid made up of several different proteins. Even deletion of many unnecessary genes in recombinant adenoviral vectors still results in an immediate innate immune response and antibody production. The significant host immune response has hindered the use of this vector in many applications (Kay 2011).

1.5.4.3 Adeno-associated viral vectors

Adeno-associated viral (AAV) vectors are minimally pathogenic, highly persistent and can be produced at a high titre (Ponnazhagan, Mukherjee et al. 1997). Twelve human serotypes and over 100 primate serotypes have been identified, each having tropism for particular cell types (Howard, Powers et al. 2008). AAV contains single stranded DNA that requires conversion into double stranded DNA once successfully transfected into the host; a process that can be slow and delays maximal expression by up to 3 weeks *in vivo* (Wang, Ma et al. 2003). The majority of viral DNA is removed in recombinant AAV (rAAV), including the genes encoding Rep and Cap proteins for capsid production and insertion into the host's chromosomes. The remaining viral DNA consists of inverted terminal repeats at both ends that are essential for transfection. Removal of inessential genes creates a larger insertion cassette for therapeutic genes.

AAV2 has a tropism for neurones, therefore is valuable when investigating overexpression or knockdown of genes in the CNS (Gardiner, Kong et al. 2005). When administered *in vivo*, rAAV2 spread is limited to around the site of injection as co-transfection of a helper plasmid containing the necessary genes for replication is required. The infection rate into the CNS is approximately 70% (Palomeque, Chemaly et al. 2007). While rAAV has the ability for a larger gene to be inserted than AAV, the size of the cassette is still smaller than other vectors (4.5kb vs. <18kb for lentivirus). To overcome this, trans-splicing vectors can be engineered (Yan, Zhang et al. 2000). The cassette size can be doubled with the independent infection of complimentary rAAV vectors that recombine in the cytoplasm. A benefit of rAAV is that

stable expression seems to persist for several months despite the DNA being present as an episome. Transfection of rAAV containing glucokinase has previously been successful *in vivo* in our laboratory (Hussain, Richardson et al. 2014).

1.6 Summary

The brain has developed a complex set of neuronal circuits to control food intake and homeostasis. Many of these circuits involve neurones in the arcuate nucleus of the hypothalamus, where nutrients and hormones from the blood and CSF provide feedback to fine tune neuronal responses. Hypothalamic glucose sensing neurones have previously been described to control counterregulatory responses to hypoglycaemia and hyperglycaemia. However, a specific role for arcuate nucleus glucose sensing neurones in regulating food intake has not has not been investigated. The work in this thesis investigates arcuate nucleus glucose sensing and its role in food intake using rats.

Chapter two: Materials and methods

2.1. Methods used to produce plasmids containing GK and to produce rAAV

2.1.1 Production of rAAV

Recombinant AAV was produced by Dr J Gardiner (Division for Diabetes, Endocrinology and Metabolism), Dr SS Hussain (Division for Diabetes, Endocrinology and Metabolism) and Dr E Richardson (Division of Women's Health, King's College London). Full length glucokinase cDNA was isolated and amplified by PCR from the plasmid pCMV4.GKB1 encoding full length glucokinase cDNA (gift from Prof. Magnuson, Nashville).

GK DNA were cloned into the plasmid pTR-CGW (gift from Dr. Verhaggen, Amsterdam) in the forward and reverse orientation to produce GK sense (GKS) and antisense (GKAS), respectively. Recombinant AAV particles were produced using the two-plasmid system with a helper plasmid pDG (Grimm, Kern et al. 1999), then recovered and purified using a Sepharose column. This was used to make rAAV-GKS and rAAV-GKAS.

2.1.2 Digestion of PCR products

The previous PCR products from isolated GK cDNA were cut to isolate the fragment of interest.

Materials

GK-pTR-CGW plasmid (AAV-CMV-eGFP-WPRE-Amp)

Restriction endonucleases: BamHI, PSTI (New England Biolabs)

10x Restriction buffer (appendix 1)

10x Bovine serum albumin (BSA) (New England Biolabs)

Shrimp alkali phosphatase (SAP) 4U/µl (GE Healthcare)

Phenol/chloroform pH8 (VWR)

2M Sodium acetate pH5.2 (appendix 1)

100% ethanol (VWR)

Methods

GK-pTR-CGW was diluted twice in GDW in separate microcentrifuge tubes. Restriction buffer and BSA were added to give a final concentration of 1x. Eight microlitres of BamHI and PstI (30U each) were added to give the volume of enzyme added as less than 10% of the final volume. The reaction was incubated at 37°C for at least 1 hour and 8U SAP added to one reaction 30 minutes before the end of the incubation. SAP removes 5‟ phosphate groups preventing self-ligation of the plasmid. The reactions were extracted with an equal volume of phenol/chloroform and the phases separated by centrifugation for 3 minutes at 13,000xg. The DNA was ethanol precipitated with 0.1 volumes sodium acetate pH5.2 and 2.5 volumes absolute ethanol and was incubated at -20°C for at least one hour. The DNA was recovered by centrifugation for 7 minutes at 13,000xg.

2.1.3 Electroelution of DNA fragments

Following the PCR reaction it is advantageous to purify the DNA fragment of interest and remove any contaminating fragments. This is especially true for plasmids as restriction digests are not 100% efficient and a small amount of closed plasmid DNA can produce a high background during transformations. The DNA was therefore size fractionated by electrophoresis on an agarose gel and the bands of interest electroeluted.

Materials

Agarose, type II-A medium EEO (VWR)

50x TAE (Appendix I)

Ethidium Bromide (10mg/ml) (VWR)

Dialysis tubing (VWR)

Gel loading buffer (Appendix I)

1Kb plus DNA marker (Invitrogen)

DNA fragments

Methods

A 1% (w/v) agarose gel was prepared by boiling 3g agarose and 6ml 50X TAE in 300ml GDW, allowing this to cool, then adding 13µl ethidium bromide before pouring into a cassette. The precipitated

DNA was dissolved in 20µl GDW and 6µl loading buffer added. One microlitre of DNA marker was added to 9µl GDW and 3µl loading buffer added. Samples were loaded onto the gel and electrophoresed at 10V/cm.

The DNA was visualised by illumination with UV light (300nm), the band of interest was cut out from the gel using a scalpel and placed into dialysis tubing. Four hundred microlitres of 0.5x TAE was added to the gel slice, air excluded from the end of the tubing and the other end sealed with a clip. The DNA was eluted from the gel by electrophoresis at 20V/cm for 20 minutes. The TAE was removed from the tubing, phenol/chloroform extracted and the DNA was recovered by ethanol precipitation (as described in section 2.1.2).

The DNA was then quantified spectrophotometrically: 10µl DNA was diluted 1:100 and placed into a quartz cuvette. Absorbance was read at 260 and 280nm UV 1101 spectrophotometer (WPA). The reading at 280nm gives an indication of the purity of the sample as proteins and phenol absorbs more strongly at 280nm than DNA. The concentration of the DNA was calculated using the following formula:

Concentration (µg/ml) = (A260 x dilution factor) x 50

2.1.4 Ligation of PCR product into pTR-CGW

Materials

T4 DNA ligase, 6U/µl (New England Biolabs)

10x Ligase buffer (New England Biolabs)

Digested plasmid: insert (27ng/µl) and cut plasmid (46ng/µl)

Methods

DNA ligation was used to insert the digested GK into pTR-CGW plasmid. Twenty nanograms of cut plasmid DNA were dissolved in GDW and a fourfold molar excess of PCR product added. Ligase buffer was added to a final concentration of 1x and 6U T4 DNA ligase added to give a final volume of 10µl. The reaction was incubated at 16°C overnight.

2.1.5 Transformation of competent bacteria by heat shock

A sudden increase in temperature opens transient pores in the bacteria plasma membrane allowing the plasmid to move into the cell. pTR-GCW contains an ampillicin resistance gene. Calcium chloride is added to the environment to reduce electrostatic repulsion between the plasmid and bacterial cell membrane. Subsequent incubation allows the expression of the resistance genes before exposure to antibiotic.

Materials

LB culture medium (Appendix I)

LB(amp) plates (Appendix I)

E. coli BL21 bacteria (Invitrogen) in frozen aliquots of 0.1M $CaCl_2$ and 15% glycerol

Methods

On ice, 5ng of ligation products were added to an aliquot of thawed bacteria, mixed gently and incubated on ice for 10 minutes. The mixture was heated to 42°C for 45 seconds, then immediately incubated on ice again. 450µl LB was added and was shaken rigorously at 250 rpm for 1 hour at 37°C. Agar plates (supplemented with 100µg/ml ampicillin) were warmed and 150µl of the transformed bacteria added to the plate. The bacteria were spread over the surface of the agar, the plate inverted and incubated at 37°C overnight. Efficiently transformed colonies were collected and sequenced.

2.1.6 DNA sequencing

Sequencing of GKS-pTR-CGW plasmid was performed by the Imperial College Genomics Core Laboratory.

Materials

GKS-pTR-CGW

20µM GK forward primer 5'-ACGTACCGGTATTCACATCTGGTACCTGGG -3' (Oswel DNA Service)

20µM GK reverse primer 5'-AGCTCGTACGTATTAGGACAAGGCTGGTGG-3' (Oswel DNA Service)

Methods

Prior to sequencing 200ng of plasmid DNA was diluted and mixed with 3.2pmole of either the forward or reverse primer that was used during the initial production of the plasmid. Samples were cycle sequenced using BigDye v3.1 (Applied Biosystems Ltd, Warrington, UK). Sequencing results were analysed for homology to known rat GK gene sequences using the Basic Local Alignment Search Tool (BLAST) on the National Centre for Biotechnology Information (NCBI) internet site.

2.1.7 Large scale preparation of plasmid

A large scale preparation of a plasmid or maxi preparation is used to obtain a large supply of high quality plasmid.

Materials

LB(amp) (Appendix I)

GTE (Appendix I)

Lysozyme (Sigma)

0.2M sodium hydroxide/1% (w/v) SDS (Appendix I)

5M potassium acetate (KAc) (VWR)

Propan-2-ol (VWR)

100x TE (Appendix I)

DNase free RNase A 10mg/ml in GDW (GE Healthcare)

Phenol/Chloroform (VWR)

Methods

A small quantity of bacteria containing pTR-CGW was inoculated into 500ml LB(amp) and incubated at 37°C overnight with shaking at 250 rpm. The bacteria were split into two and each recovered by centrifugation for 8 minutes at 3000xg at 4°C. The pellets were resuspended in 12.5ml GTE supplemented with 2mg/ml lysozyme and incubated at room temperature for 5 minutes. Twenty five millilitres of NaOH/SDS were added, the samples mixed by inversion and incubated on ice for 5 minutes until they cleared. Then 18.75ml 5M KAc were added, the samples mixed by inversion and incubated on ice for 5 minutes. Bacterial debris was removed by centrifugation for 10 minutes at 9000xg at 4°C. The supernatants were transferred to a clean tube and 0.6 volumes isopropanol added. The samples were incubated on ice for 15 minutes and the DNA recovered by centrifugation for 15 minutes at 9000xg at 4°C. The pellets were dissolved in 5ml GDW and combined together, to which 100µl 100x TE was added. RNase A was added at a concentration of 0.1mg/ml and the reaction incubated at 37°C for 60 minutes. The reaction was extracted with an equal volume of phenol/chloroform and the phases separated by centrifugation for 20 minutes at 10000xg and 4°C. The DNA was recovered by addition of 0.1 volumes 2M sodium acetate pH 5.2 and one volume isopropanol and incubation at -20°C for at least one hour. The DNA was then purified by caesium chloride gradient.

2.1.8 Caesium chloride gradient purification

Large scale plasmid purification was carried out using a caesium chloride gradient (Sambrook, Fritsch et al. 1989). This purification method depends on the decrease in density of nucleic acids when bound to ethidium bromide. Because ethidium bromide binds by intercalation into the DNA, it causes unwinding of the helix. Closed circular DNA of a plasmid increases supercoiling so binding of ethidium bromide is limited and the plasmid has a higher buoyant density than linear or nicked plasmids. The difference in buoyant density allows separation of the plasmid on a caesium chloride density gradient.

Materials

TES: 50mM Tris-HCL (pH 8.0), 50mM NaCl, 5 mM EDTA in GDW (Appendix I)

Caesium chloride (Boehringer)

10mg/ml ethidium bromide (VWR)

Caesium chloride-saturated propan-2-ol (Appendix I)

Methods

DNA obtained from large scale plasmid purification was recovered by centrifugation for 20 minutes at 24,000xg and 4°C. The DNA was then dissolved in 8.20ml TES. Eight point four grams of caesium chloride were dissolved in the DNA solution and 200µl of ethidium bromide added and the solution shaken to disperse. The sample was divided into two polyallomer tubes (Ultracrimp, Du Pont), balanced, and overlaid with paraffin oil. The tubes were sealed and centrifuged for 16 hours at 20°C and 216,518xg (60,000rpm in a T-8100 rotor in a Sorvall 100SE centrifuge, Fisher Scientific).

After centrifugation, DNA bands were visualised by UV illumination and the band containing the closed pTR-CGW DNA removed using a 20-gauge needle and a 2ml syringe. Ethidium bromide was removed from the plasmid by repeated extraction with an equal volume of caesium chloride saturated isopropanol until both phases were colourless. The DNA was precipitated by addition of two volumes of GDW and six volumes of room temperature absolute ethanol. DNA was recovered by centrifugation at 24,000xg and 20°C for 20 minutes. The supernatant was poured off and the DNA pellet was dissolved in 0.4ml GDW, ethanol precipitated with 0.1 volume of sodium acetate and 2.5 volumes of absolute ethanol at -20°C for 60 minutes and recovered by centrifugation for 7 minutes at 13,000xg. The DNA was then air dried for 10 minutes and dissolved in 1ml GDW. GK-pTR-CGW was quantified by spectrophotometric measurement at a wavelength of 260nm. Negligible protein contamination was confirmed by a low absorbance at 280nm.

2.1.9 Plasmid digestion for dot blot and *in situ* hybridisation

GK-pTR-CGW plasmid was cut to produce a linear cDNA fragment that could be used for dot blot analysis and in situ hybridisation. Restriction endonucleases were used to digest the DNA fragments of interest as previously sequenced in 2.1.6.

Materials

GK-pTR-CGW (1.6mg/ml) and pTR-CGW (4.5mg/ml)

Restriction endonucleases: BamHI, PSTI (New England Biolabs)

10x Restriction buffer (appendix 1)

10x Bovine serum albumin (BSA) (New England Biolabs)

Phenol/chloroform pH8 (VWR)

2M Sodium acetate pH5.2 (appendix 1)

100% ethanol (VWR)

Methods

Samples were subjected to endonuclease digestion (as described in 2.1.2, without SAP). GK-pTR-CGW was digested by BamHI and PstI in separate reactions to produce antisense and sense probes, respectively. pTR-CGW containing WPRE, which was previously prepared by Dr Errol Richardson, was digested with BamHI and EcoRI. Products were diluted in GDW to a final concentration of 200ng/µl.

2.1.10 Quantification of total virus titre by dot-blot analysis

The concentration of rAAV depicts the level of transgene expression so the total particle number was determined by dot-blot analysis. Similar to northern and southern blotting techniques, dot-blot analysis measures RNA or DNA using a radio-labelled probe. Rather than being separated by size and transferred to a membrane, the sample being analysed is placed directly onto a membrane. Analysis of DNA by dot-blot is more accurate than other techniques such as RT-PCR in that a probe with a higher specificity can be used because the original genome sequence is used.

Materials

rAAV-GFP and rAAV-GKAS viral preparations

Solution A: 10mM Tris-HCl (pH 8.0), 1mM MgCl2 and 8U/ml DNase I in GDW (Appendix I)

Solution B: 10mM Tris-HCl (pH 8.0), 100mM NaCl, 10mM EDTA, 0.5% SDS and 1mg/ml proteinase K in GDW (Appendix I)

Phenol: chloroform: iso-amyl alcohol (pH 8.0) 25:24:1 (VWR)

5M Glycogen (5mg/ml) (Life Technologies)

100% Ethanol (VWR)

75% Ethanol

2M Sodium acetate (pH 5.2) (Appendix I)

Denaturing solution: 2M NaCl in 0.5M NaOH (Appendix I)

Neutralising solution (pH 7.5): 2M NaCl, 0.5M Tris-HCl (Appendix I)

pTR-CGW plasmid (4.5mg/ml)

Hybridisation buffer (Appendix I) 5mg/ml dried milk powder, 2.5mM EDTA, 0.25M Na phosphate buffer, 5% SDS and 25µM ATA in GDW (Appendix I)

Woodchuck post-transcriptional regulatory element (WPRE) cDNA fragment

5x ABC Buffer containing deoxynucleotides, random oligonucleotides and mercaptoethanol (Appendix I)

BSA, fraction V (10mg/ml) (Sigma)

(α-32P)-dCTP: 10Ci/ml, 3Ci/mol (Perkin Elmer)

DNA polymerase I, Klenow fragment (9U/µl) (GE Healthcare)

Sephadex G50 (Appendix I)

1x TE (pH 7.5) (Appendix I)

Amasino wash buffer: 1mM Na phosphate buffer (pH 7.2), 1mM EDTA and 2% SDS in GDW (Appendix I)

Universal wash buffer: 0.2% SDS and 0.02x SSPE in GDW (Appendix I)

Nylon filter paper (Hybond N+, GE healthcare)

Methods

Forty five microlitres of solution A were added to 5µl rAAV virus stock and incubated for thirty minutes at 37°C. Two hundred microlitres of solution B were added and the sample was incubated at 55°C for one hour. DNA was extracted by adding an equal volume of phenol/chloroform and the phases separated by centrifugation for three minutes at 13,000xg. The top phase containing the DNA was ethanol precipitated by adding 0.1 volumes sodium acetate, 40µg glycogen and 2.5 volumes ice cold 99.7-100% ethanol. After one hour at -20°C the solution was centrifuged for seven minutes at 8,000xg and 4°C and the supernatant discarded. The pellet was washed in 450µl 75% ice cold ethanol with centrifugation as before, supernatant removed and air-dried. The pellet was re-suspended in 10µl GDW and 1µl applied to a nylon membrane. A series of dilutions of the original plasmid pTR-CGW (50 to 0.1ng) were also applied to the membrane to act as a standard curve. The membrane was washed for five minutes in denaturing solution then washed twice for five minutes in neutralising solution. The membrane was then baked at 80°C for two hours. Pre-hybridisation was carried out by placing the membrane into a heat sealed polythene bag containing 10ml hybridisation buffer without probe. The membrane was incubated at 60°C for four hours.

A cDNA fragment of WPRE was used as a probe for rAAV transgenes. To radio-label the probe, 20ng of DNA in a total volume of 13µl of GDW were boiled for five minutes. After boiling, the solution was made up to a total volume of 25µl containing 1x ABC buffer, 2mg/ml BSA, 10µCi dCTP and 1U Klenow. The reaction was incubated at 37°C for at least one hour. Incorporation of radio-labelled nucleotide into the DNA probe was measured using a mini Sephadex G50 column. The column was prepared by plugging a glass Pasteur pipette with glass wool, and adding Sephadex G50. The labelling reaction volume was made up to 200µl 1x TE and loaded onto the column. The column was

then eluted with 1x TE and 200µl fractions collected. The fractions were counted and the percentage incorporation calculated. The hottest two fractions were pooled and half was boiled and added to 10ml hybridisation buffer. Hybridisation was carried out overnight at 60°C by emptying the pre-hybridisation buffer from the polythene bag, adding fresh buffer containing probe and resealing.

The following day the membrane was washed to remove any non-specifically bound probe. Three twenty minute washes at 60°C were carried out in amasino wash buffer followed by a further three twenty minute washes at 60°C in universal wash buffer. The filter was then sealed in a clean plastic bag and exposed to a storage phosphorimager screen (GE Healthcare) for two days. Radio-labelled areas were visualised and quantified by image densitometry using ImageQuant software (GE Healthcare). Quantification was performed by comparing viral DNA to known amounts of pTR-CGW in the standard curve.

2.1.11 *In vitro* transfection of GKAS pTR-CGW into cultured cells

The ability of GKAS plasmid to transfect mammalian cells was tested using a human hepatocellular carcinoma (HEPG2) cell line, which express large quantities of GK, by Dr E Richardson (Division of Women's Health, King's College London).

Materials

Human hepatocellular carcinoma (HEPG2) (ATCC)

Dulbeccos modified eagle medium (DMEM) (Invitrogen)

Foetal Bovine Serum, heat inactivated (FBS) (Invitrogen)

2.5% Trypsin in hanks balanced salt solution (Invitrogen)

Versene (appendix I)

2x HEPES-buffered saline (HBS) (appendix I)

2M calcium chloride (appendix I)

40µg/ml plasmid DNA in 0.1x TE

DMEM (Invitrogen)

Methods

HEPG2 cells were cultured in DMEM containing 4.5mg/ml glucose and 1mM sodium pyruvate supplemented with 10% (v/v) FBS at 37°C in 5% carbon dioxide. The medium was changed every three days and the cells sub-cultured when 70-80% confluent using 0.25% trypsin in versene. The medium was aspirated and cells incubated at 37°C for 5 minutes with fresh trypsin/versene until they detached from the flask. The trypsin was inactivated by the addition of 10ml of fresh medium and the cells recovered by centrifugation for 5 minutes at 100xg. The cells were resuspended in fresh medium and transferred to a new flask at a 1:10 dilution.

Cells at approximately 60% confluence were sub-cultured and plated at a density of $1x10^4$ cells/cm^2 in 90mm Petri dishes. The following day, the medium was replaced with fresh medium. A calcium phosphate co-precipitation was used to transfect large quantities of exogenous DNA. Briefly, a co-precipitate was formed by mixing 300µl 10xHBS with 28µg plasmid DNA in 2.5ml GDW and slowly adding 180µl 2M calcium chloride, while gently mixing using air expelled from a pipette aid. The solution was incubated at room temperature for 5 minutes to allow formation of the precipitate. The precipitate was added to the cells and they were incubated at 37°C in 5% carbon dioxide for 18 hours. The medium containing the precipitate was replaced with fresh media, cells were incubated for 48 hours after which time, cells were lysed in GK extraction buffer and a GK activity assay was performed as described below in 2.3.1.

2.2 Methods used for physiological and pharmacological measurement of glucose sensing in vivo

2.2.1 Animal maintenance

Male Wistar rats (specific pathogen free, Charles River UK Ltd) were maintained under a controlled environment (temperature 21-23°C, 12 hour light-dark cycle, lights on at 07:00) with *ad libitum* access to standard chow (RM1 diet, Special Diet Services UK Ltd), except where stated, and water. All animal procedures were approved under the British Home Office Animals (Scientific Procedures) Act 1986 (Project Licence no. 70/7229). Prior to all experiments animals were acclimatised to the Imperial College animal holding rooms for 7 days. Animals were pseudo-randomised to treatment and control groups of approximately equal mean and standard error of mean bodyweight.

2.2.2 Optimisation of successful stereotactic injection

Stereotactic micro-injection into the rat ARC is technically challenging as the structure is approximately $1mm^3$ each side of the third ventricle. Glucokinase mediates glucose homeostasis in other areas of the hypothalamus, namely the VMN adjacent to the ARC. Therefore, if rAAV-GKAS is delivered inaccurately, GK knockdown will occur in CNS areas other than, or as well as, the ARC. This will make the phenotype inconsistent and difficult to interpret. For this reason, stereotactic micro-injection was optimised with injection of Indian ink. This allowed improvements in technique and accuracy of micro-injection into the ARC until there was a bilateral accuracy rate of 85% or greater. Furthermore, after the following experiments requiring stereotactic surgery, accuracy of each injection was confirmed histologically. Animals that were not injected into the correct area were not included in the analysis.

2.2.3 Stereotactic injection of rAAV-GK antisense into the arcuate nucleus of rats

Recombinant AAV-GKAS (titre: $1.85x10^{13}$ genome particles/ml) (n=12 per group) or AAV-GFP (titre: $8.57x10^{13}$ genome particles/ml) was bilaterally injected into the ARC of male Wistar rats. GFP has previously been used as a marker of successful gene transfer in mammalian cells (Zhang, Gurtu et al. 1996).

Materials

Isoflurane (Abbott Laboratories Ltd)

Betadine (10% w/v povidine-iodine solution) (Seton Scholl Healthcare Ltd.)

rAAV-GFP (titre: 8.57x1013 genome particles/ml)

Amoxicillin powder for injection (500mg) (CP Pharmaceuticals)

Flucloxacillin powder for injection (500mg) (CP Pharmaceuticals)

0.9% NaCl (Braun Medical Ltd., Sheffield, UK)

Buprenorphine hydrochloride (Temgesic) (0.3mg/ml) (Schering-Plough Ltd.)

Internal cannula custom cut to length (Plastics One)

Guide cannula custom cut to length (Plastics One)

Method

Male Wistar rats of approximately 250g were anesthetised with 2L/minute oxygen and 4% isoflurane and held in a Kopf stereotactic frame. Under aseptic conditions, the surgical area was shaved then cleaned with betadine. A 1cm rostro-caudal incision was made in the skin over the vertex of the skull and the periosteum removed from the underlying bone to expose bregma. Using an electric drill, which was mounted onto the stereotactic frame, bilateral burr holes were drilled according to coordinates calculated previously and by using the 'The rat brain in stereotactic coordinates' (Franklin and Paxinos, 2007). The ARC coordinates were 3.4mm posterior to bregma, ±0.5mm lateral to bregma and 10.5mm below the skull surface. Each rat received an intra-ARC injection of 1µl both sides (n=12 per group). The injection was delivered over five minutes using a stainless steel injector and an infusion pump. The cannula and injector were left in position for five minutes to limit back-diffusion and then slowly withdrawn. The scalp incision was sutured with a 4.0 polypropylene suture (Ethicon).

After surgery, rats were placed in a warming chamber. Prophylactic flucloxacillin and amoxicillin (50mg/kg each) were administered intraperitoneally and 2.5ml 0.9% NaCl were given by intraperitoneal injection for rehydration. Analgesia was administered by subcutaneous injection of 0.12mg/kg buprenorphine hydrochloride at anaesthetic induction.

2.2.4 Stereotactic cannulation of the left arcuate nucleus in rats

Stereotactic cannulation of the ARC allows intra-nucleus injection of drugs directly into the arcuate in freely moving animals. This is particularly useful for acute feeding studies as food intake can be measured immediately after the injection.

Materials

Isoflurane (Abbott Laboratories Ltd)

Betadine (10% w/v povidine-iodine solution) (Seton Scholl Healthcare Ltd.)

Amoxicillin powder for injection (500mg) (CP Pharmaceuticals)

Flucloxacillin powder for injection (500mg) (CP Pharmaceuticals)

0.9% NaCl (Braun Medical Ltd.)

Buprenorphine hydrochloride (Temgesic) (0.3mg/ml) (Schering-Plough Ltd.)

Guide cannula custom cut to length (Plastics One)

Acrylic dental cement and powder (Kemdent)

Miniature 1.6 x 3 stainless steel screws (Montrose Fasteners)

Dummy cannula custom cut to length (Plastics One)

Methods

Animals were prepared and mounted onto a stereotactic frame as described previously. Anaesthetic, analgesia and antibiotics were administered as previously described. A hand drill was used to score three marks into the skull where stainless steel screws were lightly tightened to act as anchors. A unilateral burr hole was drilled according to coordinates calculated previously; 3.4mm posterior to bregma and -0.5mm lateral to bregma. A stainless steel cannulae held by an arm mounted onto the stereotactic frame was inserted 9.5mm below the skull surface. Dental acrylic was used to form a

pedestal fixing the cannulae into a stationary position with support from the mounting screws. This was left to dry and the scalp incision was sutured over the pedestal if necessary with a 4.0 polypropylene suture (Ethicon, Gargrave). A cap was screwed onto the cannula to prevent infection.

2.2.5 Feeding studies with genetically altered animals

Animals that were injected bilaterally into the ARC with rAAV-GKAS or rAAV-GFP were monitored for changes in chow intake and body weight three times per week for 33 days.

In some cohorts, glucose feeding studies were then performed. Appropriate concentrations of glucose solution were calculated previously. For acute studies, animals were acclimatised to a 2% (w/v) glucose solution provided *ad libitum* in pouches alongside the water bottles. After a period of at least 24 hours without glucose, animals were provided with 2% glucose, chow and water *ad libitum* from 19:00h. Glucose and chow intake was measured at 0, 1, 2, 4, 8, 12, 16 and 24 hours.

For chronic glucose feeding studies, animals were provided with 10% (w/v) glucose solution provided *ad libitum* in pouches alongside the water bottles. Body weight, glucose and chow intake was measured three times per week for 33 days. For both acute and chronic glucose feeding studies, total caloric intake was measured. Total energy intake was calculated using 14.75 kJ/g for RM1 diet (appendix II) and 16.0 kJ/g for glucose.

2.2.6 Twenty four hour feeding studies with intra-ARC injections

Unless stated otherwise, animals were fasted for two hours before injection and the animals were placed in a clean cage to ensure no food remained. Water was provided *ad libitum* in a bottle with a lick-type nozzle. For studies requiring measurement of 2% (w/v) glucose solution via a nozzle, water was provided via a smaller bottle situated in the food hopper. Animals were acclimatised to the glucose solution over approximately 72 hours, after which 24 hour feeding studies commenced twice per week for up to four weeks.

For studies involving CpdA, glibenclamide and diazoxide a single injection of 1µl was administered using an internal injector cut 1.0mm longer than the cannula to ensure microinjection into the left

arcuate nucleus. The injection was delivered over thirty seconds using an infusion pump. The injector was left in position for thirty seconds to limit back-diffusion and then withdrawn. The animal was placed back in its cage and provided with chow and glucose measurements initiated.

For studies involving calcium channel blockers, animals had two intra-nuclear injections fifteen minutes apart. Glucose measurements started after injection of the second substance.

For studies involving NPY antagonists, animals were given the first treatment by intraperitoneal injection of 100µl. The second treatment delivered by intra-nuclear injection was given after thirty minutes to give enough time for the circulation of the first treatment.

2.2.7 Collection of tissue samples

In all studies, unless otherwise stated in the methods, rats were euthanised in the early light phase by carbon dioxide asphyxiation followed by cervical dislocation.

Materials

Isopentane (Sigma)

Dry ice (BOC)

1.25% India ink (VWR)

4% paraformaldehyde diluted in 0.01M PBS (Appendix I)

30% sucrose solution (Appendix I)

Methods

For *in situ* hybridisation and glucokinase activity assay brains were rapidly removed after cervical dislocation and snap-frozen by immersion in ice cold isopentane on dry ice. Tissues were stored at -80°C.

For cresyl violet staining 1µl intra-arcuate injection of india ink was injected after euthanisation. Brains were then rapidly removed and fixed by placing into 4% formaldehyde solution for 24 hours. The tissue was then dehydrated in 30% sucrose solution for 3 days and snap-frozen by immersion in ice cold isopentane on dry ice.

2.3 Methods used for ex vivo measurement of glucose sensing

2.3.1 Glucokinase activity assay

The glucokinase activity assay measures production of NADPH in a two-step reaction. First, glucokinase catalyses the phosphorylation of glucose to G-6-P in the presence of ATP. Second, G-6-P dehydrogenase converts G-6-P to 6-phophate-D-gluconolactone and generates NADPH. The assay was modified from a previously reported G-6-P dehydrogenase assay to measure GK activity in small tissue samples (Goward, Hartwell et al. 1986).

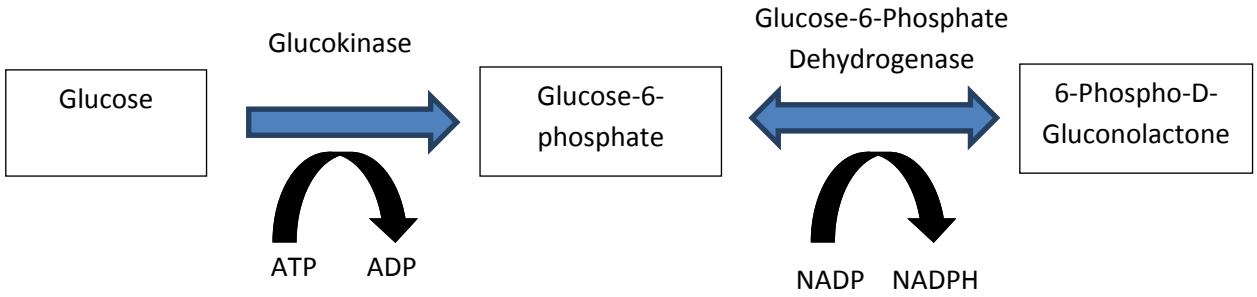


Figure 2.1 Schematic of the two step reaction in the GK activity assay.

Absorbance of NADPH is measured to calculate the concentration of NADPH produced in the reaction and therefore GK activity. Inhibitors of hexokinases are added to the reaction to ensure that only GK can catalyse the reaction. The advantage of this assay over previously used GK activity assays is that small amounts of tissue can be used. Measurement of GK from Bacillus stearothermophilus indicates that the assay has a high sensitivity even at very small concentrations of enzyme. In this study, glucokinase from rat hypothalamic nuclei were individually quantified and samples did not require pooling to increase sensitivity.

Materials

GK extraction buffer (Appendix I)

Micropunch needles (custom made 1mm diameter)

Cryostat (Bright)

Poly-D-lysine glass slides

Glucokinase from Bacillus stearothermophilus (0.25µg/ml)

Reaction Mix: (Appendix I)

Glycine buffer (50mM) (VWR)

5-Thio-D-glucose-6-phosphate (45µM) (Sigma)

$MgCl_2$ (7.5mM) (VWR)

ATP (10mM) (VWR)

NADP (0.75mM) (VWR)

Glucose (100mM) (VWR)

3-O-methyl-N-acetylglucosamine (0.5mM) (Enzo Life Science)

G-6-PD (type IX, from Baker's yeast) (1.25 units) (VWR)

Methods

Three hundred micrometre thick coronal sections of brain tissue was cut using a cryostat with a chamber temperature of -7°C and adhered using slight defrosting onto glass slides. Slides were kept on dry ice to keep frozen and the ARC, PVN and VMN were identified using a rat brain atlas (Paxinos & Watson, 1998) and removed using a micropunch needle and placed in separate microcentrifuge tubes. Nuclei were homogenised with a handheld homogeniser and 200µl extraction buffer added. The samples were centrifuged at 13,000 RPM at 4°C for 40 minutes. Fifty microlitres of each supernatant were added to 500µl reaction mix and incubated at 37°C for thirty minutes. Fifty microlitres of GK standard at a series of dilutions were simultaneously added to 500µl reaction mix to provide a standard curve. Samples were then placed into cuvettes.

Absorbance of each sample was read at 340nm using a spectrophotometer. Concentration of NADPH was calculated using the following equation:

Absorbance at 340nm (A) = Molar absorptivity of NADPH (ε) x Concentration (c) x length (l)

$A = 6.2x10^3\ Lmol^{-1}cm^{-1} \times c\ molL^{-1} \times 1\ cm$

GK concentration was calculated by extrapolating values with the standard curve. Samples were normalised to protein content using a Pierce bicinchoninic acid (BCA) assay. Twenty microlitres of each sample were incubated with 180µl extraction buffer and 500µl BioRad dye reagent for 5 minutes. Absorbance at 595nm was compared with known protein concentrations on a standard curve constructed using BSA. Samples were thus measured in units of GK activity per mg protein.

2.3.2 Production of radiolabelled RNA probes for *in situ* hybridisation

Single stranded mRNA probes significantly improve the sensitivity of examination of gene expression by *in situ* hybridisation (Cox, DeLeon et al. 1984). The RNA is complimentary to the gene of interest therefore uniquely binds to any endogenous mRNA. There are multiple ways to label a probe, including using nucleotides bound to different radioactive isotopes, digoxigenin, biotin and fluorescent markers. ^{35}S labelled radio-probes are considered the most sensitive method for brain sections (Wilcox 1993).

Materials

200ng/µl of linearised GK template (from section 2.1.9)

100M DTT (VWR)

RNase inhibitor RNase Out (40U/µl) (Invitrogen)

10x nucleotide mix (10mM of each ATP, UTP, GTP) (New England Biolabs)

T3 and T7 RNA polymerase (20U/µl) (Thermo Fisher Scientific)

5x RNA polymerase buffer (Promega)

[^{35}S]-CTPαS (46.2TBq/mmol, 2.6GBq/ml) (Perkin Elmer)

DNase 1 (2U/µl) (Thermo Fisher Scientific)

10x DNase buffer (Appendix I)

7.5M Ammonium acetate (Appendix I)

100% ethanol stored at -20°C (VWR)

Methods

RNA was radioactively labelled in a transcription reaction to act as a probe for ex vivo mRNA. Two hundred nanograms of template were added to an eppendorf containing 9.5µl GDW warmed to 37°C. To this the following was added in order: 1µl DTT, 1µl RNase inhibitor, 1µl NTP mix, 4µl 5x buffer, 0.5µl CTPαS, 1µl RNA polymerase. T3 polymerase was used to transcribe GK and WPRE antisense whereas T7 was used for GK and WPRE sense. The reaction was incubated for at least 2 hours at 37°C. Six microlitres of GDW, 1µl 10x DNase buffer and 3µl DNase 1 was then added followed by 15 minutes incubation. RNA was then precipitated by addition of ammonium acetate to a final concentration of 2.5M and 2.5 volumes of ice cold absolute ethanol. The mixture was left at -20°C for at least 1 hour. RNA was recovered by centrifugation at 8,000xg for 8 minutes and the pellet was dissolved in 200µl GDW. The level of the radioactively labelled probe was measured by sampling 1µl in triplicate in a microbeta liquid scintillation counter (Wallace). Probes were considered successfully transcribed when radioactive counts were above 200,000/µl.

2.3.3 *In situ* hybridisation for glucokinase and WPRE mRNA

In situ hybridisation is similar in technique to northern blot except that the tissues are not homogenised and the cellular structure of the tissue is preserved.

Materials

4% (v/v) formaldehyde in 0.01M phosphate buffered solution (Appendix I)

0.25% (v/v) acetic anhydride in 0.1M TEA pH8.0 (Appendix I)

20x SSC (Appendix I)

50, 70, 95 and 100% ethanol in GDW (VWR)

Chloroform (VWR)

De-ionised formamide (VWR)

5M sodium chloride (VWR)

1M Tris-HCl, pH 8.0 (VWR)

0.5M EDTA (VWR)

1M DTT (VWR)

10mg/ml Baker's yeast tRNA (VWR)

100x Denhart's solution (Appendix I)

50% (w/v) dextran sulphate (mw >500,000) in GDW at 60°C (Sigma)

1x RNase A (10g/ml) (Appendix I)

Biomax film (Kodak)

Developing solution (Jet X-Ray)

Fixing solution (Jet X-Ray)

Methods

Twelve micrometre brain sections were cut on a cryostat at -21°C (Bright Instrument Company), mounted onto poly-D-lysine coated slides and stored at -80°C until hybridisation. For *in situ* hybridisation, slides were allowed to thaw and fixed in 4% formaldehyde for 20 minutes on ice. Slides were washed twice in 0.01M PBS for 5 minutes and briefly in autoclaved GDW. Slides were acetylated in 0.25% acetic anhydride in 0.1M TEA for 10 minutes and washed twice in 0.01M PBS for 2 minutes. Slides were dehydrated in ascending concentrations of ethanol (50, 70, 95 and 100%) for 2 minutes each and delipidated in chloroform for 5 minutes. Finally, slides were slightly rehydrated in descending concentrations of ethanol (100 and 95%) for 2 minutes and allowed to air dry.

Hybridisation buffer was made by adding 1ml of 50% dextran sulphate to a 3ml solution containing final concentrations of 375mM NaCl, 31% (v/v) formamide, 0.5mg/ml tRNA, 1.25X Denhart's solution, 12.5mM Tris, 10mM DTT and 1.25mM EDTA. Individual probes for sense and antisense were added to make 1 million counts per 70µl. Seventy microlitres of hybridisation buffer were pipetted onto coverslips in a linear streak and were stuck onto the slides. At least one Sense slide was made to measure non-specific binding of the probe. Slides were incubated overnight at 60°C in slightly humid conditions in a water bath.

Coverslips were removed in 4 X SSC and slides washed a further 4 times in 4 X SSC for 5 minutes each. Slides were incubated in RNase solution containing 20mg/ml RNase A, 0.5M NaCl, 10mM Tris and 1mM EDTA for 30 minutes at 37°C. Stringency washes followed to remove incompletely bound probe. Slides were washed twice in 2 X SSC for 5 minutes, 1 X SSC for 10 minutes, 0.5 X SSC for 10 minutes and 0.1 X SSC for 30 minutes at 60°C. Slides were cooled in 0.1 X SSC, dehydrated in ascending concentrations of ethanol and allowed to completely dry. Slides were then placed into a photoplate cassette and exposed to chromatography paper for between 2-10 days. To develop, the paper was washed in developing solution until the slides appeared, rinsed briefly in water and fixed using fixing solution for at least 3 minutes. Slides could then be visualised on a light box or high resolution scanner.

2.3.5 Hypothalamic explant static incubation system

The static incubation system used was a modification of the method previously described to measure neurotransmitter release from hypothalamic explants in response to glucose or pharmacological agents (Dhillo, Small et al. 2002). It is a useful tool to investigate the response of basal hypothalamic neurones ex vivo. This method has the advantage that the neuropeptide response from explants can be compared to basal levels so act as their own controls. The limitations of this technique are that the saturation of 95% oxygen during the experiment is not sufficient to prevent cell death. Therefore the tissue under investigation is partially necrotic, particularly in the centre. As the ARC is situated on the outside of the tissue the damage may be limited. However to confirm that the explants still remained viable throughout the experiment, widespread neurotransmitter release was stimulated by potassium enriched aCSF. Only hypothalami that showed a 100% secretion over baseline in response to 56 mM KCl were used in the analysis.

Materials

Artificial CSF (appendix I)

Potassium enriched aCSF (Appendix I)

5% CO2/ 95% O2 (BOC)

30µM Glucokinase activator, CpdA (Merck)

100 µM Glibenclamide (Sigma)

200 µM Diazoxide (Sigma)

Methods

Male Wistar rats were killed by decapitation and the brain was immediately dissected. The brain was mounted with ventral surface uppermost and placed in a vibrating microtome (Microfield Scientific Ltd). The blade was adjusted until it abutted the median eminence and a 1.7mm slice was taken from the basal hypothalamus and cut lateral to the Circle of Willis to include the arcuate nucleus (Seal, Small et al. 2001). The hypothalamic slice was incubated in individual chambers containing 1 ml aCSF, equilibrated with 95% O_2 and 5% CO_2. The tubes were placed on a platform in a water bath maintained at 37°C. After an initial 2 hours equilibration period, the hypothalami were incubated for 45 min in 600µl aCSF (basal period) before being challenged with the test drug (test period) for 45 min. The viability of the tissue was verified by a final 45 min of exposure to aCSF containing 56 mM KCl; isotonicity was maintained by substituting K+ for Na+. Hypothalamic explants that failed to show peptide release above that of basal in response to aCSF containing 56 mM KCl were excluded from the data analysis. This was less than 10% of explants. At the end of each period, the aCSF was collected and stored at -20°C until measurement of NPY and α-MSH by radioimmunoassay.

2.3.6 Measurement of NPY and α-MSH in aCSF samples

Release of neuropeptides was measured by radioimmunoassay (RIA). The measurement of peptides by RIA relies on competition between radioactivity-labelled and unlabelled peptide for a specific binding site of an antibody. The amounts of antibody and labelled peptide are fixed; the only variable is the unlabelled peptide. The higher the concentration of unlabelled peptide, the less radioactively labelled peptide will be bound to the antibody. The bound and free peptide is separated by addition of dextran-coated charcoal which binds free antigen in the charcoal pellet. The activity in the bound and free components is measured in a γ counter and the data used to construct a standard curve.

Hypothalamic α-MSH –like immunoreactivity was calculated using a specific and sensitive in-house method and NPY –like immunoreactivity was calculated using a commercial kit from Bachem, San Carlos, USA. α-MSH was iodinated using the iodogen or Bolton and Hunter method by Professor Mohammed Ghatei and purified by HPLC (Wood, Wood et al. 1981). A label test was performed to

identify the best fraction. Standard curves for each assay were prepared using synthetic peptide. Dilution factors of samples were based on previous studies within this laboratory (Dhillo, Small et al. 2002).

2.3.6.1 α-MSH radioimmunoassay

Materials

0.06 M phosphate buffer (pH 7.2) containing 0.3% BSA (Appendix I)

125I labelled α-MSH (Produced by Prof M. Ghatei)

α-MSH standard peptide (Bachem)

Undiluted aCSF sample from hypothalamic explant

Rabbit anti- α-MSH antibody (1:120,000 dilution) (Chemicon International Inc.)

Sheep anti-rabbit antibody (Pharmacia & Upjohn, Sweden)

Methods

Three millilitre RIA tubes were labelled in RIA racks holding 128 tubes. Each assay began with duplicated tubes of; NSB (non-specific binding; without antibody), ½ x label, 2 x label, zeros (no sample), standard curve dilutions, zeros. All unknown samples were assayed in singlet separated by duplicated zeros every 24 samples. An additional standard curve was inserted at the end of the assay and finally duplicated excess antibody tubes. Each tube was made up to a total volume of 400µl buffered with phosphate buffer. The assay was incubated for 3 days at 4°C before separation of the free from antibody-bound label by sheep anti-rabbit antibody. These free and bound fractions were counted for 180 seconds in a gamma scintillation counter and sample concentrations were calculated using a data reduction programme (NE1600, NE Technology, UK). All samples were measured in one assay to avoid inter-assay variation.

2.3.6.2 NPY radioimmunoassay

Materials

0.06 M phosphate buffer (pH 7.2) containing 0.3% BSA

125I labelled NPY (Bachem, San Carlos, USA)

NPY standard peptide (Bachem, UK)

Undiluted aCSF sample from hypothalamic explant

Rabbit anti- NPY antibody (Bachem, San Carlos, USA)

Goat anti-rabbit antibody (Bachem, San Carlos, USA)

Methods

NPY-like immunoreactivity was measured using the same set-up described earlier. Each tube was made up to a total volume of 400µl buffered with phosphate buffer. The assay was incubated overnight at 4°C before separation of the free from antibody-bound label by goat anti-rabbit antibody. These free and bound fractions were counted for 180 seconds in a gamma scintillation counter and sample concentrations were calculated using a data reduction programme (NE1600, NE Technology, UK). All samples were measured in one assay to avoid inter-assay variation.

2.3.7 Cresyl violet staining of ink injected rat brains

Materials

Acetic acid (VWR)

Ethanol (VWR)

1% Cresyl violet stain (Appendix I)

Xylene (VWR)

DPX (Thermo Fisher Scientific)

Poly-D-lysine glass slides (VWR)

Methods

Rat brains were fixed onto a cold block and sliced with a Shandon sled microtome (Thermo Fisher Scientific). Forty micrometre coronal sections were cut and placed into wells containing anti-freeze. These were stored at -20°C until required. Sections were mounted onto glass slides and allowed to dry for at least four hours. Slides were fixed in a solution of 5% acetic acid in 100% ethanol, and then stained in cresyl violet for 15 minutes. Slides were washed twice in GDW, dehydrated in 70% ethanol and delipidated in xylene overnight. The following morning, slides were mounted with DPX and coverslips. Animals with ink more than 0.2mm outside the ARC when viewed under the microscope (Nikon, Eclipse 50i) were removed from subsequent analysis.

2.4 Statistical analysis

Results are displayed as mean and standard error of the mean (SEM) unless indicated. Generalised estimating equation (GEE) was used to compare cumulative data (namely body weight, chow, glucose and caloric intake) between control and treatment groups. GEE, based on generalised linear models, analyses longitudinal data and accounts for small variation in two groups that are time-dependently different. Individual data points were further analysed by Mann-Whitney post-hoc test where appropriate. Data from multiple groups for glucokinase activity assays and hypothalamic explant studies were analysed using one-way statistical analysis of variance (ANOVA) followed by post-hoc Holm-Sidak test. Data from multiple groups for Calcium channel and NPY receptor experiments were analysed using one-way ANOVA followed by post-hoc Holm-Sidak test for specific columns. A paired Student's t-test was used to compare absolute food and glucose intake data from cross-over studies. An unpaired Student's t-test was used to compare all other data. Significance was set at $P<0.05$ unless indicated otherwise. Data analysis was performed using Graphpad Prism 6.05 software (Graphpad Software, Inc.) except for GEE, which was performed using Stata 9 software (Stata).

Chapter 3: The effect of altered ARC glucokinase activity on glucose intake

3.1 Introduction

Energy homeostasis is regulated by an array of neuronal circuits that control food intake and energy expenditure (Schwartz, Woods et al. 2000). Glucose sensing neurones play an integral role in allowing the brain to detect glucose levels (Anand, Chhina et al. 1964). These neurones are important for maintaining glucose homeostasis by regulation of downstream peripheral mechanisms and food intake (Dunn-Meynell, Sanders et al. 2009, Levin, Magnan et al. 2011). While the contribution of glucose sensing neurones in responding to hypoglycaemia is well known, their role in regulating food intake and body weight remains poorly understood.

3.1.1 The glucostatic control of food intake

Over 60 years ago, Mayer's "glucostatic theory" suggested that changes in blood glucose are detected by the brain to alter hunger signals (Mayer 1953). It has since been demonstrated that alterations in CNS glucose concentration affects food intake. ICV injection of glucose decreases food intake in rats (Panksepp and Rossi 1981, Kurata, Fujimoto et al. 1986). ICV injection of 2-DG, an analogue of glucose that cannot undergo glycolysis, increases food intake (Tsujii and Bray 1990). The effects on food intake is specific to glucose, as ICV of glucose epimers such as D-mannose and D-galactose do not have any effect on food intake (Kurata, Fujimoto et al. 1986). Also, ICV fructose, which is not metabolised by GK, increases food intake (Miller, Martin et al. 2002). These studies implicate sensors of CSF glucose levels as mediators of appetite.

3.1.2 Glucokinase and food intake

Glucokinase is the primary enzyme that glucose sensing neurones use for translating glucose levels into neuronal signals. Neurones within the ARC exert a powerful effect on food intake as demonstrated by the potent effects of leptin and other metabolic signals (Cone, Cowley et al. 2001). GK activity in the ARC is also regulated by altered ambient glucose levels (Hussain, Richardson et al. 2014). Fasting increases GK activity in the ARC, but not in the VMN (Hussain, Richardson et al. 2014). However, GK mRNA expression in the VMN is

increased when challenged with insulin-induced hypoglycaemia (Kang, Sanders et al. 2008). It is likely that specific populations of neurones in the CNS are responsible for controlling particular aspects of glucose sensing and any physiological response. This is in contrast to other areas of glucose sensing; pancreatic GK levels remain unperturbed by altered glucose levels (Iynedjian, Pilot et al. 1989).

Differences in nutrient availability between neurones in the VMN and ARC have already been described (Wang, Liu et al. 2004, Mullier, Bouret et al. 2010, Langlet, Levin et al. 2013). In addition, a robust network of neurones controlling the CRR to hypoglycaemia has been demonstrated across the VMN, brainstem and medial amygdala nucleus (Kang, Routh et al. 2004, Dunn-Meynell, Sanders et al. 2009, Zhou, Podolsky et al. 2010). However, the role of CNS glucose sensing in influencing daily food intake remains to be investigated.

3.1.3 Techniques used to alter glucokinase *in vivo*

In order to investigate the role of ARC glucose sensing on food intake, approaches to alter the intracellular mechanisms of glucose sensing neurones can be used. Mice with homozygous or heterozygous deletion for the GK gene are diabetic, due to the combined effects of decreased GK in the liver, pancreas and CNS (Grupe, Hultgren et al. 1995, Baker, Atkinson et al. 2014). As gene expression is affected throughout the prenatal and growth stages of the animal in these models, it is possible that compensatory mechanisms can affect their phenotype. Therefore, the phenotypes may not represent the physiological role of GK in these models. An alternative approach is to develop transgenic mice with a 'floxed' GK gene to restrict genetic modification to a particular tissue or region, for example in the ARC. Stereotactic injection of rAAV containing Cre recombinase into the ARC ensures knockdown of GK is restricted to the area surrounding the injection site. This technique is more appropriate for investigating the specific role of ARC GK on the regulation of food intake. However, due to the difficulty in targeting the small mouse ARC, and in order to compare with previous studies of GK overexpression in rats, a model of glucokinase knockdown in rats is used in the present study. Transgenic alterations in rats are not widely used so a GK 'floxed' rat is currently unavailable.

As discussed in chapter 1, AAV2 is an effective vector for gene delivery to neurones (Howard, Powers et al. 2008). Maximal viral infection occurs at approximately 21 days in rodents and can last for at least 50 days (Hussain, Richardson et al. 2014). Recombinant AAV containing GK has previously been used to demonstrate selective overexpression of GK in the ARC of rats (Hussain, Richardson et al. 2014). In order to selectively decrease ARC GK expression in rats, rAAV containing antisense RNA can be injected to create long term expression of a molecule with sequence complimentary to that of the endogenous mRNA. Antisense RNA interferes with gene expression by hybridising to the mRNA sequence and disabling its translation (Kumar and Carmichael 1997). In the present chapter I utilise antisense technology to inhibit endogenous GK expression *in vivo*. Recombinant AAV containing GK antisense (rAAV-GKAS) was produced using the two-plasmid system as described previously (Grimm, Kern et al. 1999, Gardiner, Kong et al. 2005).

In summary, ARC GK is hypothesised to regulate food intake. However, the exact role of GK in controlling glucose homeostasis has not been elucidated in the ARC and requires further investigation. Previous work within this laboratory has shown that chronic overexpression of ARC GK results in increased food intake and body weight gain (Hussain, Richardson et al. 2014). The work in this chapter will build on this previous finding by investigating the effects of altered ARC GK activity using two different approaches. The first will be to acutely increase ARC GK activity using a pharmacological activator, and the second will be to chronically knock down ARC GK using rAAV encoding for GK antisense.

3.2 Hypothesis and Aims

3.2.1 Hypothesis

Acute activation of ARC GK will result in an increase in glucose-specific appetite, similar to previous findings, which chronically overexpressed ARC GK. In contrast, chronic reduction of ARC GK will result in a decrease in glucose-specific appetite, when measured in both an acute and cumulative setting.

3.2.2 Aims

To investigate my hypothesis I will:

1. Identify endogenous GK expression in the ARC of rats using *in situ* hybridisation.
2. Inject the pharmacological activator compound A into the ARC of rats via stereotactically inserted cannula, to investigate the effect of increased GK activity on short term food intake.
3. Investigate altered preference for glucose in rats with increased ARC GK activity, by providing them with standard chow and glucose solution.
4. Stereotactically inject rAAV-GK antisense into the ARC of rats, and confirm knockdown in the ARC.
5. Investigate the acute effects of ARC GK knockdown, by measuring 24 hour glucose intake.
6. Investigate the long-term effects of ARC GK knockdown, by measuring food intake, body weight and long-term glucose intake.

3.3 Results

3.3.1 Localisation of GK expression in the hypothalamus

In situ hybridisation was performed on coronal sections from wild-type rats provided with *ad libitum* standard chow. Expression of GK mRNA was observed in the VMN, ARC and MAN (figure 3.1a). Expression was not due to non-specific binding of the radio-labelled probe (figure 3.1b).

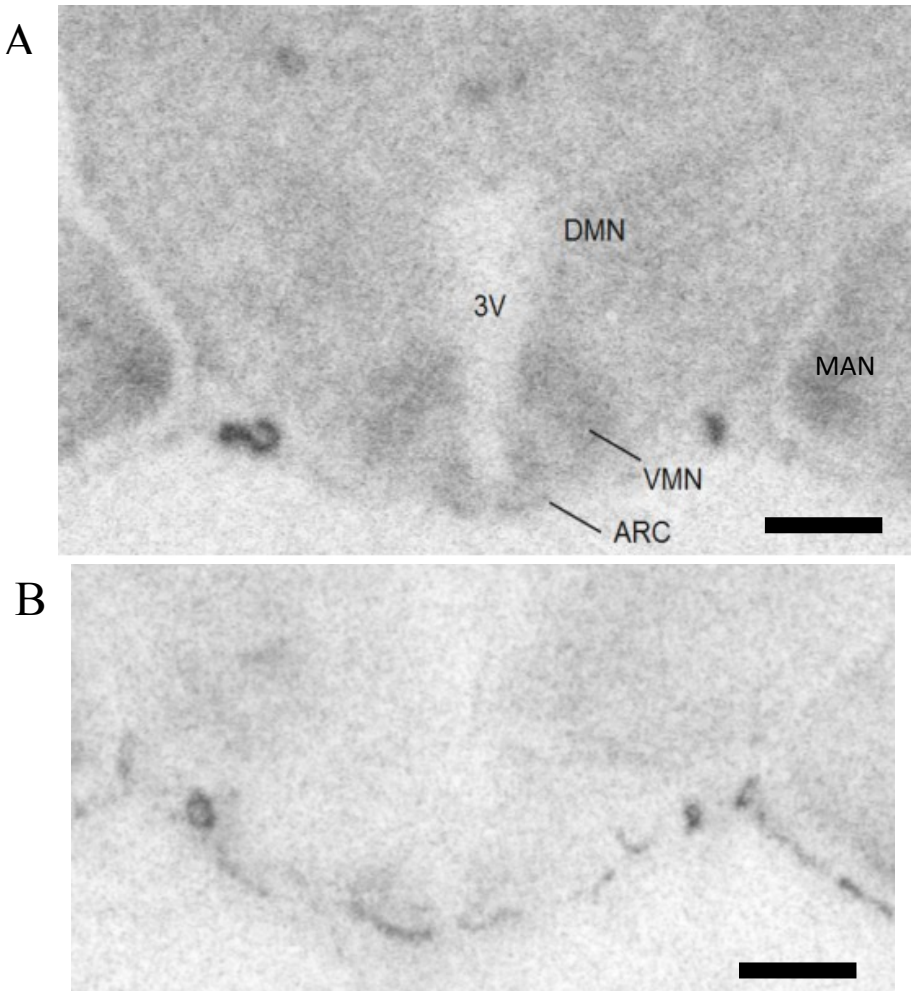


Figure 3.1 Endogenous GK mRNA expression in the rat hypothalamus. *In situ* hybridisation with: (A) GK antisense-labelled probe, (B) GK sense-labelled probe in 12µm coronal sections at -3.3 mm from bregma at 4x magnification. Abbreviations: 3v, third ventricle; ARC, arcuate nucleus; VMN, ventromedial nucleus; DMN, dorsal medial nucleus; MAN, medial amygdala nucleus. Black bars indicate 1mm length.

3.3.2 Effect of pharmacologically increasing ARC GK activity on chow and glucose intake

ARC GK activity was increased acutely using the glucokinase activator CpdA (Kamata, Mitsuya et al. 2004). Following injection, rats were allowed access to either; chow alone, a 2% (w/v) glucose solution alone, or both chow and glucose. Acute activation of ARC GK caused a significant increase in chow intake when chow was presented alone during the first hour, compared with vehicle injected controls (control, 0.38±0.13g; CpdA, 1.07±0.27g; n=10 per group, p <0.05) (figure 3.2a). This increase in chow intake was observed over 8 hours from injection but was not statistically significant beyond the first hour (after 8 hours: control, 3.17±0.64g; CpdA, 4.47±0.90g, n=8 per group, p =0.25) (figure 3.2b). Acute activation of ARC GK also caused a significant increase in glucose intake when glucose was presented alone, during the first hour compared with vehicle injected controls (control, 4.56±1.00g; CpdA, 8.36±1.24g, n=8 per group, p <0.05) (figure 3.3a). Glucose intake was significantly increased over 8 hours (control, 5.83±1.16g; CpdA, 11.2±1.64g, n=8 per group, p <0.05) (figure 3.3b). When both chow and glucose were available, only glucose intake was significantly increased during the first hour (control, 3.06±1.12g; CpdA, 7.70±1.55g; n=7 per group, p <0.05) (figure 3.4a). There was no change in chow intake during the first hour (control, 1.68±0.43g; 1.43±0.70g, n=7 per group) (3.4b). The increase in glucose intake was maintained over eight hours but was not statistically significant (control, 6.10±2.39g; CpdA, 10.6±2.64g, n=7 per group, p =0.23) (figure 3.4c). There was no change in chow intake over 8 hours (control, 6.50±1.30g; CpdA, 5.81±0.89g, n=7 per group) (figure 3.4d).

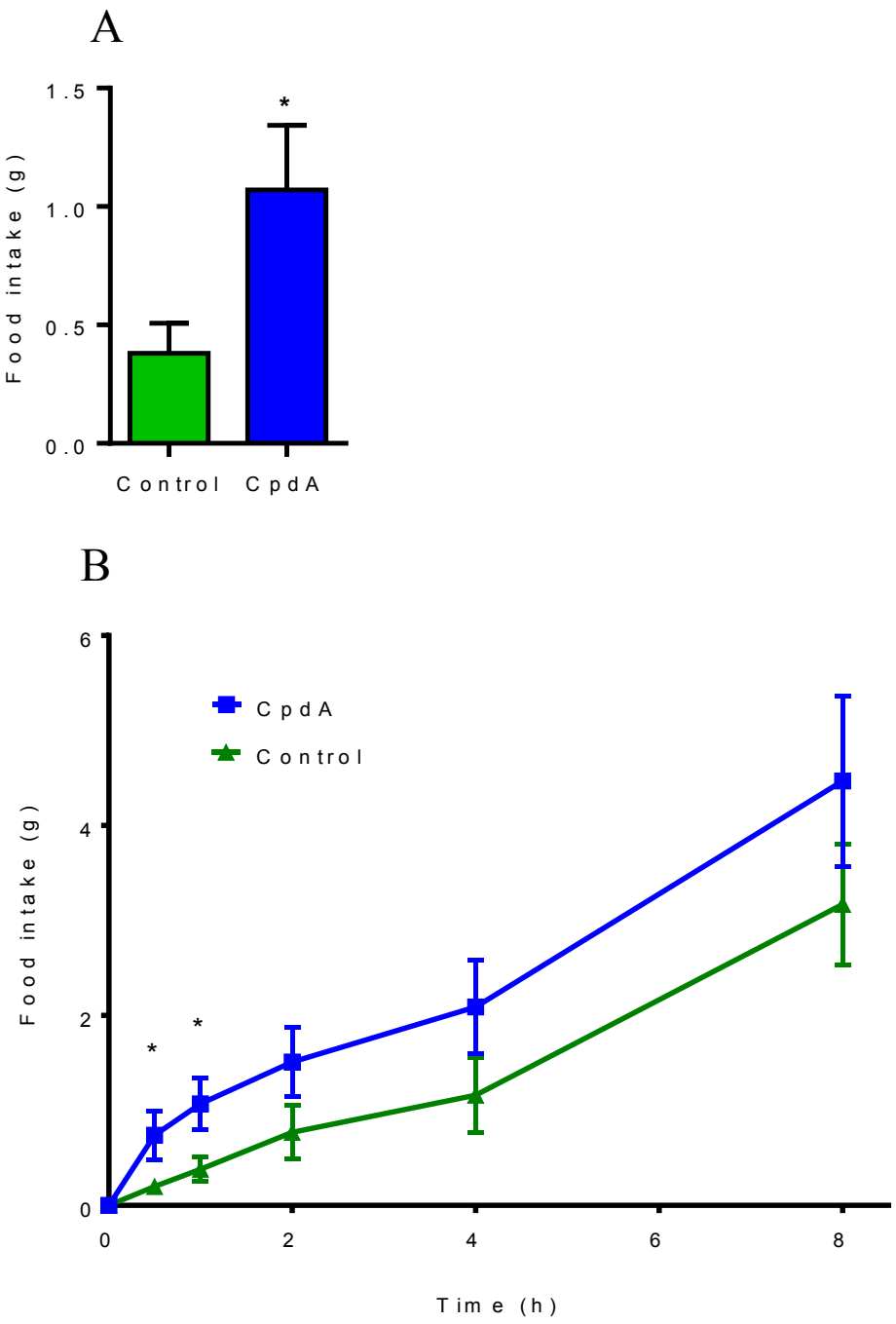


Figure 3.2 Effect of increasing ARC GK activity on food intake. (A) Food intake one hour after ARC GK activation using stereotactic injection of 0.5 nmol CpdA as compared to the vehicle injected controls during a crossover study. (B) Eight hour food intake after ARC GK activation using stereotactic injection of 0.5 nmol CpdA as compared to the vehicle injected controls during a crossover study. Data are presented as mean±SEM, n=10 per group. Statistical significance was analysed by paired Student's t-test: *= p <0.05.

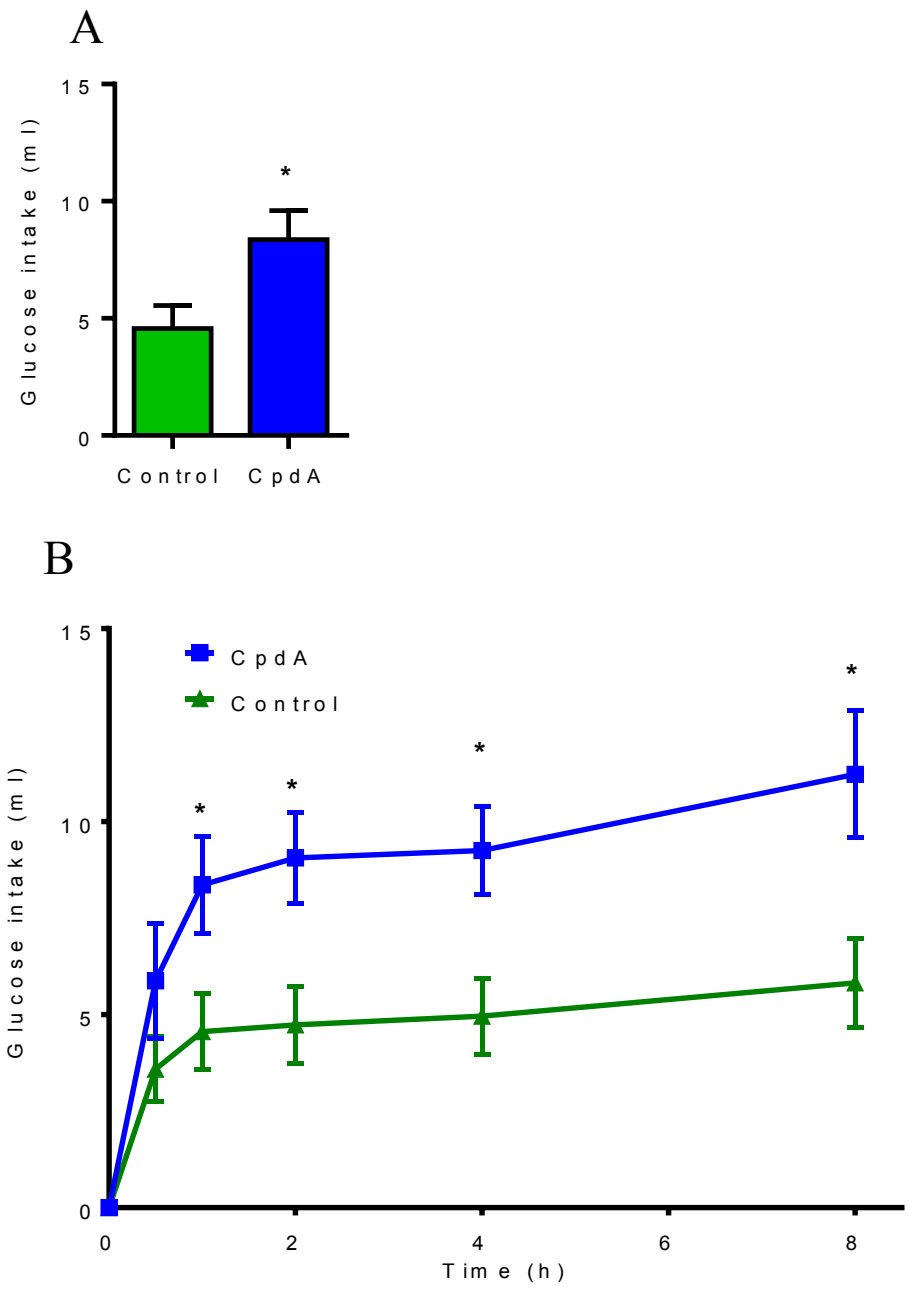


Figure 3.3 Effect of increasing ARC GK activity on 2% glucose intake. (A) Glucose intake one hour after ARC GK activation using stereotactic injection of 0.5 nmol CpdA as compared to the vehicle injected controls during a crossover study. (B) Eight hour glucose intake after ARC GK activation using stereotactic injection of 0.5 nmol CpdA as compared to the vehicle injected controls during a crossover study. Data are presented as mean±SEM, n=8 per group. Statistical significance was analysed by Student's t-test: *= p <0.05.

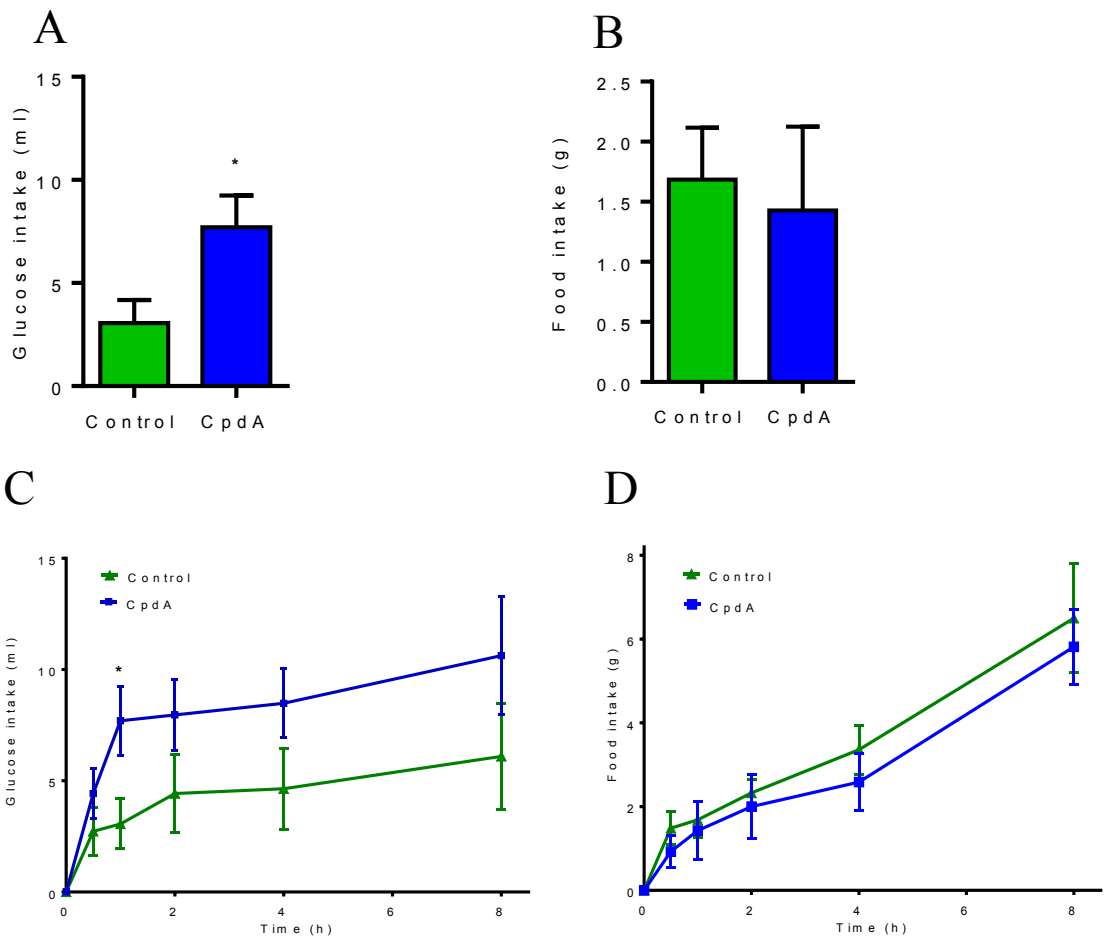


Figure 3.4 Effect of increasing ARC GK activity on chow and 2% glucose intake. (A) Glucose and (B) chow intake one hour after ARC GK activation using stereotactic injection of 0.5 nmol CpdA as compared to the vehicle injected controls during a crossover study. (C) Eight hour glucose and (D) chow intake after ARC GK activation using stereotactic injection of 0.5 nmol CpdA as compared to the vehicle injected controls during a crossover study. Data are presented as mean±SEM, n=7 per group. Statistical significance was analysed by Student's t-test: *= p <0.05.

3.3.3 Visualisation of accurate ARC injection

Permanent cannulas were stereotactically implanted 1mm above the ARC of rats (figure 3.5). Pharmacological agents could be injected directly into the ARC via a 1mm projection beyond the implanted cannula. Only animals that had correct cannula placements were included in the analysis.

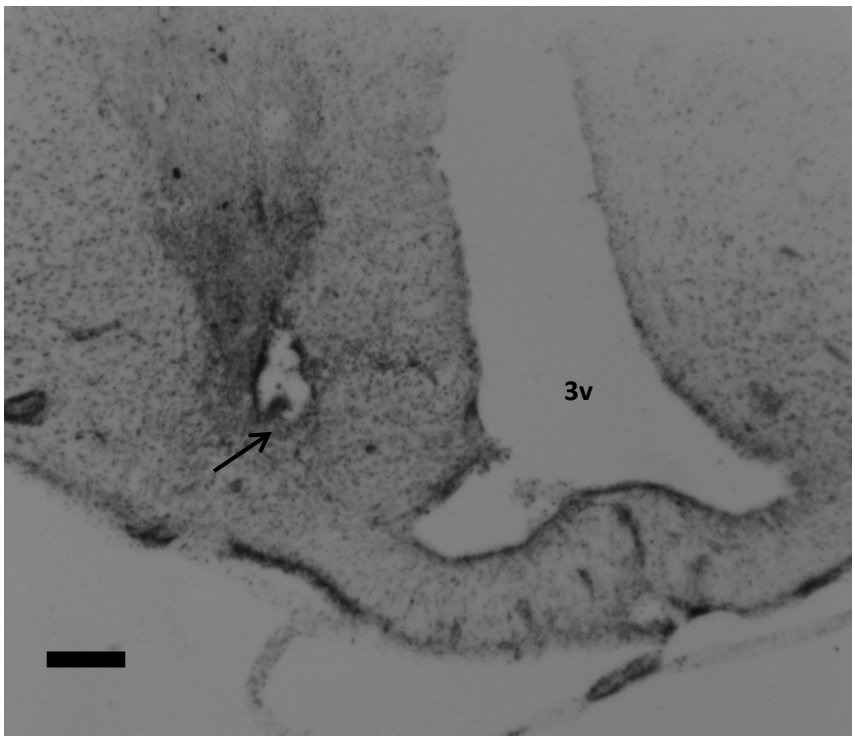


Figure 3.5 Confirmation of cannula placement in rats cannulated into the ARC. Cresyl-violet stained 30µm sections at 100x magnification showing edge of guide cannula (arrow) in a representative animal. Administered solutions are delivered into the ARC via an injector projecting 1mm from the end of the cannula. 3v, third ventricle. Bar = 100µm.

3.3.4 Measurement of total viral titre by dot blot analysis

The total virus titres for rAAV encoding GK antisense (rAAV-GKAS) and rAAV encoding enhanced green fluorescent protein (rAAV-GFP) were $1.85x10^{13}$ and $8.57x10^{13}$ genome particles/ml respectively.

3.3.5 Quantification of GK knockdown *in vitro*

Transfection of HEPG2 cells with GKAS-containing plasmid resulted in decreased GK activity in lysates compared to pTR-CGW transfected controls (control, 0.31 ± 0.024 units/mg protein; GKAS, 0.19 ± 0.011 units/mg protein, n=4 per group, p <0.05) (figure 3.6).

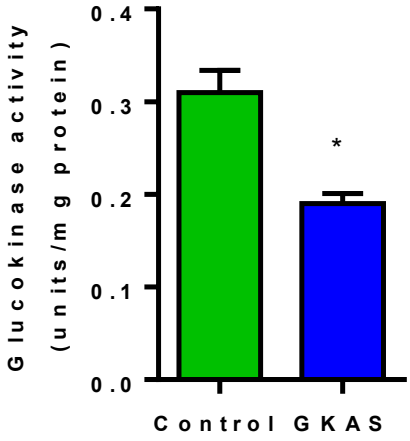


Figure 3.6 **Effect of *in vitro* GKAS-pTR-CGW plasmid transfection on GK activity:** GK activity in HEPG2 cells 48hr after transfection with either GKAS-pTR-CGW plasmid (blue bar) or pTR-CGW plasmid (green bar). Data presented as mean±SEM, n=4 per group. Statistical significance was analysed by Student's t-test: * p <0.05 versus corresponding control values.

3.3.6 Quantification of knockdown of ARC GK *in vivo*

Recombinant AAV encoding for GKAS was stereotactically injected into the ARC of rats. To ensure that the reduction in GK activity was exclusive to the ARC and that the VMN was not affected, GK activity was quantified. Animals were killed 11 weeks after stereotactic injection of either rAAV-GKAS or rAAV-GFP and GK activity was measured in the ARC, VMN and PVN of animals. There was a significant decrease in GK activity in the ARC in rAAV-GKAS injected animals compared with controls (iARC-GFP, 9.82±0.42U/mg; iARC-GKAS, 4.08±0.74U/mg; n=9-11 per group, p <0.001) (figure 3.7). There was no difference in GK activity in either the VMN (iARC-GFP, 7.13±0.19U/mg; iARC-GKAS, 6.628±0.82U/mg; n=9-11 per group) or PVN (iARC-GFP, 6.14±0.44U/mg; iARC-GKAS, 5.89±0.46U/mg; n=9-11 per group) between the two groups (figure 3.7).

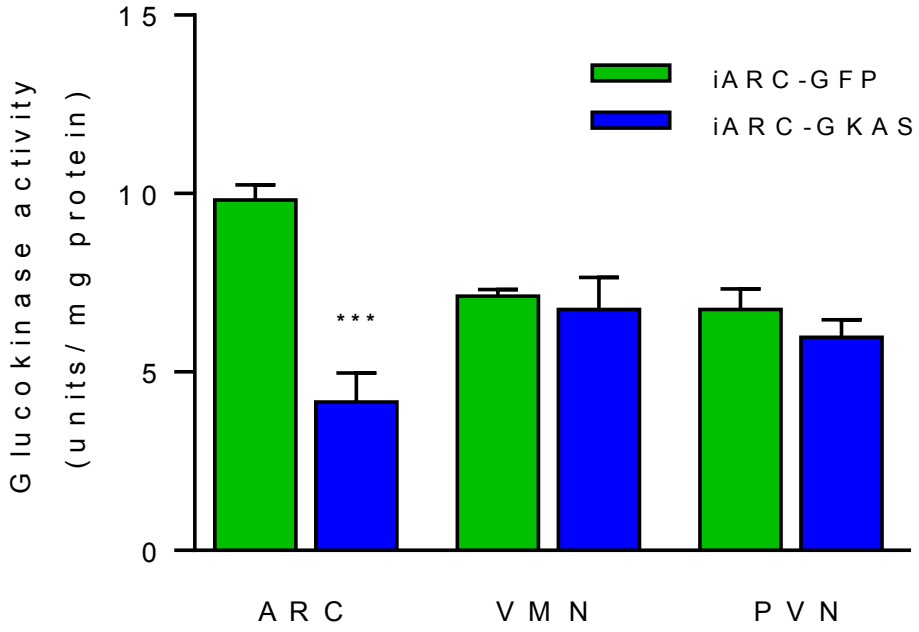


Figure 3.7 Confirmation of GK knockdown by activity assay. Glucokinase activity in the arcuate nucleus (ARC), ventromedial nucleus (VMN) and paraventricular nucleus (PVN) of male Wistar rats following intra-ARC injection of either rAAV-GFP (iARC-GFP) or rAAV-GK antisense (iARC-GKAS). Data presented as mean±SEM, n=9-11 per group. Statistical significance was analysed by ANOVA with post-hoc Holm-Sidak test *** p <0.001 versus corresponding control values.

3.3.7 Effect of ARC GK knockdown on body weight

Rats were maintained on a diet of standard chow for 33 days after recovery from rAAV injections. Knockdown of ARC GK slightly, but not significantly reduced body weight gain compared to controls (iARC-GFP, 153.9±6.06g; iARC-GKAS, 143.2±6.95g; *p* =0.37, n=9-11 per group) (figure 3.8).

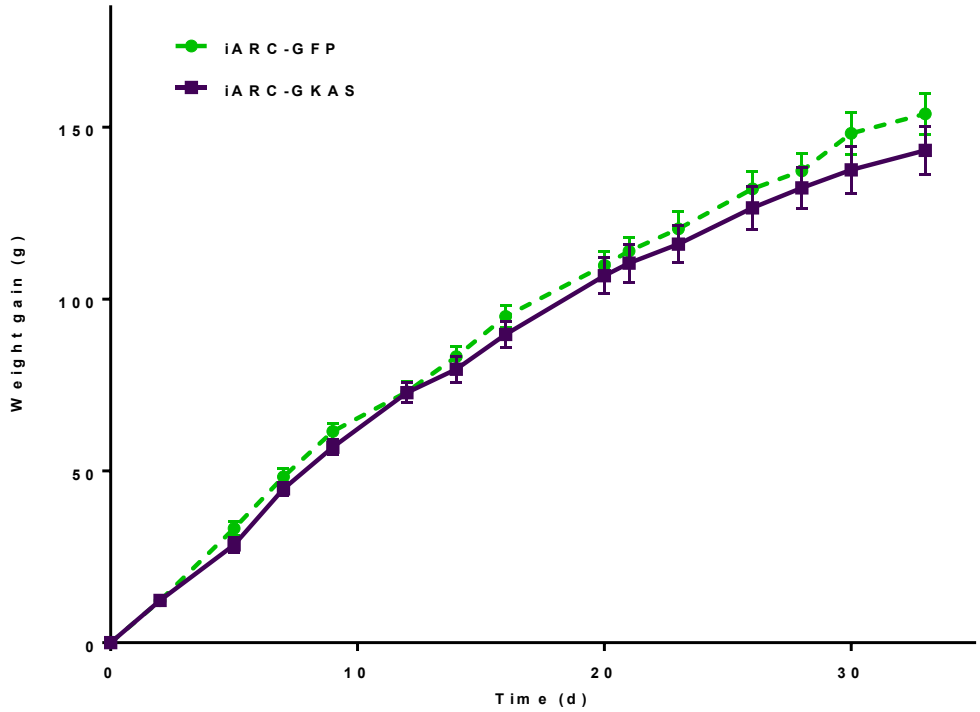


Figure 3.8 Effect of decreasing ARC GK on body weight. Cumulative body weight following intra-ARC injection of either rAAV-GFP (iARC-GFP) or rAAV-GK antisense (iARC-GKAS) (n=9-11 per group). Data presented as mean±SEM. Statistical significance was analysed by GEE.

3.3.8 Effect of ARC GK knockdown on food intake

Thirty three days after recovery from surgery there was a slight but non-significant decrease in chow intake compared with control rats (iARC-GFP, 1039.3±17.9; iARC-GKAS, 994.2±14.1g; n=9-11 per group, *p* =0.0747) (figure 3.9).

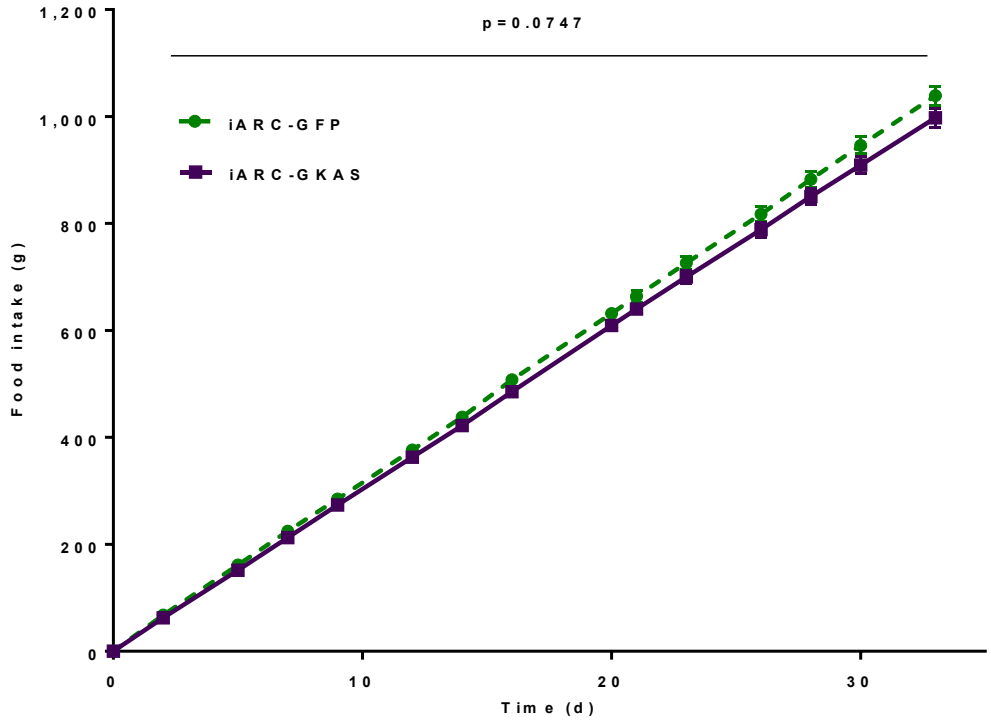


Figure 3.9 Effect of decreasing ARC GK on food intake. Cumulative chow intake when provided *ad libitum* following intra-ARC injection of either rAAV-GFP (iARC-GFP) or rAAV-GK antisense (iARC-GKAS) (n=9-11 per group) Data presented as mean±SEM. Statistical significance was analysed by GEE.

3.3.9 Effect of ARC GK knockdown on acute glucose intake

Forty days after surgery, *ad libitum* glucose and chow intake were measured for 24 hours from the start of the dark period. Knockdown of ARC GK resulted in a significant decrease in cumulative glucose intake from 2 to 24 hours, compared to control rats (at 24 hours: iARC-GFP, 72.4±6.79g; iARC-GKAS, 46.8±4.01g; n=8-9 per group, p <0.05) (figure 3.10a). However there was no significant difference in chow intake (at 24 hours: iARC-GFP, 30.6±0.78g; iARC-GKAS, 32.4±1.14g; n=8-9 per group) (figure 3.10b). There was no significant difference in total energy intake between GK antisense or control injected rats (at 24 hours: iARC-GFP, 477.0±19.4kJ; iARC-GKAS, 494.1±17.2kJ, n=8-9 per group) (figure 3.10c).

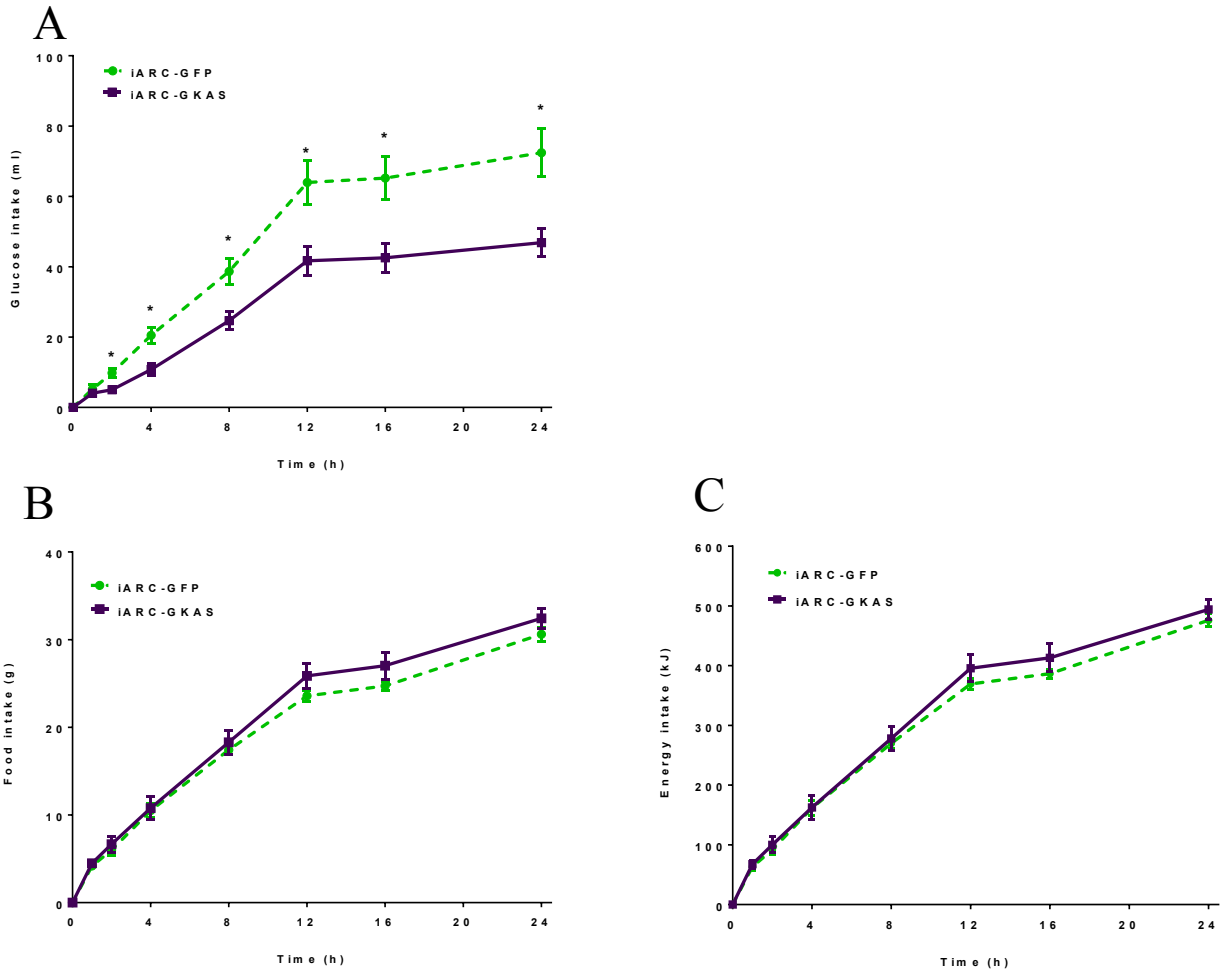


Figure 3.10 Effect of decreasing ARC GK on acute glucose and chow intake. Cumulative (A) 2% glucose intake, (B) chow intake and (C) caloric intake when provided *ad libitum* for 24 hours, 40 days after intra-ARC injection of either rAAV-GFP (iARC-GFP) or rAAV-GK antisense (iARC-GKAS) (n=8-9). Data presented as mean±SEM. Statistical significance was analysed by GEE with Mann-Whitney post-hoc test * p <0.05 versus corresponding control values.

3.3.10 Effect of ARC GK knockdown on cumulative glucose intake

Standard chow and 10% (w/v) glucose intake were measured for 33 days, 44 days after stereotactic injection of either rAAV-GKAS or rAAV-GFP. ARC GK knockdown resulted in a significant decrease in cumulative glucose consumption compared to controls (after 33 days: iARC-GFP, 3675±174ml; iARC-GKAS, 3090±264ml; n=9-11 per group, p <0.05) (figure 3.11). There was no significant difference in chow intake (after 33 days: iARC-GFP, 684.8±21.2g; iARC-GKAS, 711.5±22.2g; n=9-11 per group) (figure 3.12). There was no significant difference in total energy intake (after 33 days: iARC-GFP, 16.82±0.37MJ; iARC-GKAS, 16.36±0.49MJ; n=9-11 per group) (figure 3.13). There was also no significant difference in body weight gain when the animals were challenged with a high glucose diet (after 33 days: iARC-GFP, 66.6±3.3g; iARC-GKAS, 71.4±6.1g; n=9-11 per group) (figure 3.14).

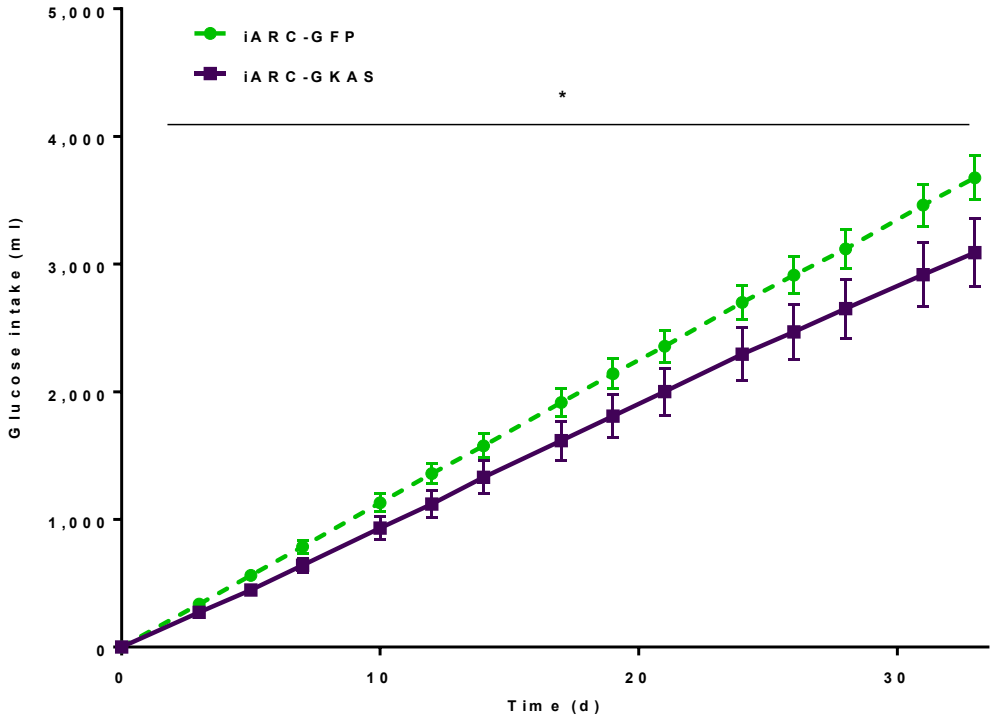


Figure 3.11 Effect of decreasing ARC GK on glucose intake. Cumulative 10% glucose intake when provided *ad libitum* with chow 44 days after intra-ARC injection of either rAAV-GFP (iARC-GFP) or rAAV-GK antisense (iARC-GKAS) (n=9-11). Data presented as mean±SEM. Statistical significance was analysed by GEE * p <0.05 versus corresponding control values.

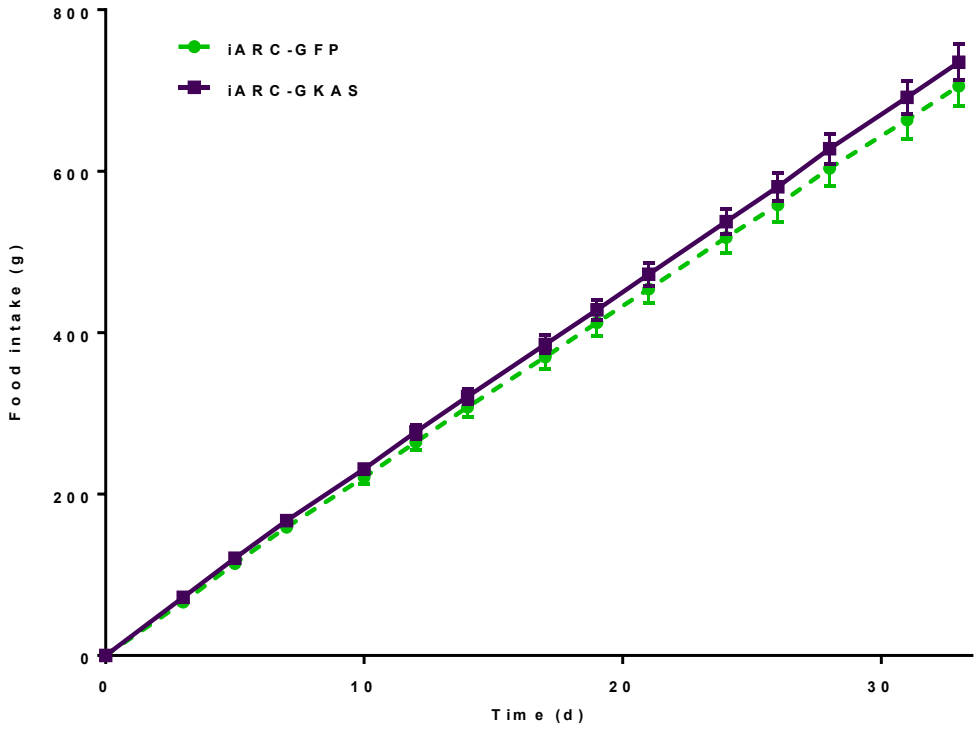


Figure 3.12 Effect of decreasing ARC GK on food intake. Cumulative chow intake when provided *ad libitum* with 10% glucose 44 days after intra-ARC injection of either rAAV-GFP (iARC-GFP) or rAAV-GK antisense (iARC-GKAS) (n=9-11 per group). Data presented as mean±SEM.

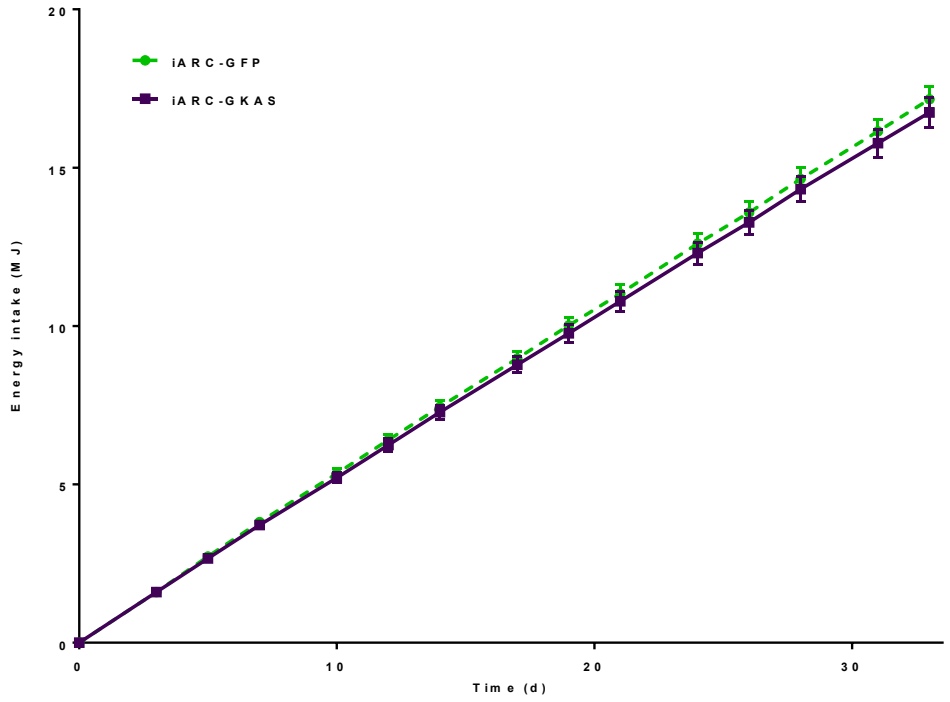


Figure 3.13 Effect of decreasing ARC GK on energy intake. Cumulative total energy intake when provided with 10% glucose and chow *ad libitum* 44 days after intra-ARC injection of either rAAV-GFP (iARC-GFP) or rAAV-GK antisense (iARC-GKAS) (n=9-11 per group). Data presented as mean±SEM.

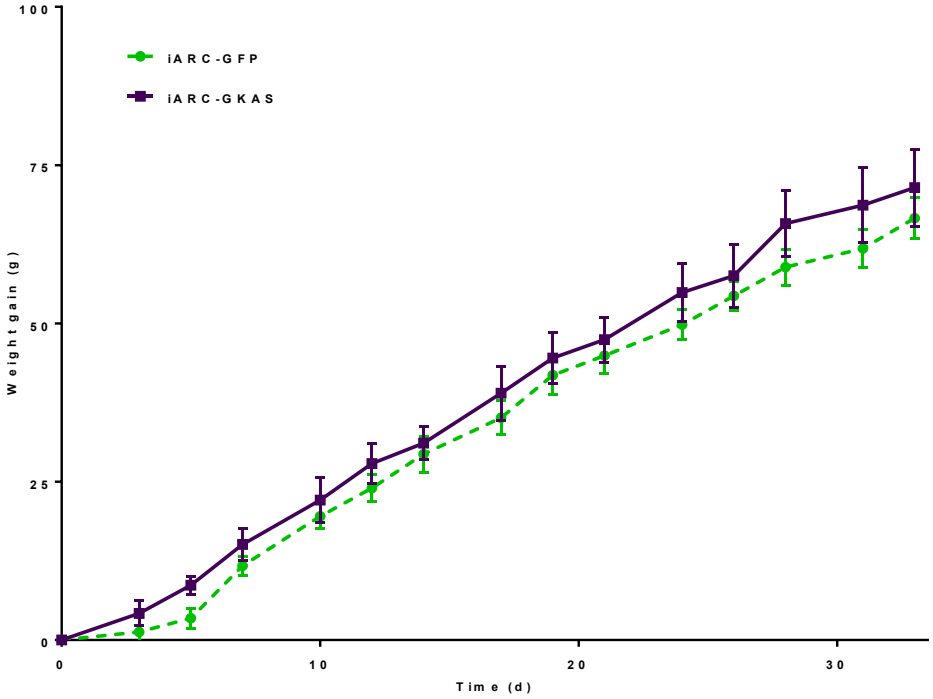


Figure 3.14 Effect of decreasing ARC GK on body weight. Body weight gain when provided with *ad libitum* chow and 10% glucose 44 days after intra-ARC injection of either rAAV-GFP (iARC-GFP) or rAAV-GK antisense (iARC-GKAS) (n=9-11 per group). Data presented as mean±SEM.

3.4 Discussion

3.4.1 Endogenous expression of GK in the rat hypothalamus

In situ hybridisation revealed that GK is expressed in the ARC, VMN and the MAN. This was not due to non-specific binding of the radio-labelled probe as there was no expression observed when "GK-sense" probe was applied [see review (Wilcox 1993)]. These observations agree with previous reports detailing GK expression in the hypothalamus (Jetton, Liang et al. 1994, Lynch, Tompkins et al. 2000). It is difficult to quantify expression using *in situ* hybridisation therefore the GK activity assay was performed to measure GK activity.

3.4.2 Increasing arcuate glucokinase activity increases glucose intake

Alteration of glucokinase activity affects the cell's ability to sense glucose, thus altering the regulation of glucose homeostasis and appetite. Pharmacological activation of ARC GK by stereotactic injection of CpdA results in an increase in glucose intake from 1 hour. Doses of CpdA were based on previous experiments (Kamata, Mitsuya et al. 2004, Levin, Becker et al. 2008). Previously, injection of CpdA into the VMH has been shown to induce peripheral hormone release from 30 minutes after injection (Levin, Becker et al. 2008). In contrast, the present study demonstrates that injection of CpdA into the ARC increases glucose intake from 30 minutes after injection. An increase in glucose intake is in agreement with my hypothesis and suggests that ARC GK promotes glucose intake.

Activation of ARC GK also increased intake of standard chow. However when both glucose and chow were provided together, activation of ARC GK only increased glucose consumption. I propose that this is because pure glucose alters blood and CSF glucose levels more quickly than chow, which is sensed by ARC glucose sensors to affect appetite. Consistent with this hypothesis, glucose is also preferred over fructose and other sweeteners in animals with increased GK expression (Hussain, Richardson et al. 2014).

3.4.3 Accurate injection of substances into the ARC

Histological techniques were used to confirm effective ARC injection. In cannulated animals, post-mortem localisation of the cannula placement was determined by staining with cresyl violet. Correct cannula placement was confirmed in over 90% of animals; those that did not seem to project into the left ARC were not included in the final analysis. I found that the majority of injections appeared to project into the lateral portion of the ARC, as insertion of the cannula into the medial ARC risked disturbing the 3rd ventricle. The majority of GE neurones have been identified in the lateral ARC, in accord with this finding (Wang, Liu et al. 2004). It is possible that the injections could diffuse into other regions as direct localisation of the injection was not confirmed. Therefore VMN neurones could be affected and may contribute to the response.

3.4.4 Methods and measurements of altered glucokinase activity

Recombinant AAV was used to decrease ARC GK expression. AAV was preferred over adenoviral and retroviral vectors because it is non-immunogenic and the effects on gene expression are highly persistent *in vivo* (Ponnazhagan, Mukherjee et al. 1997). The plasmid used to make rAAV particles consists of an original backbone (pTR-CGW) that was engineered to include the complimentary (antisense) sequence for neuroendocrine glucokinase so that base pairing and suppression of translation would occur (Kumar and Carmichael 1998, O'Keefe 2013). The efficacy of the plasmid to alter glucokinase was first tested *in vitro* using HEPG2 cells, a liver cell line that express GK. HEPG2 cells were transfected with GKAS plasmid and cell lysates were assayed for GK activity after 48 hours. Transfection with GKAS plasmid resulted in a 38% reduction of GK activity compared with control plasmid. The level of knockdown achieved was slightly lower than previous studies using antisense AAV. RIN56 NPY-containing cells showed a 56% knockdown of NPY expression when transfected with antisense AAV (Gardiner et al, 2005).

To test the efficacy of the plasmid to alter GK *in vivo*, I determined glucokinase activity in dissected hypothalamic nuclei of iARC-GKAS rats. Glucokinase activity was calculated using a modified NADPH assay as described previously (Goward, Hartwell et al. 1986, Hussain, Richardson et al. 2014). GK activity was reduced by more than 50% in the ARC and not

altered in the VMN or PVN, compared with iARC-GFP. This demonstrates that rAAV-GKAS can significantly alter GK activity *in vivo*.

GK activity was measured using a modified $NADP^+$-coupled activity assay rather than using previously used techniques. Previous assays for measuring GK activity were not specific to GK as hexokinases have a higher affinity and lower Km for glucose than GK (Printz, Magnuson et al. 1993). Other methods measure $NADP^+$ in two separate experiments at high (20mM) and low (0.5mM) concentrations of glucose where GK activity should be lower than hexokinase activity in the second experiment. A comparison between the two experiments is necessary to eliminate the effects of other hexokinases, but total elimination cannot be confirmed (Osundiji, Lam et al. 2012). To circumvent the effects of hexokinases, I added hexokinase inhibitors to increase the accuracy of the assay. The glucose analogue 5-thio-D-glucose is an antagonist for hexokinases except for GK (Wilson and Chung 1989). Similarly, 3-O-methyl-N-acetylglucosamine inhibits glucose phosphorylation by N-acetylglucosamine kinase but not GK (Miwa, Mita et al. 1994). Accurate GK activity measurement was previously demonstrated in vitro and an improved sensitivity to GK was shown (Richardson 2011).

3.4.5 Decreasing arcuate glucokinase activity decreases glucose intake

To investigate the physiological role of GK in the ARC, I injected rAAV encoding for antisense GK into rats. Selectively decreasing ARC GK in rats results in a decrease in glucose intake in both an acute and long-term study. This data backs up my hypothesis and correlates with my previous investigation of the role of ARC GK using pharmacological activators. Furthermore, knocking down ARC GK is in agreement with previous studies conducted in this laboratory. Overexpression of ARC GK (iARC-GKS), using rAAV encoding for GK sense, resulted in increased food intake and body weight gain (Hussain, Richardson et al. 2014). When iARC-GKS animals were provided with standard chow and glucose solution in a long-term study, they consumed significantly more glucose than control rats whereas chow intake remained the same. In the present study, knockdown of ARC GK using a comparable approach decreased glucose intake. This provides evidence for the hypothesis that ARC GK regulates glucose-specific appetite over other foods.

3.4.6 ARC glucokinase and the control of overall calorie intake

Decreasing ARC GK activity decreases glucose intake but not total energy intake. This is due to a slight but non-significant increase in normal chow intake as compensation. Body weight gain between the two groups was not significantly different. A decrease of glucose consumption is consistent with previous findings that increased ARC GK expression increases glucose intake (Hussain, Richardson et al. 2014). However, iARC-GKS also caused a significant increase in body weight gain by around 6% (Hussain, Richardson et al. 2014). Further analysis of this increase revealed that it was due to a rise in percentage bodyweight of fat. While there was not a statistically significant decrease in body weight gain in iARC-GKAS animals, there was a reduction by around 7% after 33 days, similar to the 6% increase observed in iARC-GKS animals (Hussain, Richardson et al. 2014). Therefore it is likely that GK does alter overall body weight gain, particularly fat, but in the present study there was an increased variation between animals.

3.4.7 Two separate physiological roles for hypothalamic glucokinase

The findings in this chapter describe a novel role for ARC GK independent of the role previously described. Classically, hypothalamic GK has been shown to be involved in the CRR to hypoglycaemia. Infusion of insulin in rats to induce hypoglycaemia triggers adrenalin, noradrenalin and glucagon release to promote glucose availability and maintain homeostasis (Levin, Becker et al. 2008). Injection of CpdA into the VMH reduced adrenalin, noradrenalin and glucagon secretion in rats under conditions of insulin-induced hypoglycaemia, suggesting that increased GK inhibits the production of glucose (Levin, Becker et al. 2008). Glucose consumption was not reported in these experiments, and there were no reported changes in acute chow intake. This is contrary to the findings using CpdA in the present chapter, where glucose and chow intake were increased. However, CpdA injection sites were different between the two studies, and the model of insulin-induced hypoglycaemia was not used in this chapter. The reason why there were no reported changes in appetite may be because insulin directly inhibits food intake therefore the effects of CpdA would be masked (Woods, Lotter et al. 1979, Levin, Becker et al. 2008). Also, hypoglycaemia can indirectly affect appetite; as observed in humans by increasing anxiety,

dizziness and perspiration (Mitrakou, Ryan et al. 1991). Furthermore, Levin, Becker et al. (2008) used animals that were subjected to extra surgical procedures, such as jugular vein catheterisation, which could affect baseline measurements by inducing stress.

The effects of reduced ARC GK in this chapter are not consistent with previous investigations in the hypothalamus. Injection of adenovirus containing short-hairpin RNA (shRNA) for GK reduced VMN GK expression by 70% over 10 days in rats but did not alter feeding (Dunn-Meynell, Sanders et al. 2009). However, this experiment was not consistent with other studies by the same group who have shown robust changes in the CRR to hypoglycaemia with altered VMN GK activity (Kang, Routh et al. 2004, Levin, Magnan et al. 2011). VMN GK reduction by shRNA did not alter blood glucose or glucagon release when induced with hypoglycaemia (Dunn-Meynell, Sanders et al. 2009). This could be due to an immediate immunogenic response from adenoviral infection or as a result of decreased hexokinase 1 expression (Levin, Becker et al. 2008, Dunn-Meynell, Sanders et al. 2009). In accord with the findings in previous models of GK knockdown, it is possible that the decrease in food intake with knockdown of ARC GK could be due to alterations in glucagon, adrenalin or insulin release (Levin, Becker et al. 2008).

Alternative methods to decrease GK activity have similar limitations. Injection of the toxic glucose analogue alloxan into the VMN did not alter glucose tolerance or appetite (Dunn-Meynell, Sanders et al. 2009). However this drug produces significant toxicity in glucose sensing cells and ICV injection of comparable doses has been shown to alter gene expression and behaviour (Šalković-Petrišić and Lacković 2003). Other studies investigating the effects of decreased GK have used the hexokinase inhibitor glucosamine but as it affects other hexokinases as well as GK, intracellular glucose metabolism is likely to be compromised (Zhou, Yueh et al. 2011). Therefore previous studies have not completely identified the effects of decreased GK activity so the reduction in glucose intake observed in the present study provides novel evidence of an alternate role for GK in the hypothalamus.

The difference in effects between the techniques used in the present study and those by Levin et al. could also be due to variances in injection coordinates. While the VMN and ARC are located adjacent to each other in the hypothalamus, there are some notable differences between them. These have been described in chapter 1, but could primarily be due to the

different populations of neurones in the ARC and the increased tanycyte projections from the median eminence. Previous studies that investigated the effects of hypoglycaemia targeted the divide between the VMN and ARC (-8.5 to -9.5mm from the dura) (Levin, Becker et al. 2008, Dunn-Meynell, Sanders et al. 2009), whereas I target the ARC exclusively (-10.5mm from the dura). The powerful influence of ARC neurones on appetite and energy homeostasis demonstrates that these neurones are part of an important pathway to control feeding. Therefore the differences observed between GK expressing neurones in the ARC and VMN may be due to differences in neuronal circuitry that are investigated.

It was not confirmed that direct injection of substances only affected ARC neurones. With regard to genetic knockdown of ARC GK, a GK activity assay was performed to show that VMN GK activity was not altered. While it was assumed that each cannula projected into the ARC, diffusion of substances outside of the ARC could occur. Immunoreactivity of a neuronal activation marker, such as c-fos, could achieve confirmation of exclusive ARC activation.

There is a possibility that pharmacologically increasing GK activity using CpdA results in intracellular hypoglycaemia by artificially driving metabolism of available glucose. Theoretically this could increase food intake as central hypoglycaemia has been shown to affect feeding. However there are several reasons why this is not likely to be due to hypoglycaemia. First, pharmacological and genetic activation of ARC GK does not increase fructose consumption, indicating that the effect of CpdA is specific for glucose (Hussain, Richardson et al. 2014). Second, GLUT control the transport of glucose into cells and have a high affinity for glucose. This means that under normal physiological conditions any available extracellular glucose will be taken up into the cell. Third, G6P; not glucose, controls metabolism therefore the rate of phosphorylation of glucose by other hexokinases determines cellular function. If there was a large increase in G6P with an increase of GK activity then food intake would decrease, according to previous reports (Dunn-Meynell, Sanders et al. 2009). It therefore seems unlikely that CpdA drive feeding by indirectly triggering hypoglycaemia.

In summary, the different approaches between the two studies may influence the behaviour observed with CpdA injection. Both approaches may still be beneficial for describing the physiological role of GK.

3.4.8 The physiological relevance of ARC GK in the regulation of food intake

The finding that ARC GK regulates glucose appetite is not supported by evidence regarding glucose homeostasis in the VMN. The question arises as to the physiological relevance for a positive feedback where rising glucose levels further increase glucose consumption. However all energy homeostasis pathways comprise of orexigenic and anorexigenic signals working in parallel. A relevant example is the hedonic value of food, which plays a major part in the regulation of food intake (Berthoud and Morrison 2007). The principle of reward processing is that feeding promotes positive feelings and emotion therefore positive feedback mechanisms are powerful mediators of food intake. ARC GK represents an orexigenic pathway that promotes the consumption of the substrate that is a vital energy source for the brain. This might be a conserved behaviour to make use of any glucose when it becomes available. It is likely that this behaviour involves hedonic centres to communicate the reward value of glucose. This hypothesis is supported by findings that fasting results in an increase in ARC GK expression in rats (Hussain, Richardson et al. 2014). This is in accord with previous data showing an increase in hypothalamic GK expression (Zhou, Roane et al. 2003, Sanz, Roncero et al. 2007, Kang, Sanders et al. 2008), even though pancreatic GK expression does not change (Iynedjian, Pilot et al. 1989). In addition, rat LH and VMH slices exhibit an increase in GK activity when glucose concentration decreases (Sanz, Roncero et al. 2007). Therefore it is likely that ARC GK plays a physiological role in food intake. If GK was present to only maintain homeostasis then fasting should have decreased GK activity to promote feeding (Levin, Magnan et al. 2011). In the next chapter I investigate the neuronal mechanisms of GK activation to better understand this pathway.

3.4.9 Conclusion

Activation of ARC GK activity in rats increases appetite specifically for glucose. Conversely, chronic knockdown of ARC GK in rats decreases food intake in both an acute and cumulative setting. Appetite for pure glucose is decreased but appetite for other foods is not. In addition, total energy intake is not affected by a decrease in glucose intake as overall food intake is slightly increased. These findings compliment previous investigations where chronic overexpression of ARC GK increases glucose appetite.

Chapter 4: Pharmacological manipulation of arcuate nucleus glucose sensing

4.1 Introduction

The data presented in chapter 3 suggests that ARC GK regulates glucose appetite. Pharmacological activation of ARC GK increases glucose intake at 1 hour. While it is likely that this response is mediated by direct activation of GK, the intracellular mechanisms and neuronal circuitry that are involved in driving glucose intake are not known. Investigating the mechanisms of ARC glucose sensing is necessary in order to understand why regulation of glucose appetite only occurs in the ARC and not elsewhere in the hypothalamus. To identify the types of neurones involved and how GK may alter depolarisation, I will investigate the intracellular mechanisms that are involved in mediating the effects of ARC GK on appetite. To explore the neuronal pathways involved in glucose sensing neurones, I will investigate the neurotransmitters released as a result of ARC GK activation.

4.1.1 The role of ATP-sensitive potassium channels

K_{ATP} channels play a key role in glucose-stimulated insulin release from β-cells (Ashcroft and Rorsman 2013). The K_{ATP} channels involved in this glucose sensing pathway likely consist of 4 $K_{ir}6.2$ and 4 SUR1 subunits arranged to form an ion channel. The ratio of ATP to ADP dictates K_{ATP} channel opening probability. ATP binds to $K_{ir}6.2$ to keep the channel closed and prevent K^+ ions exiting the cell while ADP binds to SUR1 with an opposite effect on channel opening (Gribble, Tucker et al. 1997, Tucker, Gribble et al. 1998). ATP concentrations rise with an increase in GK activity in β-cells to stimulate further K_{ATP} channel closure and trigger insulin release. A similar mechanism has also been identified in GE neurones to trigger depolarisation. K_{ATP} channels are highly expressed in many cells including NPY and POMC neurones (Ibrahim, Bosch et al. 2003, van den Top, Lyons et al. 2007). Selective knockout of $K_{ir}6.2$ in POMC neurones results in an impaired glucose tolerance and glucose-stimulated hypothalamic α-MSH release (Parton, Ye et al. 2007). However the role of K_{ATP} channels in regulating glucose intake is not known.

The role of ion channels can be investigated by altering channel opening using pharmacological activators and inhibitors. Diazoxide stimulates channel opening by increasing the actions of ADP and Mg^{2+} (Kozlowski, Hales et al. 1989, Gribble, Tucker et al. 1997). Sulfonylureas such as glibenclamide inhibit channel opening to cause depolarisation.

Many sulfonylureas have had some success as therapeutic treatments for type II diabetes to stimulate insulin release (U. K. Prospective Diabetes Study Group 1998, Turner, Cull et al. 1999). The SUR1 subunit has at least two ligand binding sites for drugs that induce K_{ATP} closure: a benzamide-binding site and a tolbutamide-binding site (figure 1.3). Many sulfonylureas including tolbutamide and gliclazide bind to the tolbutamide-binding site but glibenclamide is thought to bind to both sites (Nagashima, Takahashi et al. 2004).

The role of K_{ATP} channels in the CRR to hypoglycaemia has been investigated by direct administration of pharmacological agents into the brain. Injection of glibenclamide in the VMN impairs the compensatory increase in glucagon in response to hypoglycaemia (Evans, McCrimmon et al. 2004). In contrast, injection of diazoxide in the VMN amplifies the CRR to hypoglycaemia response by increasing adrenaline and glucagon (McCrimmon, Evans et al. 2005). I aim to investigate the role of K_{ATP} channels in ARC GK-regulated glucose intake using these pharmacological agents. The previous studies investigating the role of K_{ATP} channels in the CRR to hypoglycaemia injected primarily into the VMN so the physiological role of K_{ATP} channels in the ARC has not yet been studied.

4.1.2 The role of voltage-gated calcium channels in ARC GK-regulated glucose intake

Voltage-gated calcium channels (VGCC) are important regulators of electrochemical gradients in neurones. The tight regulation of calcium influx requires the combination of many different types of VGCC with different physiological and pharmacological profiles. These are mainly dependant on the type of α1 subunit expressed, which forms the channel pore, voltage sensor and gate (Catterall, Perez-Reyes et al. 2005). High voltage-activated channels, including L, N and P/Q type channels, have ancillary subunits to further control the voltage required to trigger activation and inactivation of the channel. Neurones express many different types of channels to control many different physiological functions. For example; L, N, P/Q and R type channels all contribute to the calcium-induced increase in membrane currents in rat cerebellar granule neurones (Randall and Tsien 1995). The family of L type VGCC comprise of at least 4 different sub-types with different subunit composition ($Ca_V1.1$-1.4). Of note, $Ca_V1.2$ and 1.3 are expressed in neurones and endocrine cells and have been shown to regulate hormone secretion, action potential propagation and gene

expression (Catterall 2000). Most $Ca_V1.2$ and 1.3 channels are located on the post-synaptic terminal of neurones and are not associated with release of cortical neurones vesicles at the presynaptic terminal as they do not possess a motif for interactions with SNARE proteins. $Ca_V1.3$ are activated at a relatively hyperpolarised potential and have been shown to modulate post-synaptic activity in neurones (Xu and Lipscombe 2001). Dihydropyridines such as nifedipine are potent blockers of L type channels and have been used to identify the role of hippocampal VGCC in memory (Quevedo, Vianna et al. 1998). L type channels have been shown to regulate the orexin-A-induced activation of a minor population of ARC neurones (Wu, Wu et al. 2013); and to some extent, β-cells (Smith, Rorsman et al. 1989). Though the role of ARC GK on appetite does not likely involve AMPK (Hussain, Richardson et al. 2014) , L type channels may still play a role.

P/Q type VGCC, also known as $Ca_V2.1$, are associated with vesicle release and are located very close to SNARE proteins at pre-synaptic terminals (Catterall, Perez-Reyes et al. 2005, Weiss and Zamponi 2012). P and Q type channels have slight variations in inactivation kinetics but are not easily distinguished. Both are blocked by ω-agatoxin IVA but at a slightly higher potency at P type channels (Llinas, Sugimori et al. 1989, Randall and Tsien 1995).

N type VGCC ($Ca_V2.2$) are also associated with vesicle release at pre-synaptic terminals (Catterall, Perez-Reyes et al. 2005). They have a high single-channel conductance in order to quickly induce a transient increase in Ca^{2+} so are ideal for vesicle release (Weber, Wong et al. 2010). The voltage dependence of N type channels varies considerably, presumably due to different vesicle release requirements, therefore the most accurate identifier of N type channels is via their sensitivity to cone snail neurotoxin ω-conotoxin GVIA (Casali, Gomez et al. 1997). Both P/Q and N are also expressed in dendrites and play a role in dendritic Ca^{2+} transients (Catterall 2000).

R type channels, also known as $Ca_V2.3$, are expressed in cell bodies, dendrites and nerve terminals to trigger Ca^{2+}-dependent action potentials and neurotransmitter release. While expressed in the cortex and hippocampus, their expression is not as high as other Ca_V2 channels (Dunlap, Luebke et al. 1995).

It is worth noting that as well as the actions of VGCC in vesicle release, P/Q, N and $Na_V1.2$ of L type channels are also likely to be involved in action potential repolarisation rates due to

their association with potassium channels (Simms and Zamponi 2014). I aim to investigate the involvement of VGCC in mediating ARC GK-regulated glucose intake.

4.1.3 The neurotransmitters involved in ARC GK-regulated increase in glucose intake

Both POMC and NPY neurones express GK in the ARC (Muroya, Yada et al. 1999, Ibrahim, Bosch et al. 2003, Parton, Ye et al. 2007) therefore the neuronal mechanism of ARC GK action could be via these pathways. NPY is a widely distributed neurotransmitter in the CNS (Li, Xi et al. 2003) and is a potent orexigenic peptide (Mercer, Chee et al. 2011). The majority of NPY in the hypothalamus is produced by ARC neurones, which co-express AgRP (Broberger, Johansen et al. 1998). ARC NPY neurones innervate and inhibit nearby POMC neurones. NPY is contained in large dense core vesicles, which are exocytosed into the synapse by calcium-mediated vesicular release (Pelletier, Guy et al. 1984). The vesicles containing NPY can also be released at sites along the axon, indicating that it also acts as a neuromodulator on neighbouring neurones (Morris and Pow 1991). NPY binds to Y1 and Y2 receptors on the post-synaptic terminal to hyperpolarise POMC neurones (Broberger, Landry et al. 1997, Roseberry, Liu et al. 2004). Regulation of feeding also requires the Y5 receptor and stimulation of this receptor in the ARC inhibits α-MSH release (Galas, Tonon et al. 2002). NPY neurones also project to glutamatergic neurones in the VMN, GABAergic neurones in the PVN and MCH and orexinergic neurones in the LH (Tiesjema, Adan et al. 2007, Mercer, Chee et al. 2011). Interestingly, the majority of glucose sensitive VMN neurones are also sensitive to NPY (Chee, Myers et al. 2010). In addition, NPY injection in the PVN stimulates food intake (Stanley, Chin et al. 1985).

Alpha-MSH is cleaved from the POMC precursor and acts as an anorexigenic peptide (Rossi, Kim et al. 1998, Cone, Cowley et al. 2001). Alpha-MSH release from hypothalamic explants increases with increasing glucose concentrations (Parton, Ye et al. 2007). Alpha-MSH binds to melanocortin 4 receptors to inhibit food intake (Kim, Rossi et al. 2000). Pathways for melanocortin action have been demonstrated throughout the CNS, notably forming positive feedback within VMH neurones and inhibiting appetite in the PVN (Balthasar, Dalgaard et al. 2005, Parker and Bloom 2012). Alpha MSH signalling in the central amygdala is also linked with alterations in preferences for dietary fats (Boghossian, Park et al. 2010).

In summary, the mechanisms of ARC GK control of glucose appetite require further investigation. K_{ATP} channels play a key role in glucose sensing in the ARC. The types of neurones involved in ARC glucose sensing remain to be determined but likely involves POMC or NPY neurones, the predominant ARC populations involved in regulation of food intake.

4.2 Hypothesis and Aims

4.2.1 Hypothesis

Pharmacologically closing K_{ATP} channels will affect food intake and glucose intake in a similar way to increasing GK activity. Similarly, opening K_{ATP} channels will have the opposite effect. The mechanism of ARC GK mediated glucose intake is likely to be mediated by neuronal pathways. Therefore alterations in ARC GK will alter neuronal firing, probably via orexigenic NPY neurones. The release of vesicular NPY at pre-synaptic terminals is likely controlled by multiple types of voltage-gated calcium channels (VGCC). Furthermore NPY likely acts at Y1 and Y5 receptors on the post-synaptic terminals of second order neurones.

4.2.2 Aims

To investigate my hypothesis I will:

1. Inhibit and stimulate ARC K_{ATP} channels by delivering pharmacological agents into the ARC via a stereotactically inserted cannula and measure food and glucose intake.
2. Pharmacologically stimulate GK and K_{ATP} channels *ex vivo* in hypothalamic explants and measure neuropeptide release.
3. Investigate the effect of pharmacologically blocking ARC VGCC on the previously described model of ARC GK-regulated increase in glucose intake.
4. Investigate the effect of pharmacologically blocking central NPY receptors on ARC GK-regulated increase in glucose intake.

4.3 Results

4.3.1 Effect of pharmacologically inhibiting ARC K_{ATP} channels on chow and glucose intake

Permanent cannulas were stereotactically implanted 1mm above the ARC nucleus of rats. ARC K_{ATP} channels were inhibited by 2 nmol injection of the sulfonylurea glibenclamide. Following injection rats were allowed access to either chow, a glucose solution or both chow and glucose. Acute inhibition of ARC K_{ATP} channels caused a significant increase in chow intake over the first 4 hours (control, 3.29±0.54g; glib, 4.43±0.70g; n=12 per group, p <0.05) (figure 4.1a). Acute inhibition of ARC K_{ATP} channels caused a slight, but not significant, increase in chow intake over 8 hours (control, 6.18±1.79g; glib, 7.39±0.93g; n=12 per group, p =0.08) (figure 4.1b). Acute inhibition of ARC K_{ATP} channels caused a significant increase in glucose intake over 4 hours (control, 5.22±1.81g; glib, 8.39±2.06g; n=11 per group, p <0.05) (figure 4.2a). This increase in glucose intake was sustained over 8 hours (control, 6.12±1.99g; glib, 9.68±2.36g; n=11 per group, p <0.05) (figure 4.2b). Acute inhibition of ARC K_{ATP} channels caused a significant increase in glucose intake when both chow and glucose were available after 4 hours (control, 7.30±1.90g; glib, 10.22±2.46g, n=10 per group, p <0.05) (figure 4.3a). This increase was maintained but was not statistically significant after 8 hours (control, 9.31±2.42g; glib, 10.45±2.47g; n=10 per group) (figure 4.3c). However, there was no significant difference in chow intake over 4 hours (control, 3.37 ±0.52g; glib, 3.35 ±0.81g; n=10 per group) (figure 4.3b) or 8 hours (control, 6.49±0.68g; glib, 6.15±1.40g; n=10 per group) (figure 4.3d).

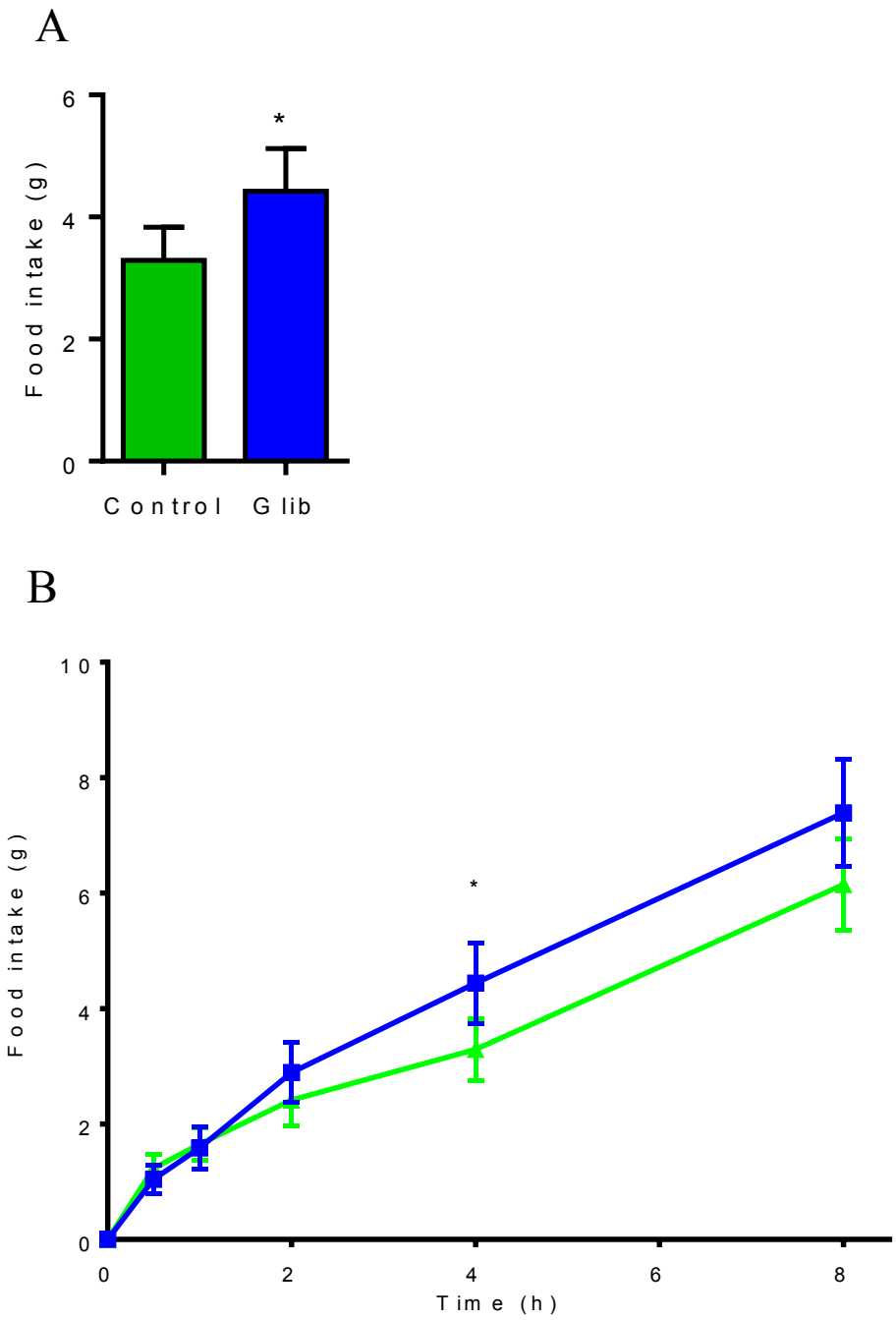


Figure 4.1 Effect of inhibiting K_{ATP} channels on food intake. Food intake; (A) four hours, (B) eight hours, after ARC K_{ATP} channel inhibition using stereotactic injection of 2 nmol glib as compared to the vehicle injected controls during a crossover study. Data are presented as mean±SEM, n=12 per group. Statistical significance was analysed by paired Student's t-test: *= p <0.05.

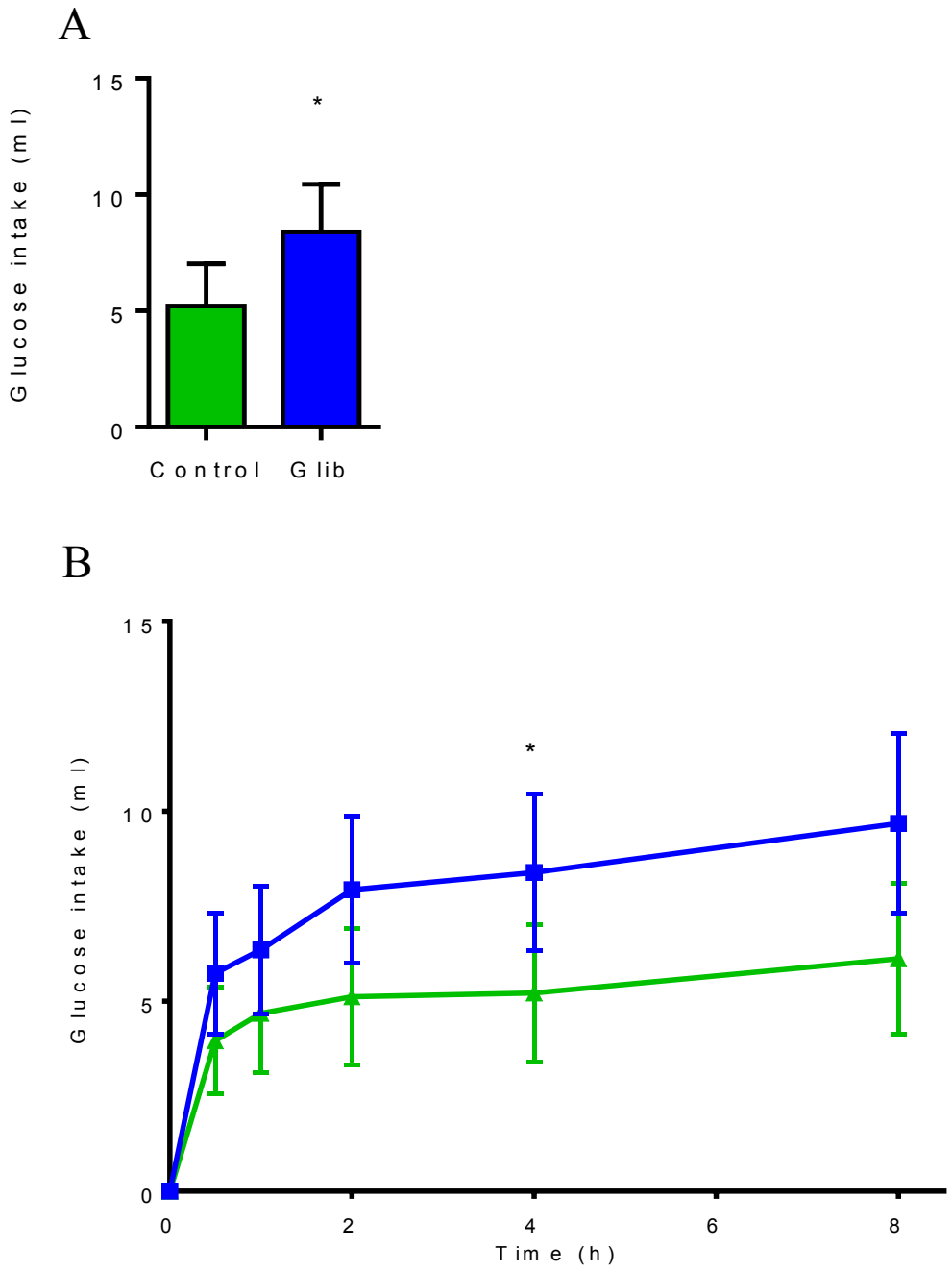


Figure 4.2 Effect of inhibiting K_{ATP} channels on glucose intake. 2% glucose intake; (A) four hours, (B) eight hours, after ARC K_{ATP} channel inhibition using stereotactic injection of 2 nmol glib as compared to the vehicle injected controls during a crossover study. Data are presented as mean±SEM, n=11 per group. Statistical significance was analysed by Student's t-test: *= p <0.05.

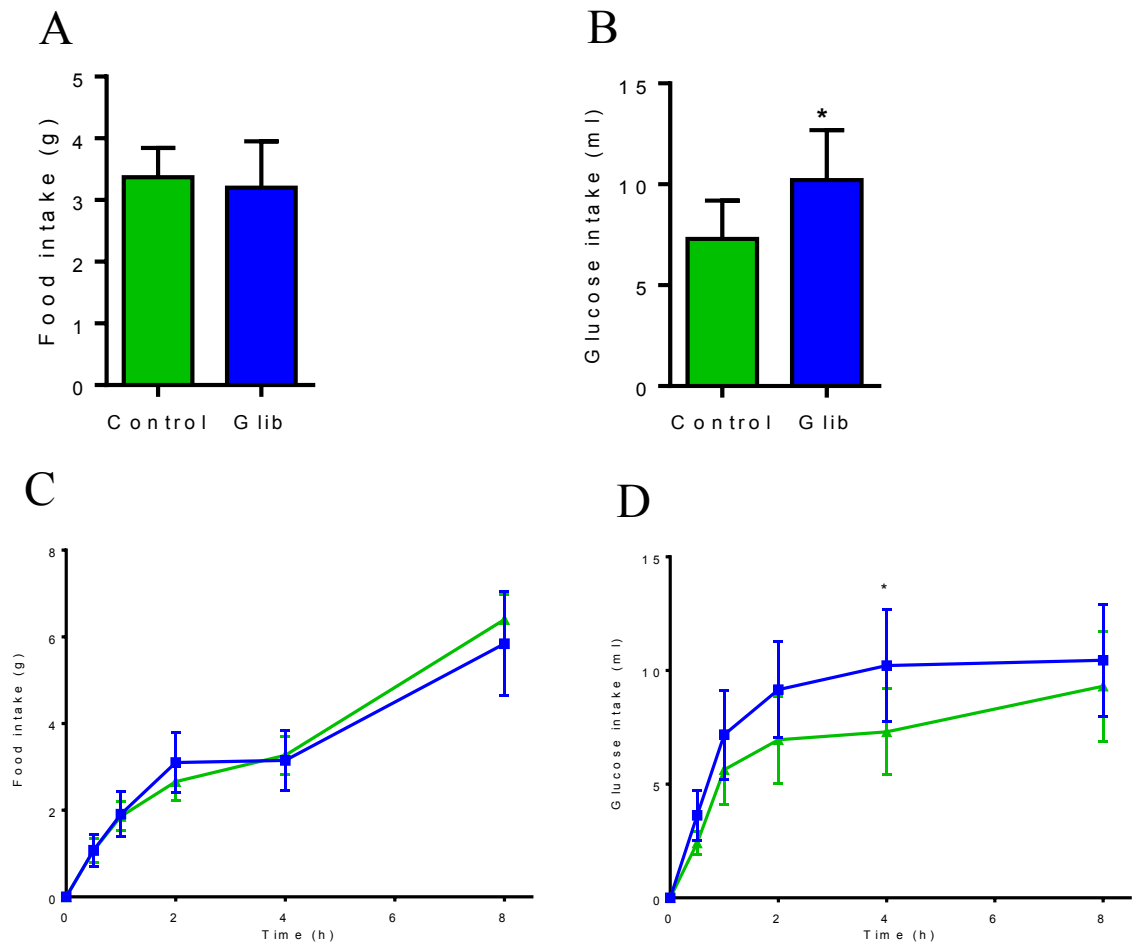


Figure 4.3 Effect of inhibiting K_{ATP} channels on chow and glucose intake. Food intake; (A) four hours, (C) eight hours, and 2% (w/v) glucose intake; (B) one hour, (D) eight hours, after ARC K_{ATP} channel inhibition using stereotactic injection of 2 nmol glib as compared to the vehicle injected controls during a crossover study. Data are presented as mean±SEM, n=10 per group. Statistical significance was analysed by Student's t-test: *= p <0.05.

4.3.2 Effect of pharmacologically activating ARC K_{ATP} channels on chow and glucose intake

Permanent cannulas were stereotactically implanted 1mm above the ARC nucleus of rats. Rats were fasted overnight and ARC K_{ATP} channels were stimulated by injection of 1 nmol of the activator diazoxide. Following injection rats were allowed access to either chow, a 2% (w/v) glucose solution or both chow and glucose. Acute activation of ARC K_{ATP} channels caused a significant decrease in chow intake over the first 30 minutes compared with controls (control, 4.81±0.42g; Dia, 3.72±0.30g; n=9 per group, p <0.01) (figure 4.4a). However chow intake was not reduced beyond 30 minutes (after 8 hours, control, 15.8±1.15g; Dia, 14.8±0.90g; n=9 per group) (figure 4.4b). Acute activation of ARC K_{ATP} channels caused a significant decrease in glucose intake over four hours (control, 25.8±4.95g; Dia, 19.3±3.97g; n=9 per group, p <0.05) (figure 4.5a). However this was not sustained over 8 hours (control, 44.1±9.59g; Dia, 44.5±13.9g; n=9 per group) (figure 4.5b). Acute activation of ARC K_{ATP} channels caused a significant decrease in glucose intake over 4 hours (control, 18.6±3.57g; Dia, 12.7±1.44g; n=9 per group, p <0.05) (figure 4.6a). There was a slight, but not significant, decrease in glucose intake after 8 hours (control, 22.5±3.58g; Dia, 19.9±1.82g; n=9 per group, p =0.12) Figure 4.6c). However there was no difference in chow intake during the first thirty minutes (control, 3.63±0.79g; Dia, 3.69±0.51g; n=11 per group) (figure 4.6b) or over 8 hours (control, 14.6±1.55g; Dia, 16.5±0.90g; n=11 per group) (figure 4.6d).

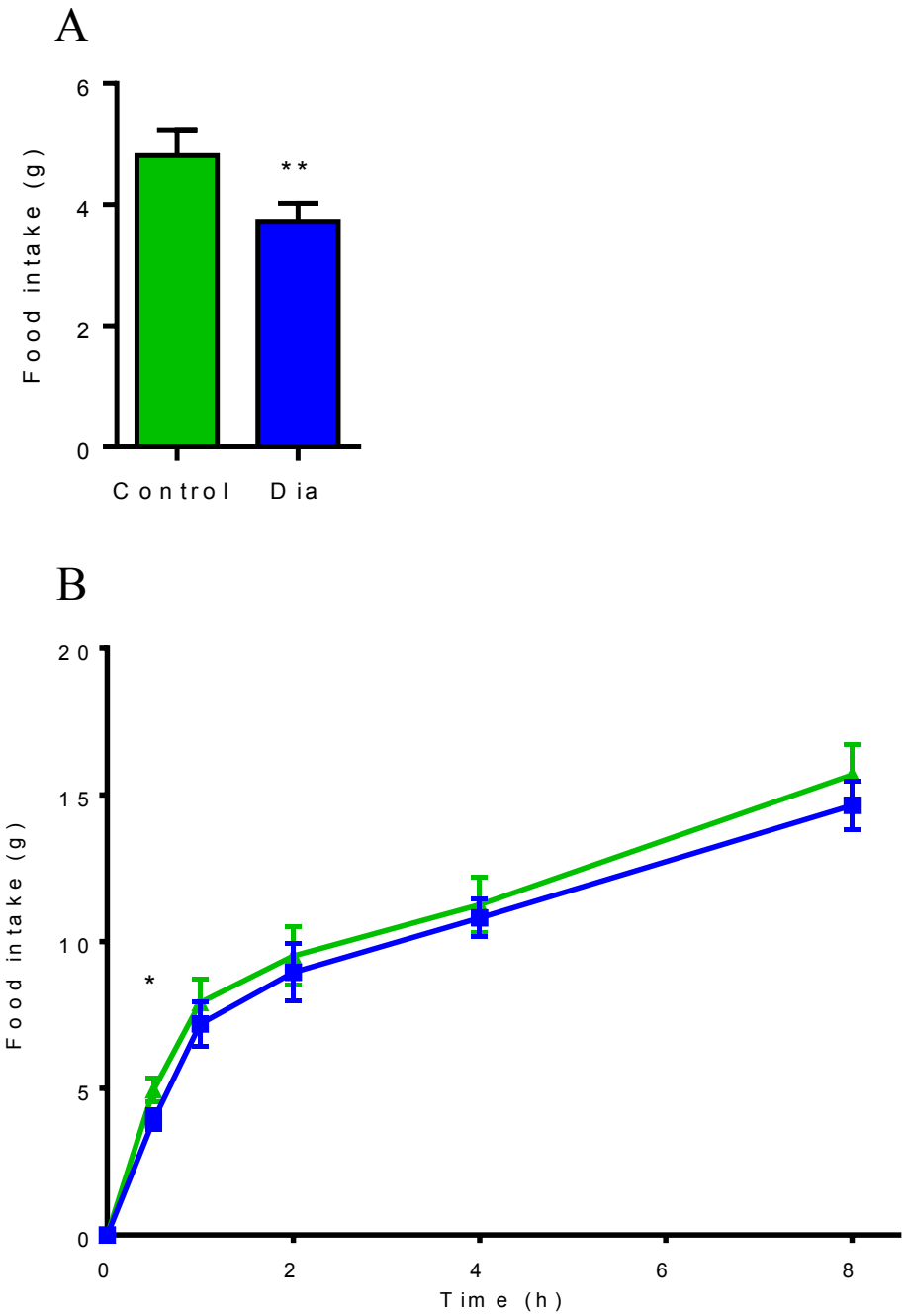


Figure 4.4 Effect of K_{ATP} channel activation on food intake. Food intake; (A) 30 minutes, (B) eight hours, after ARC K_{ATP} channel activation using stereotactic injection of 1 nmol diazoxide (dia) as compared to the vehicle injected controls during a crossover study. Data are presented as mean±SEM, n=9 per group. Statistical significance was analysed by Student's t-test: **= p <0.01, *= p <0.05.

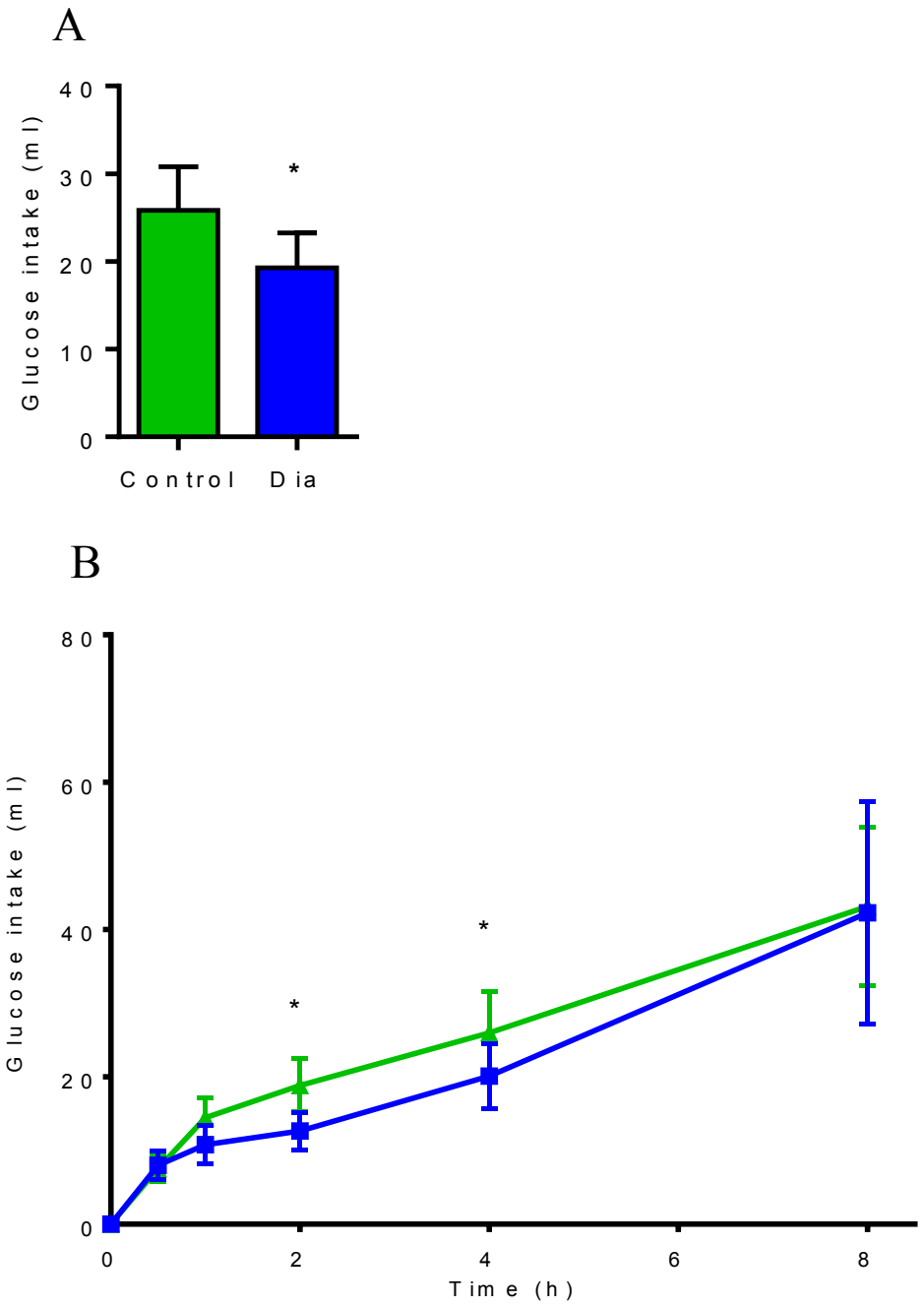


Figure 4.5 Effect of K_{ATP} channel activation on glucose intake. 2% glucose intake; (A) four hour, (B) eight hours, after ARC K_{ATP} channel activation using stereotactic injection of 1 nmol diazoxide (Dia) as compared to the vehicle injected controls during a crossover study. Data are presented as mean±SEM, n=9 per group. Statistical significance was analysed by Student's t-test: *= p <0.05.

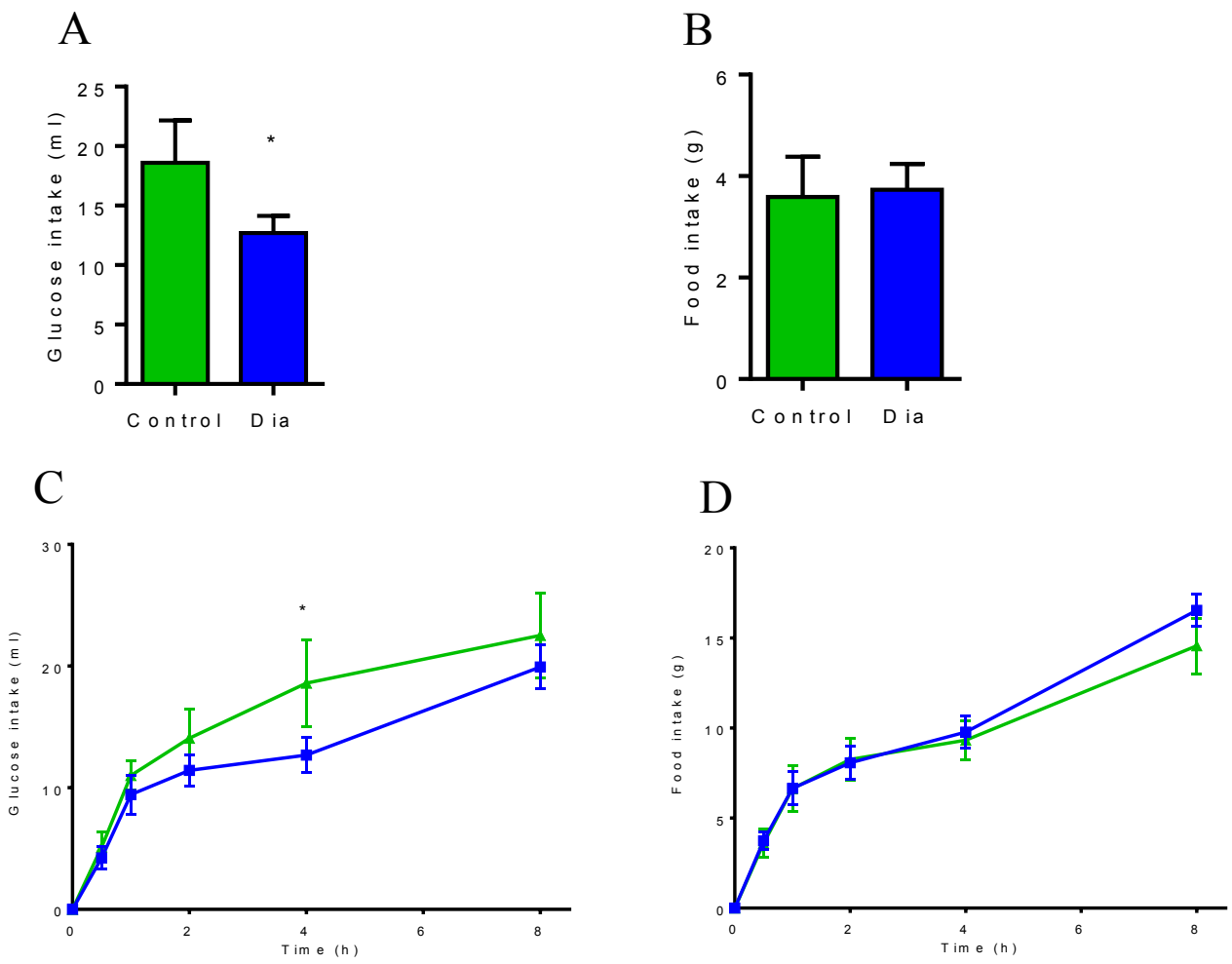


Figure 4.6 Effect of K_{ATP} channel activation on chow and glucose intake. 2% glucose intake; (A) four hours, (C) eight hours, and chow intake; (B) 0.5 hours, (D) eight hours, after ARC K_{ATP} channel activation using stereotactic injection of 1 nmol diazoxide (dia) as compared to the vehicle injected controls during a crossover study. Data are presented as mean±SEM, n=9 per group. Statistical significance was analysed by Student's t-test: *= p <0.05.

4.3.3 Effect of pharmacologically activating ARC GK and K_{ATP} channels on NPY and α-MSH release from hypothalamic neurones

Neurotransmitter release was measured *ex vivo* using rat mediobasal hypothalamus explants as described previously (Seal, Small et al. 2001). Explants were acclimatised to aCSF; basal samples were taken, and treated with one of the following: 30μM GK activator CpdA, 100μM K_{ATP} channel inhibitor glibenclamide or 200μM K_{ATP} channel activator diazoxide. These concentrations were chosen from previous similar experiments (Lam, Pocai et al. 2005, Kang, Dunn-Meynell et al. 2006, Chan, Lawson et al. 2007). Neurotransmitter release in the aCSF was measured by RIA and compared with the basal sample.

Activation of hypothalamic GK caused a significant increase in NPY release compared to basal levels (control, 8.9±1.5 fmol/explant; CpdA, 11.4±1.7 fmol/explant; n=10-12 per group, p <0.05) (figure 4.7a). Similarly, inhibition of hypothalamic K_{ATP} channels caused a significant increase in NPY release compared to basal levels (control, 9.1±1.3 fmol/explant; Glib; 12.0±1.5 fmol/explant; n=10-12 per group, p <0.05). In contrast, activation of hypothalamic K_{ATP} channels caused a significant decrease in NPY release compared to basal levels (control, 11.3±1.5 fmol/explant; Dia; 8.7±1.3 fmol/explant; n=10-12 per group, p <0.05).

Activation of hypothalamic GK did not alter α-MSH release compared to basal levels (control, 14.2±4.2 fmol/explant; CpdA, 16.2±5.6 fmol/explant; n=6-9) (figure 4.7b). Similarly, inhibition of hypothalamic K_{ATP} channels did not alter α-MSH release compared to basal levels (control, 12.1±2.2 fmol/explant; Glib, 15.7±4.1 fmol/explant; n=6-9). In addition, activation of hypothalamic K_{ATP} channels did not alter α-MSH release compared to basal levels (control, 13.7±3.2 fmol/explant; Dia, 13.2±1.7 fmol/explant; n=6-9).

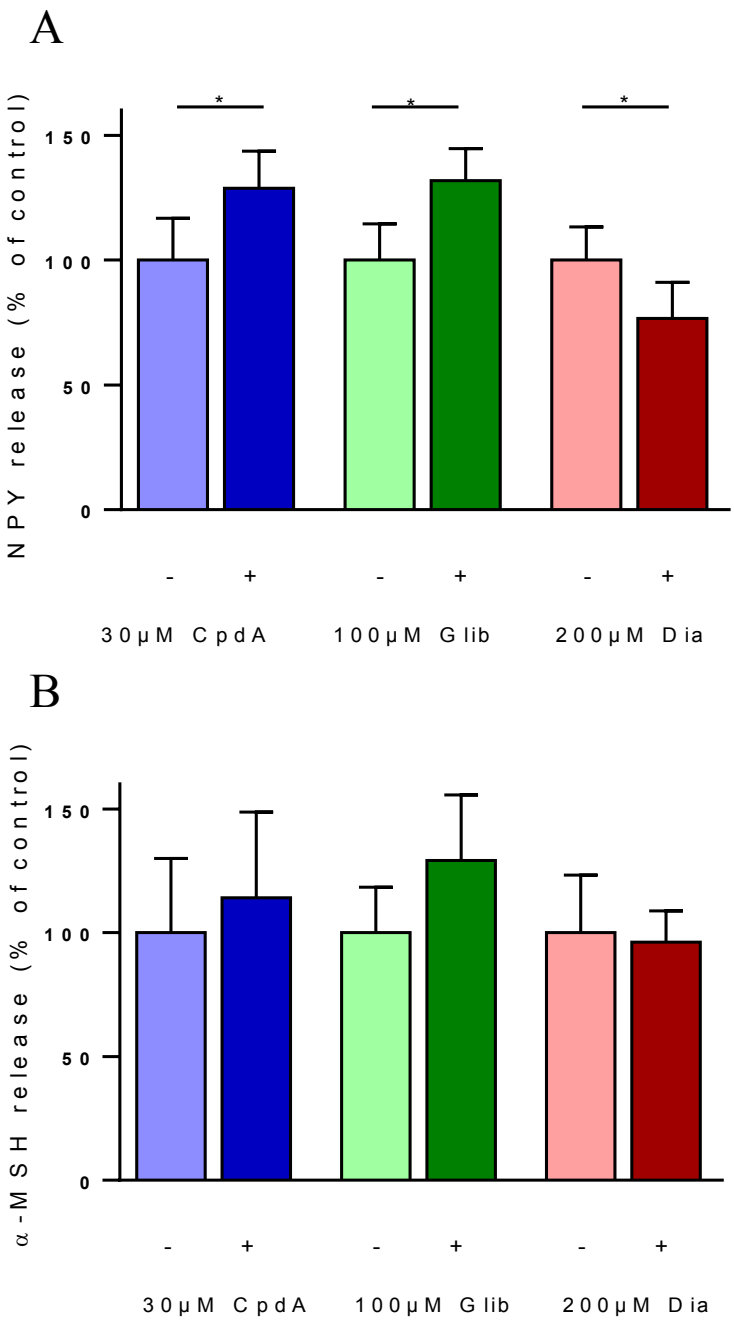


Figure 4.7 Effect of pharmacological agents on neuropeptide release from hypothalamic neurones. (A) NPY and (B) αMSH release from hypothalamic explant slices in response to pharmacological agents labelled. Addition sign (+) denotes drug wash; subtraction sign (-) denotes basal levels without drug. Data are presented as mean±SEM, NPY, n=10-12 per group, α-MSH, n=6-9. Statistical significance was analysed by ANOVA followed by post-hoc Holms-Sidak test: *= p <0.05.

4.3.4 Effect of pharmacologically activating K_{ATP} channels on the ARC GK-regulated increase in glucose intake

As demonstrated previously, pharmacological activation of ARC GK with CpdA significantly increases 2% (w/v) glucose consumption over 1 hour (figure 3.2). In contrast, pharmacological activation of ARC K_{ATP} channels with diazoxide significantly decreases glucose consumption (figure 4.5). To investigate the combined involvement of GK and K_{ATP} channels ARC glucose sensing I activated K_{ATP} channels and measured the effects of CpdA stimulated activation of ARC GK.

Permanent cannulas were stereotactically implanted into the ARC nucleus of rats. Rats were fasted overnight before 2 nmol diazoxide was administered by intra-ARC injection to open K_{ATP} channels. After 15 minutes ARC GK activity was increased by 0.5 nmol CpdA by intra-ARC injection and glucose intake was measured. Consistent with the previous studies, CpdA with pre-treatment of a control substance significantly increased glucose intake over the first hour (control, 5.22±0.22ml; CpdA, 10.86±0.69ml; n=10 per group, p <0.001) (figure 4.8a). Glucose intake stimulated by CpdA was significantly attenuated by pre-treatment with a K_{ATP} channel activator (control, 5.53±0.42ml; CpdA, 6.26±0.67ml; n=10, p <0.001). This decrease in glucose intake was not due to the activator alone as there was no significant difference when diazoxide was injected without CpdA (vehicle; 5.22±0.22ml, diaz; 5.53±0.42ml, n=10 per group). The effects of all treatments were sustained during 8 hours (figure 4.8b). These results indicate that K_{ATP} channels are involved in the ARC GK-regulated increase in glucose intake.

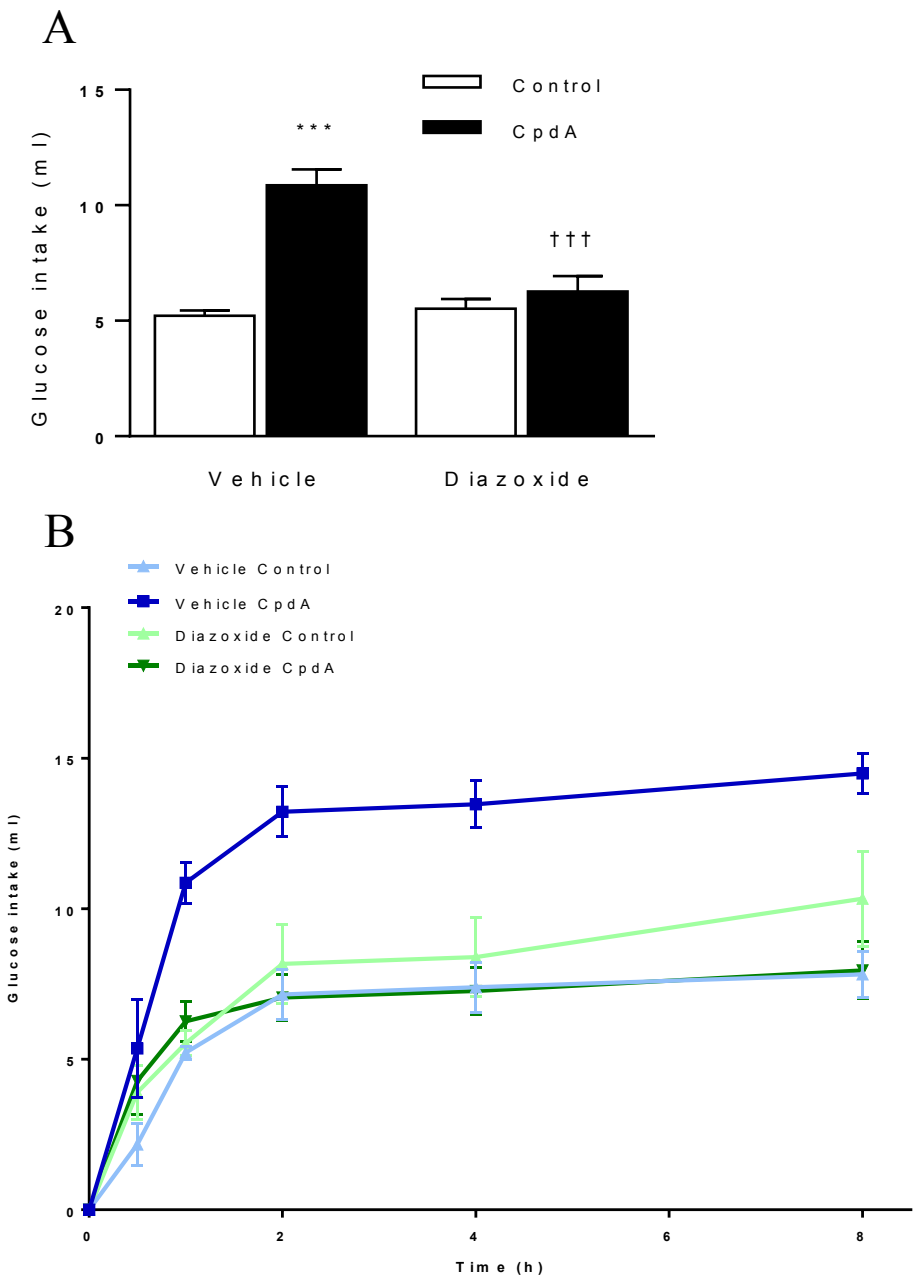


Figure 4.8 Effect of K_{ATP} channel activation on the ARC GK-regulated increase in glucose intake. 2% glucose intake one hour (A) and up to 8 hours (B) after ARC GK activation following pre-treatment with K_{ATP} channel activator over 4 sets of injections in a random order during a crossover study. Rats received intra-ARC injection of 2 nmol diazoxide or vehicle (5mM NaOH) 15 minutes before stereotactic injection of 0.5 nmol CpdA or control (0.1% DMSO). Data are presented as mean±SEM, n=10 per group. Statistical significance was analysed by one way ANOVA with Holm-Sidak's multiple comparisons test: ***= p <0.001 relative to intra-nuclear injected controls, †††= p <0.001 relative to vehicle treated and CpdA-injected group.

4.3.5 Effect of simultaneously activating ARC GK and K_{ATP} channels on hypothalamic NPY release

Activation of GK with 30μM CpdA resulted in a significant increase in NPY release from hypothalamic neurones compared to basal levels (control, 9.00±0.94 fmol/explant; CpdA, 14.3±1.40 fmol/explant; n=13 per group, p <0.01) (figure 4.9). Stimulation of K_{ATP} channels with 200μM diazoxide significantly decreased NPY release compared to basal levels (control, 17.0±3.65 fmol/explant; Dia, 8.45±1.31 fmol/explant; n=12 per group, p <0.05). NPY release is similar to previous studies under the same conditions (figure 4.7a). Activation of both GK and K_{ATP} channels with 30μM CpdA and 200μM diazoxide did not significantly alter NPY release compared with basal levels (control, 6.75±0.36 fmol/explant; CpdA + Dia, 8.07±0.85 fmol/explant; n=15). However, NPY release stimulated by CpdA was significantly attenuated by treatment with diazoxide (CpdA, 14.3±1.40 fmol/explant; CpdA + Dia, 8.07±0.85 fmol/explant; n=13-15 per group, p <0.001).

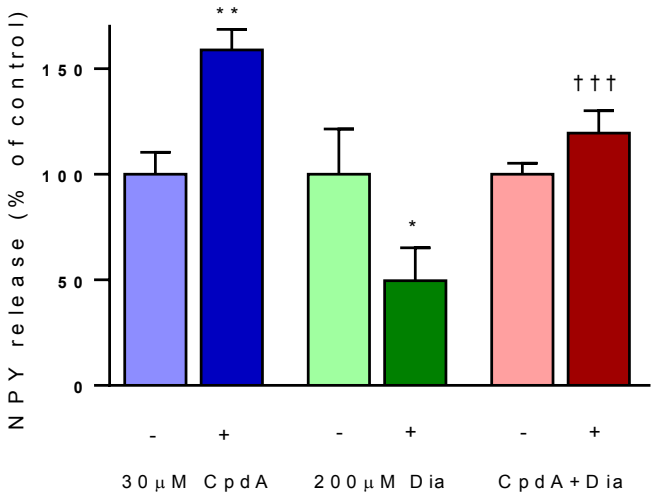


Figure 4.9 Effect of increased ARC GK and K_{ATP} channel activities on hypothalamic NPY release. NPY release from hypothalamic explant slices in response to pharmacological agents labelled. Addition sign (+) denotes drug wash; subtraction sign (-) denotes basal wash. Data are presented as mean±SEM, n=12-15 per group. Statistical significance was analysed by ANOVA followed by post-hoc Holms-Sidak test: *= p <0.05, **= p <0.01; relative to respective control, †††= p <0.001 relative to CpdA.

4.3.6 Role of voltage-gated calcium channels in the ARC GK-regulated increase in glucose intake

Pharmacological activation of ARC GK with CpdA increases glucose consumption. Stimulation of GK also releases neuropeptides from hypothalamic neurones in ex vivo hypothalamic explants indicating that the mechanism is mediated via a neuronal pathway. To further elucidate the mechanism of ARC GK action I blocked ARC VGCC and measured the effects of ARC GK-regulated increase in glucose intake.

Permanent cannulas were stereotactically implanted into the ARC nucleus of rats. P/Q and L type VGCC were blocked with 1.0μg ω-agatoxin IVA (agatox) or 1.6μg nifedipine (nifed) respectively by intra-ARC injection. Selective inhibitions of these channels were chosen because they are highly expressed in neurones. After 15 minutes ARC GK activity was increased with 0.5 nmol CpdA by intra-ARC injection and glucose intake was measured. Consistent with the previous studies, CpdA with pre-treatment of a control substance (vehicle) significantly increased glucose intake over the first hour compared with control (control, 3.10±0.51ml; CpdA, 8.90±0.54ml; n=13 per group, p <0.001) (figure 4.10a). Glucose intake stimulated by CpdA was significantly attenuated by pre-treatment with P/Q channel blocker (agatox, 3.36±0.40ml; n=13 per group, p <0.001). Glucose intake stimulated by CpdA was not altered by pre-treatment with L channel blocker (nifed, 9.44±0.67ml; n=13 per group). P/Q or L type channel antagonism did not significantly alter glucose intake alone compared with control without CpdA (control, 3.10±0.51ml; agatox, 3.05±0.54ml; nifed, 3.82±0.52ml; n=13 per group). The effects of all treatments were sustained during 8 hours (figure 4.10b). These results indicate that P/Q type, but not L type channels are involved in ARC GK-regulated increase in glucose intake.

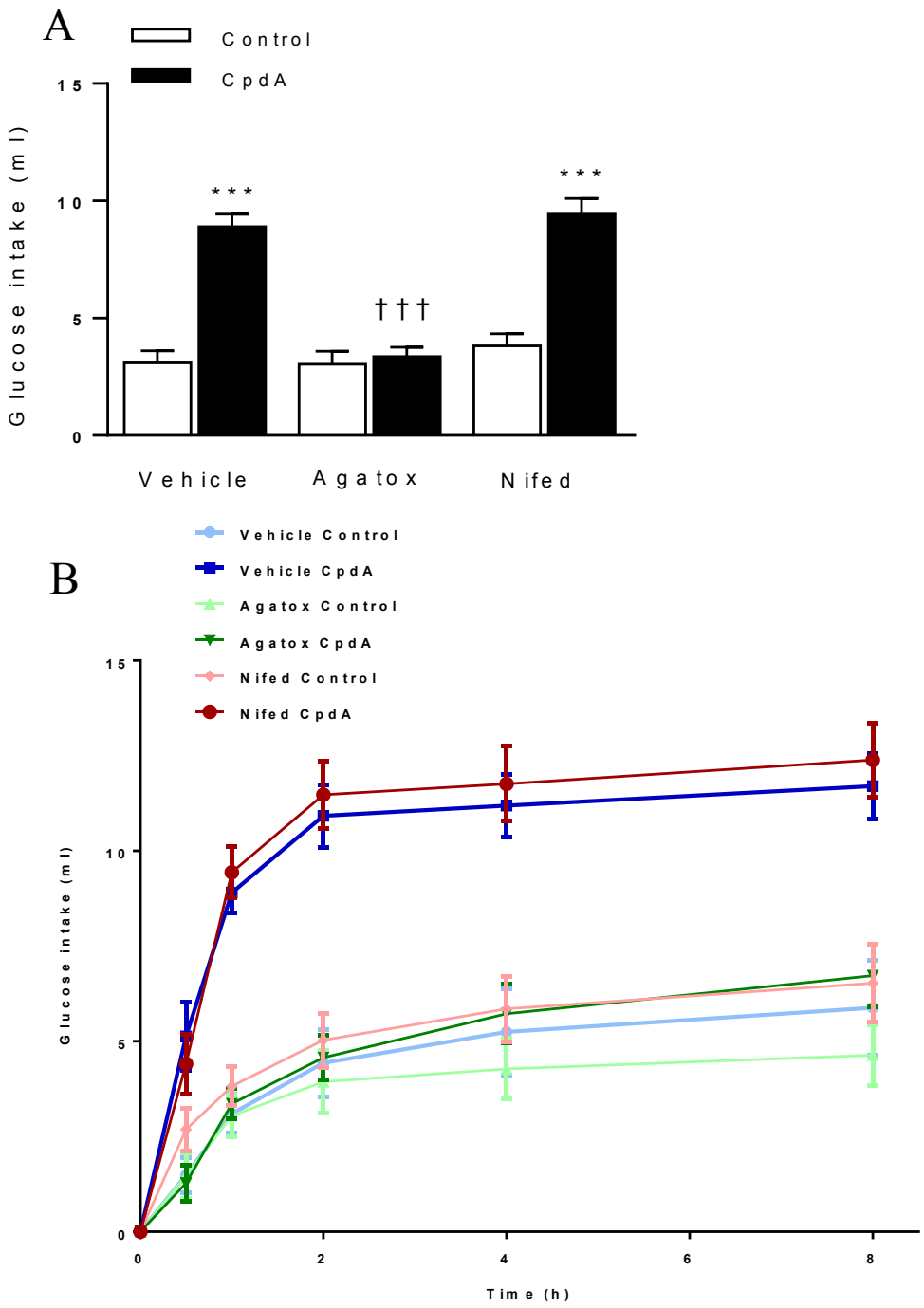


Figure 4.10 Effect of VGCC inhibition on the ARC GK-regulated increase in glucose intake. 2% glucose intake one hour (A) and 0.5-8 hours (B) after ARC GK activation following P/Q type and L type VGCC antagonism over 6 sets of injections in a random order during a crossover study. Rats received intra-ARC injection of 1.6µg nifedipine, 1µg agatoxin or vehicle (water) 15 minutes before intra-ARC injection of 0.5 nmol CpdA or control (0.1% DMSO). Data are presented as mean±SEM, n=13 per group. Statistical significance was analysed by one way ANOVA followed by post-hoc Holm-Sidak test: ***= p <0.001 relative to intra-nuclear injected controls, †††= p <0.001 relative to vehicle treated and CpdA-injected group.

4.3.7 Effect of NPY receptor inhibition on the ARC GK-regulated increase in glucose intake

Pharmacological activation of ARC GK with CpdA increases glucose consumption. Stimulation of GK also releases NPY from hypothalamic neurones in ex vivo hypothalamic explants. To further elucidate the mechanism of ARC GK action and to investigate which receptors NPY exerts its effects; I blocked NPY receptors and measured the effects of ARC GK-regulated increase in glucose intake.

Permanent cannulas were stereotactically implanted into the ARC nucleus of rats. NPY receptors Y1 or Y5 were blocked with 10mg/kg BMS193885 (BMS) or 10mg/kg CGP71683 (CGP) respectively by peripheral IP injection. After 30 minutes ARC GK activity was increased with 0.5 nmol CpdA by intra-ARC injection and glucose intake was measured. Consistent with the previous studies, CpdA with pre-treatment of a control substance (vehicle) significantly increased glucose intake over the first hour compared with control (control, 4.93±1.02ml; CpdA, 10.21±0.86ml; n=12 per group, p = <0.001) (figure 4.10a). Glucose intake stimulated by CpdA was significantly attenuated by pre-treatment with Y1 antagonist (BMS; 4.11±0.66ml; n=12 per group, p = <0.001) and Y5 antagonist (CGP; 6.32±0.75ml; n=12 per group, p = <0.001). Y1 or Y5 receptor antagonism did not significantly alter glucose intake alone compared with control without CpdA (control, 4.93±1.02ml; BMS; 3.25±0.30ml; CGP; 4.58±0.77ml; n=12 per group). The effects of all treatments were sustained during 8 hours (figure 4.11b). These results indicate that both Y1 and Y5 receptors are involved in ARC GK-regulated increase in glucose intake.

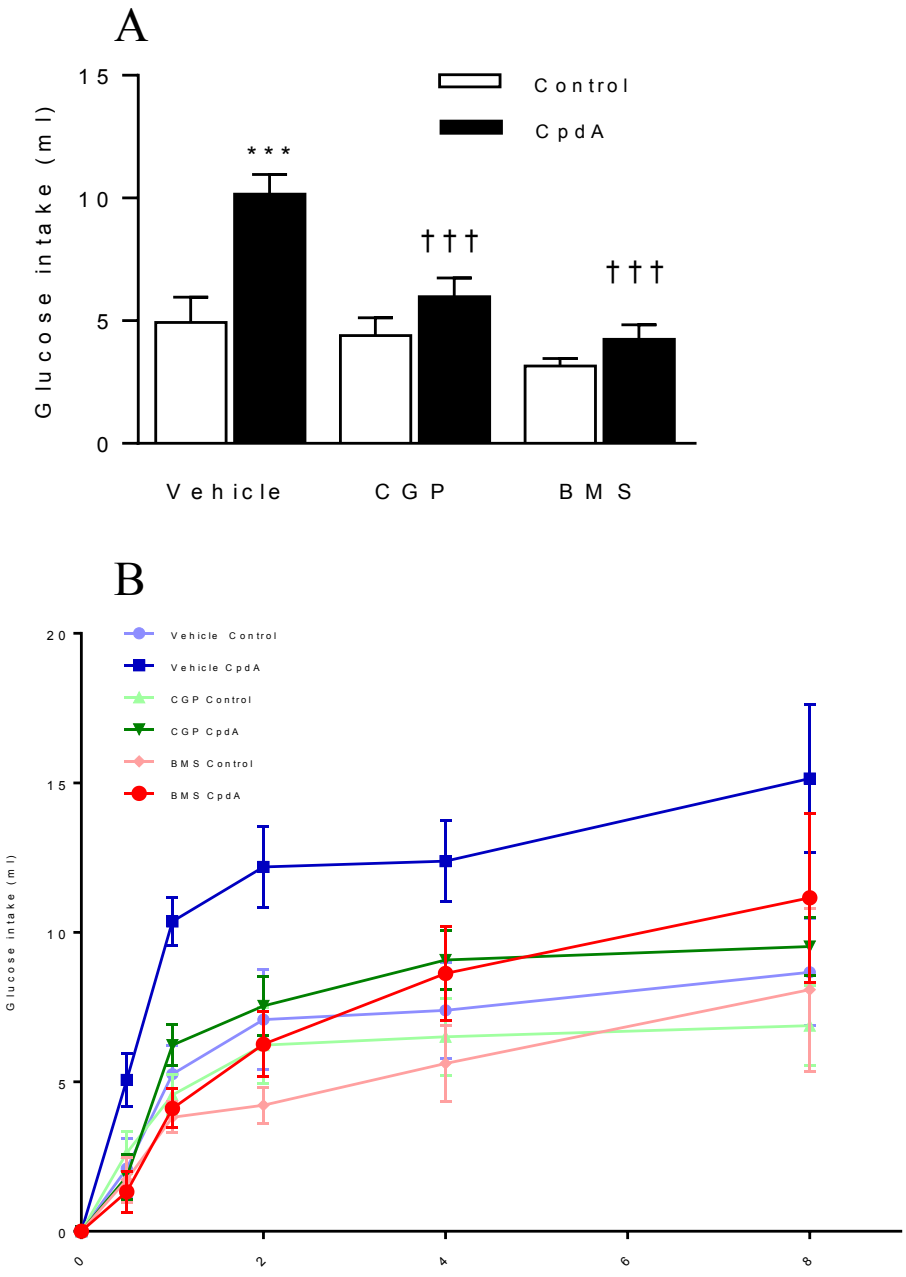


Figure 4.11 Effects of NPY receptor inhibition on the ARC GK-mediated increase in glucose consumption. 2% glucose intake one hour (A) and 8 hours (B) after ARC GK activation following NPY Y1 and Y5 receptor antagonists over 6 sets of injections in a random order during a crossover study. Rats received 100µl IP injection of 10mg/kg BMS 10mg/kg CGP or vehicle (40%DMSO) thirty minutes before stereotactic injection of 0.5 nmol CpdA or control (0.1% DMSO). Data are presented as mean±SEM, n=12 per group. Statistical significance was analysed by one way ANOVA followed by post-hoc Holm-Sidak test: ***= p <0.001 relative to intra-nuclear injected controls, †††= p <0.001 relative to vehicle treated and CpdA-injected group.

4.4 Discussion

4.4.1 The link between GK and K_{ATP} channels in ARC glucose sensing neurones

Understanding how ARC GK neurones are able to sense glucose is important for understanding the differences between ARC and other hypothalamic glucose sensing neurones. Data in chapter 3 showed that acute activation of ARC GK increases glucose intake. The present chapter demonstrates that inhibition of ARC K_{ATP} channels results increases glucose intake similar to when GK is activated. In contrast, pharmacological activation of ARC K_{ATP} channels reduces glucose intake. Regulation of appetite by K_{ATP} channel activators or inhibitors appears to be specific for glucose; when chow and glucose are provided together only glucose intake is affected.

The experiments in this chapter consistently demonstrate that acute activation of ARC GK increases glucose intake. This model is used to investigate the intracellular mechanisms involved in ARC glucose sensing. Pre-treatment with a K_{ATP} channel activator attenuates the GK-regulated increase in glucose intake by reducing glucose intake to baseline levels over 1 hour. This suggests that K_{ATP} channels are involved in the regulation of ARC glucose sensing.

In support of this finding, previous studies have proposed that K_{ATP} channels may be involved in the CRR to hypoglycaemia in other glucose sensing neurones (Miki, Liss et al. 2001, Evans, McCrimmon et al. 2004, Levin, Routh et al. 2004). Injection of diazoxide in the VMN amplifies adrenalin and glucagon release in response to insulin-induced hypoglycaemia similar to inhibition of GK activity (McCrimmon, Evans et al. 2005). This indicates that K_{ATP} channels are linked to hypothalamic GK activity albeit in the regulation of physiological responses other than appetite.

4.4.2 ARC GK neurones release NPY

The hypothalamic explant incubation system was used to investigate neuropeptide release in glucose sensing neurones. Incubation of hypothalamic slices in aCSF has previously been used to demonstrate altered neuropeptide release in response to an increasing glucose concentration (Parton, Ye et al. 2007, Hussain, Richardson et al. 2014). The procedure is optimised for mediobasal hypothalamic slices as each explant includes the VMN and ARC

and parts of the medial preoptic, PVN, DMH, and LHA (Seal, Small et al. 2001). Therefore this technique can be used to investigate neurotransmitter release but is not specific to the ARC.

Both POMC and NPY neurones have been implicated in ARC glucose sensing (Mountjoy, Bailey et al. 2007, Parton, Ye et al. 2007). However, incubation of hypothalamic explants with either a GK activator or K_{ATP} channel inhibitor increases NPY release and does not significantly alter α-MSH release. NPY is a powerful orexigenic peptide and has been shown to increase appetite when injected directly into regions of the hypothalamus (Stanley, Chin et al. 1985). The ARC is a major source of NPY neurones (Wynne, Stanley et al. 2005) therefore it is conceivable that the GK-regulated increase in glucose intake is due to an increase in NPY release. The present study describes a novel role for ARC NPY neurones as they have previously only been shown to be inhibited by glucose, albeit via an AMPK-mediated mechanism (Mountjoy, Bailey et al. 2007).

The findings of NPY in the glucose sensing pathway are consistent with previous reports showing that NPY mediates a preference for carbohydrate intake. Overexpression of NPY in neurones of mice increases food intake and body weight gain when provided with a diet consisting of 50% sucrose powder, but not with normal chow, compared with controls (Kaga, Inui et al. 2001). NPY injections into rat hypothalami increase the preference for carbohydrates and fats over proteins (Stanley, Anderson et al. 1989).

4.4.3 ARC GK-induced increase of glucose intake is mediated via P/Q-type VGCC

To demonstrate that neurotransmitter release from ARC neurones is responsible for the GK-regulated increase in glucose intake, I selectively blocked ARC VGCC. Blocking P/Q type channels, but not L type channels, within the ARC attenuated the GK-regulated increase in glucose intake. Therefore it is likely that P/Q type VGCC are involved in ARC NPY release in glucose sensing neurones. This is consistent with previous reports of P/Q channels in ARC NPY neurones. Decreasing glucose concentrations in ARC primary neurone cultures induces an influx of intracellular calcium ions as a potential marker of GI neuronal firing (Chen, Zhou et al. 2012). Blocking P/Q type VGCC and AMPK signalling, but not blocking L or N type channels, attenuates the calcium influx. However, GI neurones and AMPK are not thought to

be involved in the ARC GK-regulated increase in glucose intake therefore other populations of NPY neurones may be involved.

Most L, N and P/Q type channels are expressed in the pre-synaptic terminals of neurones therefore are able to directly stimulate vesicle release (Catterall, Perez-Reyes et al. 2005). Limited expression of VGCC occurs within axons, which may modulate action potential frequency and rates of repolarisation. However, blocking the channels in the axons will not likely alter action potential frequency during the short time period between injections of VGCC blocker and CpdA. Also, due to the significant effect of the channel blockers, it is likely that the P/Q channels are located in the pre-synaptic terminal and directly regulate vesicle release.

Other VGCC such as L type channels mediate the orexin-A effect on feeding behaviour in the ARC via an AMPK-mediated mechanism (Wu, Wu et al. 2013). As blocking L type channels did not affect the GK-regulated increase in glucose intake, it further shows that this AMPK-mediated decrease in food intake is part of a separate pathway. Both L and N type VGCC have been identified with ARC NPY neurones and may be important in release of hormones or for modulating neuronal firing rather than initiating it (Sahu, Crowley et al. 1993). Due to the lack of effect on GK-regulated glucose intake observed with the L-type VGCC blocker nifedipine, it could be contrived that an appropriate concentration was not injected to exert an effect. A positive control measuring the effect of nifedipine on muscle contractions could have been conducted to demonstrate that the compound was active, as previously described (Longo, Jain et al. 2003).

4.4.4 ARC GK-regulated increase in glucose intake is mediated by Y1 and Y5 receptors

To investigate the role of NPY in ARC glucose sensing neurones, I determined the effects of selectively blocking NPY receptors on the GK-regulated increase in glucose intake. Y1 and Y5 receptors are the major receptors involved in the regulation of feeding (Gerald, Walker et al. 1996, Mashiko, Moriya et al. 2009). Pre-treatment with Y1 antagonist attenuated the GK-regulated increase in glucose intake. Pre-treatment with Y5 antagonist had a similar effect, indicating that both of these receptors are likely to be involved in mediating the effects of NPY in ARC glucose sensing. This is in agreement with previous studies investigating

hypothalamic NPY. ARC NPY neurones project widely within the hypothalamus, acting on neurones involved in food intake in the LH, PVN, DMH and locally within the ARC (Edwards, Abusnana et al. 1999, Mercer, Chee et al. 2011, Lee, Verma et al. 2013). In particular, ARC NPY neurones provide negative feedback to POMC neurones to reduce anorexigenic signals (Broberger, Landry et al. 1997, Cowley, Smart et al. 2001). Therefore a possible pathway for NPY-regulated glucose sensing is by inhibition of POMC neurones to increase appetite. In accord with this hypothesis, the VMN has a high density of Y1 receptors on post-synaptic terminals (Bouali, Fournier et al. 1995). However, VMN Y1 receptors may be predominantly expressed in GI neurones, where activation causes hyperpolarisation and a decrease in glutamatergic activity (Chee, Myers et al. 2010). NPY receptor antagonists here could reduce appetite by promoting anorexigenic pathways via GI neurones.

Other targets of ARC NPY neurones include the PVN (Stanley, Chin et al. 1985, Mercer, Chee et al. 2011). There are two pathways that could contribute to the GK-regulated increase in glucose intake within the PVN. First, NPY acts at Y1 receptors to hyperpolarise MC4R-expressing PVN neurones and therefore inhibit anorexigenic tone (Ghamari-Langroudi, Srisai et al. 2011). Second, NPY acts at pre-synaptic Y1, Y2 and Y5 on GABAergic terminals (Pronchuk, Beck-Sickinger et al. 2002). Dense ARC projections to the PVN make these pathways a likely candidate for NPY mediated glucose sensing.

Furthermore, NPY inhibits orexin and MCH neurones involved in arousal in the LH (Broberger, De Lecea et al. 1998, Fu, Acuna-Goycolea et al. 2004). These neurones can also negatively feedback to regulate ARC NPY expression (Della-Zuana, Presse et al. 2002). However, the role of LH pathways in the control feeding is unclear. In conclusion, it is uncertain where NPY is exerting an effect in the GK-regulated increase in glucose intake, therefore further investigation is required.

ICV injection of BMS reduces NPY-stimulated food intake and slightly, but not significantly, increased food intake on its own (Antal-Zimanyi, Bruce et al. 2008). However, in the present study there was a slight decrease in glucose intake as a result of BMS injection without CpdA. The current evidence on BMS indicates that it is unlikely that a side effect of BMS is causing the decrease in glucose intake observed in the control treatment in the present study (Antal-Zimanyi, Bruce et al. 2008).

As Y1 and Y5 receptor antagonists were injected peripherally, the treatment is not targeted specifically to ARC neurones. Outside of the hypothalamus, Y1 receptors are widely expressed in the cortex, hippocampus, limbic system and NTS (Dumont, Jacques et al. 1998). Y5 receptors are highly expressed in the hippocampus, supraoptic nucleus and piriform nucleus (Morin and Gehlert 2006). Therefore, a non-specific effect of NPY receptor antagonism due to orexigenic actions of these neurones cannot be ruled out. In addition, it is not known why Y1 and Y5 antagonists produced a greater than 50% reduction in GK-regulated glucose intake each if both receptors are involved in the mechanism.

4.4.5 Other mechanisms of glucose sensing

An AMPK-mediated pathway, previously observed in GI neurones, may also be involved in ARC glucose sensing (Claret, Smith et al. 2007). Insulin and low glucose levels increase the ratio of AMP to ATP, which alters AMPK and NO signalling to depolarise neurones via chloride channels (Fioramonti, Lorsignol et al. 2004, Canabal, Potian et al. 2007). Reduced AMPK has been associated with depolarisation of some glucose sensing neurones and could contribute to the change in food intake in the present studies (Mountjoy, Bailey et al. 2007). However, previous experiments performed in this laboratory observed no change in AMPK activity due to increased ARC GK (Hussain, Richardson et al. 2014). Therefore it is unlikely that alterations in AMPK contribute to the change in food intake. This hypothesis is justified by the significant contribution of K_{ATP} channels in the GK-regulated increase in glucose intake. As diazoxide almost completely abolished the increase in glucose intake observed with CpdA injection, it is likely that K_{ATP} channels are the primary mediators of GK action. However, intracellular ATP concentrations have not been investigated to fully confirm this hypothesis.

4.5 Conclusions

A population of glucose sensing neurones in the ARC exert an orexigenic drive to increase consumption of foods rich in glucose when activated. These neurones sense ambient glucose concentrations via phosphorylation of glucose by glucokinase to increase intracellular ATP levels and close K_{ATP} channels. Neuronal depolarisation is partly triggered by increasing K^+ ion concentrations due to closure of K_{ATP} channels, resulting in neuronal firing and vesicular release of NPY via opening of P/Q type VGCC. NPY likely activates Y1 and Y5 receptors to drive orexigenic output and promote glucose intake. This mechanism is separate to neurones used to maintain glucose homeostasis.

Chapter 5: General discussion

5.1 Introduction

Understanding the mechanisms involved in the development of diabetes and obesity is vital for the development of appropriate treatments. However, we lack an in-depth knowledge of altered neuronal circuitry during these disease states. Many diet and environmental factors contribute to the diabetes and obesity pandemics. An increase in the intake of dietary sugar is undoubtedly one of the primary contributing factors, as delineated by the high sugar content in many Western-type diets. A strong effort is thus required to understand why we are designed to consume extra unnecessary sugar.

The CNS plays an important role in the control of feeding. Nutrients are sensed by specialised neurones, activating specific networks to control many different peripheral processes. The CNS is thought to regulate intake of dietary glucose, but the mechanism of this is unclear. This thesis describes work investigating the role of arcuate nucleus glucose sensing neurones in controlling our appetite for glucose.

5.2 Previous investigation of glucose sensing

Glucose sensing neurones play a crucial role in maintaining glucose appetite and homeostasis (Levin, Routh et al. 2004, Kang, Dunn-Meynell et al. 2006). Many glucose sensing neurones are positioned in the ventromedial hypothalamus and other nuclei located near the 3rd and 4th ventricles and circumventricular organs. The glucose phosphorylating enzyme glucokinase (GK) is expressed in glucose sensing neurones and is specifically involved in glucose sensing (Lynch, Tompkins et al. 2000). GK has a higher K_m for glucose than other hexokinases therefore is not saturated at glucose concentrations below 2.5mM and can phosphorylate glucose at a rate that is proportional to the ambient concentration (Printz, Magnuson et al. 1993). In pancreatic β-cells, GK plays an integral role in glucose sensing and the release of insulin (Schuit, Huypens et al. 2001). In the CNS, insulin-induced hypoglycaemia activates glucose sensing neurones and triggers neuronal pathways to alter peripheral hormone release (Levin, Routh et al. 2004, Kang, Dunn-Meynell et al. 2006). For these reasons, GK was selected as an appropriate target for investigating glucose sensing neurones with regard to appetite. Preliminary studies subsequently revealed that 24 or 48

hour fasting in rats increases GK activity in the ARC but not in the VMN or PVN (Hussain, Richardson et al. 2014). Mimicking high ARC GK activity via overexpression of ARC GK in rats increases food intake and body weight. This increase in appetite with increased GK expression challenges the previous hypothesis regarding the role of ARC GK, which was thought to be identical to that in VMN neurones (Kang, Sanders et al. 2008). This preliminary evidence suggests that ARC and VMN GK respond to altered glucose concentrations in a different way.

5.3 Investigating the role of ARC GK in appetite

I have demonstrated that acute activation of ARC GK increases food intake and glucose intake. In contrast, reduction of ARC GK activity reduces glucose intake both acutely and cumulatively. Previous findings have not identified any changes in food intake when VMH GK is altered (Levin, Becker et al. 2008). However, the CNS is thought to regulate glucose intake as it is a primary food source for the brain and has been shown to deliver a reward response via hypothalamic and limbic circuits (Sclafani 2004, Levin, Becker et al. 2008, Domingos, Sordillo et al. 2013). It is postulated that there is a mechanism to promote the consumption of glucose-rich foods, if one is available, to ensure that there is enough to supply the brain.

My findings identify an alternative role for ARC GK than previously hypothesised. In the current model of GK action, an increase in GK activity promotes a decrease in blood glucose concentrations via a counterregulatory hormone response. Insulin-induced hypoglycaemia increases VMH GK mRNA and contributes to an increased responsiveness to glucose (Kang, Sanders et al. 2008). However, I have found that ARC GK neurones act to promote further glucose intake: which likely increase blood glucose concentrations. This is not likely intended for providing homeostatic feedback for plasma glucose regulation; it is probably part of a homeostatic pathway to alter preference for glucose. Fasting induces an increase in ARC GK activity (Hussain, Richardson et al. 2014). It is possible that the palatability of foods is altered during fasting states, in order to specifically increase consumption of glucose for metabolism in the brain. In agreement with this hypothesis, chronically diet-

restricted rats show an increased preference for an artificial sweetener (Chen, Yan et al. 2010).

It is possible that ARC GK neurones involved in the regulation of glucose appetite are the same as those neurones involved in the regulation of glucose homeostasis. Injection of GK activators into the divide between the ARC and VMN produces a counterregulatory response, similar to an injection of GK activators into the VMN alone (Kang, Dunn-Meynell et al. 2006, Levin, Becker et al. 2008, Dunn-Meynell, Sanders et al. 2009, Levin, Magnan et al. 2011). In addition, preliminary unpublished investigations indicate that increasing ARC GK expression improves glucose tolerance in parallel to its effects on appetite (Richardson 2011). However, I have found that ARC GK primarily acts to regulate glucose appetite. These findings are novel and challenge the previous hypothesis that CNS GK only acts to balance glucose homeostasis (Levin, Routh et al. 2004).

5.4 Investigating the mechanisms of ARC glucose sensing

K_{ATP} channels control depolarisation of glucose sensing cells in the CNS and pancreas (Schuit, Huypens et al. 2001, McCrimmon, Evans et al. 2005). I demonstrate that K_{ATP} channels play a similar role in ARC glucose sensing neurones as inhibition of K_{ATP} channels increases glucose intake and activation of K_{ATP} channels inhibits the effects of a GK activator on glucose intake. Furthermore, I demonstrate that hypothalamic GK activation or K_{ATP} channel inhibition leads to NPY release. Blocking P/Q type VGCC or Y1 and Y5 receptors inhibits the GK regulated increase in glucose intake. Therefore it is likely that the primary mechanism for altering glucose intake by ARC GK neurones is via release of vesicular NPY.

A role of NPY in mediating the effects of glucose sensing neurones is in accord with previous electrophysiological work. Seventy five percent of NPY-sensitive neurones in the VMN are also involved in glucose sensing, thus NPY pathways from the ARC could exert an effect on extra-ARC neurones (Chee, Myers et al. 2010). My results provide novel evidence of a direct link between glucose sensing neurones and NPY release *in vivo*. In contrast, altered hypothalamic GK or K_{ATP} channels do not affect α-MSH release from POMC neurones. Consistent with this observation, selective knockout of K_{ATP} channels in POMC neurones

does not affect body weight or food intake (Parton, Ye et al. 2007). Therefore it is likely that ARC glucose sensing neurones rely on orexigenic rather than anorexigenic pathways to exert their effects on food intake. Figure 5.1 summarises the mechanism by which ARC glucose sensing neurones drive altered glucose intake in rats.

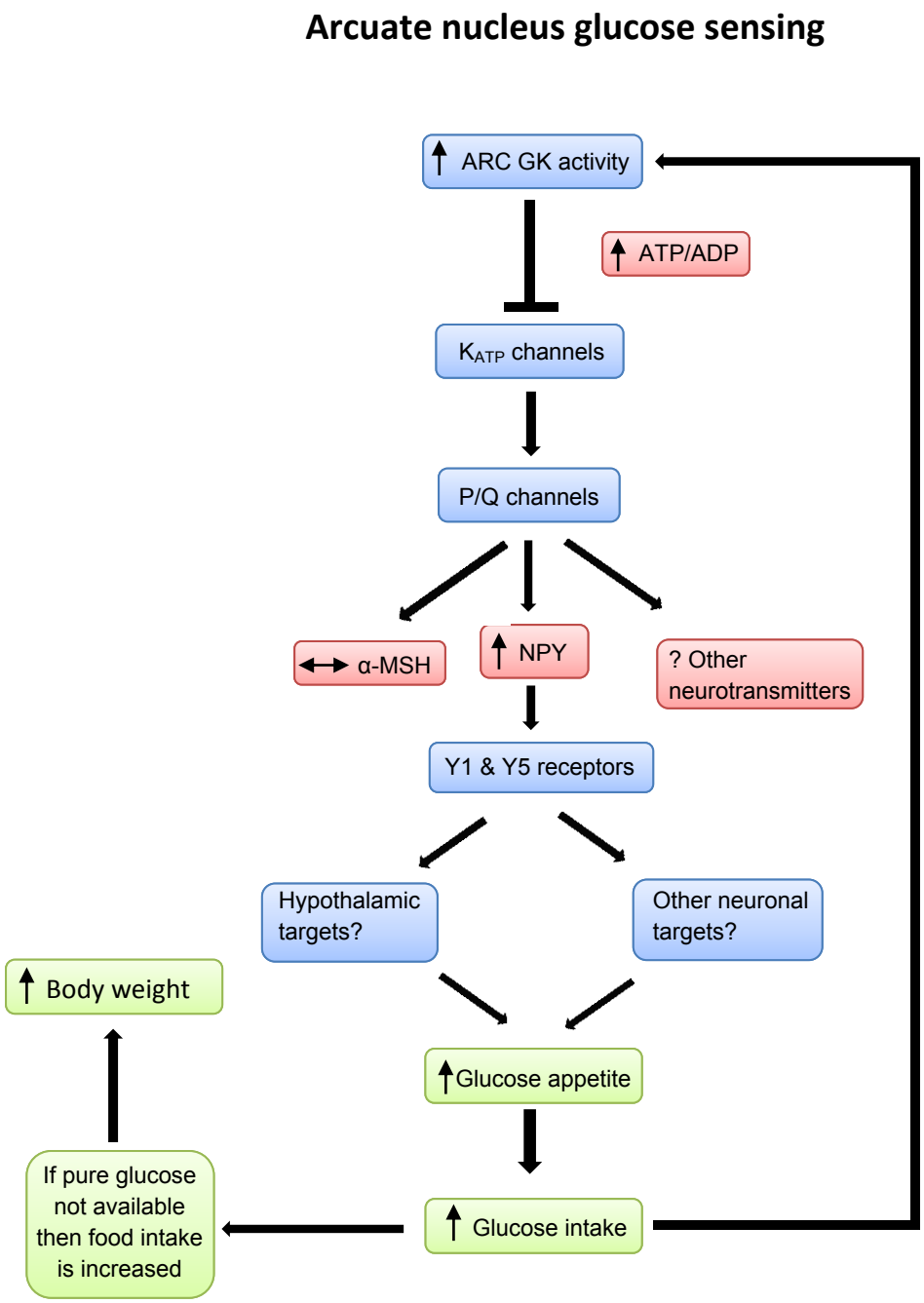


Figure 5.1 Proposed mechanism of ARC glucose sensing: ARC glucokinase activity increases with high ambient glucose concentrations to promote glucose intake if a glucose-rich food source is available. Increased glucose phosphorylation increases the ratio of ATP to ADP and inhibits K_{ATP} channels to trigger neuronal firing. Subsequent activation of P/Q type VGCC releases NPY, which acts at Y1 and Y5 receptors to increase appetite. If a glucose-rich food source is not available then normal food intake is increased, likely increasing body weight.

5.5 The significance of this work for obesity and diabetes research

This work is of clinical significance as it identifies a novel pathway for the regulation of glucose consumption. Currently, GK activators are being investigated as treatments for diabetes by pharmaceutical companies with the goal that they can be used to stimulate insulin secretion from pancreatic β-cells (Matschinsky 2009). As the effects of GK activators outside of the liver and pancreas are relatively unknown, evidence supporting a role for CNS GK is important to assess the specificity of new drugs. However, the effects of weight gain and increased food intake highlighted in the present study do not increase the confidence of the hypothesis that pharmacological activation of GK will be totally beneficial for treating diabetes (U. K. Prospective Diabetes Study Group 1998). Furthermore, weight gain is a common side effect of current treatments of diabetes using sulfonylureas such as glibenclamide. My findings suggest that ARC glucose sensing may be a contributing factor in this side effect, yet a direct link remains unexplored.

The influence of the consumption of dietary sugars to the obesity pandemic is unclear. While there is a strong trend in the increase in dietary sugars in Western-type diets causing obesity, the extent of which glucose causes obesity in relatively unknown. However, a way of inhibiting the postprandial hedonic effects of glucose and other dietary sugars would be of major interest. This work is the first study to show that a long-term alteration of hypothalamic GK activity alters body weight and food intake. Inhibition of ARC GK may be of therapeutic value to combat obesity.

Previously, alterations in food intake and body weight have not been observed in models of altered hypothalamic GK (Levin, Becker et al. 2008, Dunn-Meynell, Sanders et al. 2009). In these studies however, potentially toxic pharmacological agents or immunogenic viral vectors were used to alter GK activity, likely masking any behavioural changes. The present study builds on the previous work by decreasing GK using a non-immunogenic viral vector specifically in the ARC. Exclusive reduction of ARC GK activity by rAAV-GKAS was demonstrated by glucokinase activity assay thus conclusively showing reliability of the technique. In addition, a reproducible response was obtained after stereotactic injection of non-toxic pharmacological agents into the ARC. An increase in glucose consumption was

repeatedly observed after 1 hour from GK activator injection allowing the use of this model for investigating the effects of other pharmacological agents in the same pathway.

5.6 Limitations and unresolved questions

Possible limitations of injections of pharmacological agents into cannulated animals are that all cells within the injection range are targeted, regardless of GK expression. In particular, K_{ATP} channels are expressed in multiple cell types in the ARC therefore injection of activators and inhibitors may lead to non-specific effects. However, the effects of ARC K_{ATP} channel inhibition are similar to that of ARC GK activation and therefore are in accord with the hypothesis that K_{ATP} channels are involved in mediating the effects of GK in the CNS. Inhibition of VGCC and Y receptors may equally cause non-specific effects. However, they had no effect on glucose intake when administered alone. They were only effective in the presence of the GK activator. More specific techniques to alter the machinery involved in ARC glucose sensing could be achieved using Cre-Lox recombination. Selective knockout of GK in the ARC can be attained by inserting LoxP sites around the endogenous GK gene. Stereotactic injection of rAAV Cre recombinase into the ARC would provide knockout of GK in only the affected cells. This would eliminate the requirements for antisense technology, but is only currently available in mice.

Identification of NPY as a neurotransmitter in ARC glucose sensing neurones relied on the use of *ex vivo* hypothalamic explants and their response to pharmacological agents added to the incubating solution. The explants were not specific to the ARC; they included other parts of the mediobasal hypothalamus such as the VMN (Seal, Small et al. 2001). Although two of the major neuropeptides in the ARC were assessed, NPY and α-MSH, other neurotransmitters such as GABA and AgRP could be involved in the response. Further investigation is also required to confidently rule out a role for α-MSH. Therefore the mechanism presented here may be over simplistic as other factors are possibly involved in the response. In addition, basal and drug treatments were not randomly ordered due to the concern that elimination of the drug during washout may not fully occur. It is possible that the explants released increasing peptides over time, which may contribute to the observed effect.

A modified $NADP^+$-coupled assay was used to measure GK activity in hypothalamic tissue (Goward, Hartwell et al. 1986). Previous techniques to measure GK activity used relatively large amounts of tissue therefore it was necessary to optimise a different technique for use in individual hypothalamic nuclei (Osundiji, Lam et al. 2012). Specific hexokinase and N-acetylglucosamine kinase inhibitors were added to each experiment to inhibit phosphorylation of glucose by enzymes other than GK. While the assay was tested against known concentrations of GK and compared with previous methods to measure GK activity, further assessment of accuracy is required. Also, hypothalamic tissue was dissected using a micropunch biopsy, whereas improved methods like micro-laser dissection could more accurately dissect the VMN from the ARC. Alternatively, analysis of GK expression by RT-PCR could provide information on GK expression, but this does not necessarily correlate with GK activity.

Further work is required to understand how ARC GK activity is regulated. A 24 or 48 hour fast increases ARC GK activity in rats, however whether fasting directly influences GK activity is not known (Hussain, Richardson et al. 2014). In addition, GK mRNA expression is affected by circadian rhythms, being highly expressed in-phase with food intake (Frese, Bazwinsky et al. 2007). Real-time measurement of GK activity would be beneficial to fully investigate the regulation of GK activity. The GK activity assay is only able to measure GK activity during one time point whereas continuous real-time measurements could identify changes in activity when rats are provided with a Western-type diet. Similarly, further investigation into the effects of high glucose consumption on GK activity is required to understand whether hypothalamic GK affects adiposity in humans. However, a CSF marker or *in vivo* imaging technique for GK activity is not currently available.

Chronic knockdown of ARC GK moderately reduces cumulative food intake and body weight, providing further evidence that ARC GK regulates appetite. However energy expenditure or locomotor activity were not measured in these animals therefore it has not been confirmed whether the reduction in body weight is due to reduced energy intake or expenditure. As acute activation of ARC GK increases food intake, any changes in body weight are likely due to energy intake. To rule out altered energy expenditure, measurement of oxygen consumption and locomotor activity in ARC GK knockdown rats could be performed using a Comprehensive Laboratory Animal Monitoring System.

5.7 Future directions

Investigation of the role of ARC GK has revealed that central glucose sensing is complex and that it involves many different and intercommunicating networks, which may feedback onto many other feeding networks in the brain. I have characterised one orexigenic pathway involved in glucose sensing in the brain, however other pathways undoubtedly exist. For example the intracellular machinery involved in glucose inhibitory (GI) neurones is still debated (Mountjoy and Rutter 2007). While I demonstrate that orexigenic NPY neurones are integral to the role of ARC glucose sensing neurones in appetite, other neurotransmitters are likely involved. AgRP, ATP, GABA and GLP-1 may regulate neurotransmission or have a paracrine effect in ARC glucose sensing pathways.

I was unable to provide evidence of a direct connection with other known feeding pathways. Rapid progress is currently being made to identify and understand individual feeding pathways in the brain. These studies have made use of Designer Receptors Exclusively Activated by Designer Drugs (DREADD) technology, which can simultaneously trace and inhibit second-order neurones (Aponte, Atasoy et al. 2011, Stachniak, Ghosh et al. 2014). An important advantage of this technology is that remote and non-invasive control of neuronal signalling can be performed. DREADDs can be used to further investigate ARC glucose sensing and would be able to identify which neurones are activated upon NPY activation in the ARC GK regulated increase in glucose intake. Similarly, mice with LoxP sites flanking the GK gene are commercially available therefore could be crossed with NPY-Cre or POMC-Cre mice to selectively knockdown GK in specific neuronal populations.

The physiological roles of other CNS regions with high GK expression require further investigation. In particular, the medial amygdala nucleus and brainstem have high levels of GK therefore are possibly involved in the regulation of glucose appetite (Lynch, Tompkins et al. 2000, Maekawa, Toyoda et al. 2000). The medial NTS in the brainstem is an ideal target for investigation of glucose sensing as it is close to the AP and likely has access to glucose concentrations that are similar to those in the blood. Preliminary unpublished findings reveal that medial NTS GK activity increases due to 14 and 24 hour fasting, similar to ARC GK. Therefore medial NTS GK may regulate food and glucose intake. However, it is unclear

whether knockdown of medial NTS GK in rats alters food intake or body weight therefore further investigation is required.

Finally, GKRP is postulated to regulate CNS GK activity (Alvarez, Roncero et al. 2002). GKRP inhibits GK during low glucose levels and dis-inhibits GK during high glucose levels or upon by treatment with GK activators (Zelent, Raimondo et al. 2014). It is therefore possible that GKRP regulates GK activity in ARC glucose sensing neurones. This hypothesis is in accord with my proposed mechanism of ARC glucose sensing as it suggests that high glucose levels can promote increased GK activity, therefore providing an increased orexigenic drive.

5.8 Conclusion

This thesis identifies a role for a subset of glucose sensing neurones in the arcuate nucleus (ARC) of the hypothalamus to promote glucose intake. A population of GK neurones are able to activate orexigenic pathways in the CNS to drive glucose intake. In the absence of a pure glucose source, general food intake is increased. This pathway demonstrates a mechanism that may contribute to the obesity pandemic and therefore highlights a possible target for therapeutic treatment.

6. References

Adachi, A., M. Kobashi and M. Funahashi (1995). "Glucose-Responsive Neurons In the Brainstem." Obesity Research **3**(S5): 735S-740S.

Alvarez, E., I. Roncero, J. A. Chowen, P. Vázquez and E. Blázquez (2002). "Evidence that glucokinase regulatory protein is expressed and interacts with glucokinase in rat brain." Journal of Neurochemistry **80**(1): 45-53.

Anand, B. K. and J. R. Brobeck (1951). "Localization of a "feeding center" in the hypothalamus of the rat." Proceedings of the Society for Experimental Biology and Medicine **77**(2): 323-324.

Anand, B. K., G. S. Chhina, K. N. Sharma, S. Dua and B. Singh (1964). "Activity of single neurons in the hypothalamic feeding centers: effect of glucose." American Journal of Physiology -- Legacy Content **207**(5): 1146-1154.

Antal-Zimanyi, I., M. A. Bruce, K. L. LeBoulluec, L. G. Iben, G. K. Mattson, R. T. McGovern, J. B. Hogan, C. L. Leahy, S. C. Flowers, J. A. Stanley, A. A. Ortiz and G. S. Poindexter (2008). "Pharmacological characterization and appetite suppressive properties of BMS-193885, a novel and selective neuropeptide Y1 receptor antagonist." European Journal of Pharmacology **590**(1–3): 224-232.

Aponte, Y., D. Atasoy and S. M. Sternson (2011). "AGRP neurons are sufficient to orchestrate feeding behavior rapidly and without training." Nature Neuroscience **14**(3): 351-355.

Arkhammar, P., T. Nilsson, P. Rorsman and P. O. Berggren (1987). "Inhibition of ATP-regulated K+ channels precedes depolarization-induced increase in cytoplasmic free Ca2+ concentration in pancreatic beta-cells." Journal of Biological Chemistry **262**(12): 5448-5454.

Ashcroft, F. M., P. Proks, P. A. Smith, C. Ammala, K. Bokvist and P. Rorsman (1994). "Stimulus-secretion coupling in pancreatic beta cells." Journal of Cellular Biochemistry **55 Suppl**: 54-65.

Ashcroft, F. M. and P. Rorsman (2013). "KATP channels and islet hormone secretion: new insights and controversies." Nature Reviews Endocrinology **9**(11): 660-669.

Bady, I., N. Marty, M. Dallaporta, M. Emery, J. Gyger, D. Tarussio, M. Foretz and B. Thorens (2006). "Evidence From Glut2-Null Mice That Glucose Is a Critical Physiological Regulator of Feeding." Diabetes **55**(4): 988-995.

Baker, D. J., A. M. Atkinson, G. P. Wilkinson, G. J. Coope, A. D. Charles and B. Leighton (2014). "Characterization of the heterozygous glucokinase knockout mouse as a translational disease model for glucose control in type 2 diabetes." British Journal of Pharmacology **171**(7): 1629-1641.

Balfour, R. H., A. M. K. Hansen and S. Trapp (2006). "Neuronal responses to transient hypoglycaemia in the dorsal vagal complex of the rat brainstem." The Journal of Physiology **570**(3): 469-484.

Balthasar, N., R. Coppari, J. McMinn, S. M. Liu, C. E. Lee, V. Tang, C. D. Kenny, R. A. McGovern, S. C. Chua Jr, J. K. Elmquist and B. B. Lowell (2004). "Leptin Receptor Signaling in POMC Neurons Is Required for Normal Body Weight Homeostasis." Neuron **42**(6): 983-991.

Balthasar, N., L. T. Dalgaard, C. E. Lee, J. Yu, H. Funahashi, T. Williams, M. Ferreira, V. Tang, R. A. McGovern, C. D. Kenny, L. M. Christiansen, E. Edelstein, B. Choi, O. Boss, C. Aschkenasi, C. Y. Zhang, K. Mountjoy, T. Kishi, J. K. Elmquist and B. B. Lowell (2005). "Divergence of melanocortin pathways in the control of food intake and energy expenditure." Cell **123**(3): 493-505.

Batterham, R. L., M. A. Cowley, C. J. Small, H. Herzog, M. A. Cohen, C. L. Dakin, A. M. Wren, A. E. Brynes, M. J. Low, M. A. Ghatei, R. D. Cone and S. R. Bloom (2002). "Gut hormone PYY3-36 physiologically inhibits food intake." Nature **418**(6898): 650-654.

Berthoud, H.-R. and C. Morrison (2007). "The Brain, Appetite, and Obesity." Annual Review of Psychology **59**(1): 55-92.

Bi, S., E. E. Ladenheim, G. J. Schwartz and T. H. Moran (2001). "A role for NPY overexpression in the dorsomedial hypothalamus in hyperphagia and obesity of OLETF rats." American Journal of Physiology - Regulatory, Integrative and Comparative Physiology **281**(1): R254-260.

Biggers, D. W., S. R. Myers, D. Neal, R. Stinson, N. B. Cooper, J. B. Jaspan, P. E. Williams, A. D. Cherrington and R. T. Frizzell (1989). "Role of Brain in Counterregulation of Insulin-Induced Hypoglycemia in Dogs." Diabetes **38**(1): 7-16.
Blömer, U., L. Naldini, T. Kafri, D. Trono, I. M. Verma and F. H. Gage (1997). "Highly efficient and sustained gene transfer in adult neurons with a lentivirus vector." Journal of Virology **71**(9): 6641-6649.
Blouet, C. and Gary J. Schwartz (2012). "Brainstem Nutrient Sensing in the Nucleus of the Solitary Tract Inhibits Feeding." Cell Metabolism **16**(5): 579-587.
Boghossian, S., M. Park and D. A. York (2010). "Melanocortin activity in the amygdala controls appetite for dietary fat." American Journal of Physiology - Regulatory, Integrative and Comparative Physiology **298**(2): R385-393.
Borg, W. P., R. S. Sherwin, M. J. During, M. A. Borg and G. I. Shulman (1995). "Local Ventromedial Hypothalamus Glucopenia Triggers Counterregulatory Hormone Release." Diabetes **44**(2): 180-184.
Bouali, S., A. Fournier, S. St-Pierre and F. B. Jolicoeur (1995). "Effects of NPY and NPY 2–36 on body temperature and food intake following administration into hypothalamic nuclei." Brain Researchearch bulletin **36**(2): 131-135.
Bray, G. A. (1996). "Static Theories in a Dynamic World: A Glucodynamic Theory of Food Intake." Obesity Research **4**(5): 489-492.
Broberger, C., L. De Lecea, J. G. Sutcliffe and T. Hokfelt (1998). "Hypocretin/orexin- and melanin-concentrating hormone-expressing cells form distinct populations in the rodent lateral hypothalamus: relationship to the neuropeptide Y and agouti gene-related protein systems." Journal of Comparative Neurology **402**(4): 460-474.
Broberger, C., J. Johansen, C. Johansson, M. Schalling and T. Hökfelt (1998). "The neuropeptide Y/agouti gene-related protein (AGRP) brain circuitry in normal, anorectic, and monosodium glutamate-treated mice." Proceedings of the National Academy of Sciences **95**(25): 15043-15048.
Broberger, C., M. Landry, H. Wong, J. N. Walsh and T. Hökfelt (1997). "Subtypes Y1 and Y2 of the Neuropeptide Y Receptor Are Respectively Expressed in Pro-Opiomelanocortin- and Neuropeptide-Y-Containing Neurons of the Rat Hypothalamic Arcuate Nucleus." Neuroendocrinology **66**(6): 393-408.
Brooks, C. M. and H. F. Lambert (1946). "A study of the effect of limitation of food intake and the method of feeding on the rate of weight gain during hypothalamic obesity in the albino rat." American Journal of Physiology **147**(4): 695-707.
Brunetti-Pierri, N., G. E. Stapleton, D. J. Palmer, Y. Zuo, V. P. Mane, M. J. Finegold, A. L. Beaudet, M. M. Leland, C. E. Mullins and P. Ng (2007). "Pseudo-hydrodynamic Delivery of Helper-dependent Adenoviral Vectors into Non-human Primates for Liver-directed Gene Therapy." Molecular Therapy **15**(4): 732-740.
Buijs, R. M., S. J. Chun, A. Niijima, H. J. Romijn and K. Nagai (2001). "Parasympathetic and sympathetic control of the pancreas: a role for the suprachiasmatic nucleus and other hypothalamic centers that are involved in the regulation of food intake." Journal of Comparative Neurology **431**(4): 405-423.
Burggraf, K. K., A. E. Willing and H. S. Koopmans (1997). "The Effects of Glucose or Lipid Infused Intravenously or Intragastrically on Voluntary Food Intake in the Rat." Physiology & Behavior **61**(6): 787-793.
Canabal, D. D., J. G. Potian, R. G. Duran, J. J. McArdle and V. H. Routh (2007). "Hyperglycemia impairs glucose and insulin regulation of nitric oxide production in glucose-inhibited neurons in the ventromedial hypothalamus." American Journal of Physiology - Regulatory, Integrative and Comparative Physiology **293**(2): R592-R600.
Casali, T. A., R. S. Gomez, T. Moraes-Santos, M. A. Romano-Silva, M. A. Prado and M. V. Gomez (1997). "Different effects of reducing agents on omega-conotoxin GVIA inhibition of [3H]-acetylcholine release from rat cortical slices and guinea-pig myenteric plexus." British Journal of Pharmacology **120**(1): 88-92.

Catterall, W. A. (2000). "Structure and regulation of voltage-gated ca2+ channels." Annual Review of Cell and Developmental Biology **16**(1): 521-555.
Catterall, W. A., E. Perez-Reyes, T. P. Snutch and J. Striessnig (2005). "International Union of Pharmacology. XLVIII. Nomenclature and structure-function relationships of voltage-gated calcium channels." Pharmacology Reviews **57**(4): 411-425.
Centre, H. S. C. I. (2014). Statistics on Obesity, Physical Activity and Diet - England, 2014 Health and Social Care Information Centre. **London, UK**.
Chan, O., M. Lawson, W. Zhu, J. L. Beverly and R. S. Sherwin (2007). "ATP-Sensitive K+ Channels Regulate the Release of GABA in the Ventromedial Hypothalamus During Hypoglycemia." Diabetes **56**(4): 1120-1126.
Chee, M. J. S., M. G. Myers, C. J. Price and W. F. Colmers (2010). "Neuropeptide Y Suppresses Anorexigenic Output from the Ventromedial Nucleus of the Hypothalamus." The Journal of Neuroscience **30**(9): 3380-3390.
Chen, K., J. Yan, Y. Suo, J. Li, Q. Wang and B. Lv (2010). "Nutritional status alters saccharin intake and sweet receptor mRNA expression in rat taste buds." Brain Research **1325**: 53-62.
Chen, Y., J. Zhou, N. Xie, C. Huang, J. Q. Zhang, Z. l. Hu, L. Ni, Y. Jin, F. Wang, J. G. Chen and L. H. Long (2012). "Lowering glucose level elevates [Ca2+]i in hypothalamic arcuate nucleus NPY neurons through P/Q-type Ca2+ channel activation and GSK3beta inhibition." Acta Pharmacologica Sinica **33**(5): 594-605.
Claret, M., M. A. Smith, R. L. Batterham, C. Selman, A. I. Choudhury, L. G. D. Fryer, M. Clements, H. Al-Qassab, H. Heffron, A. W. Xu, J. R. Speakman, G. S. Barsh, B. Viollet, S. Vaulont, M. L. J. Ashford, D. Carling and D. J. Withers (2007). "AMPK is essential for energy homeostasis regulation and glucose sensing by POMC and AgRP neurons." The Journal of Clinical Investigation **117**(8): 2325-2336.
Cone, R., M. Cowley, B. A, D. L. Fan W Fau - Marks, M. J. Marks Dl Fau - Low and M. J. Low (2001). "The arcuate nucleus as a conduit for diverse signals relevant to energy homeostasis." Int, J. Obes Relat Metab Disord Suppl **5**:563-67.
Cowley, M. A., J. L. Smart, M. Rubinstein, M. G. Cerdan, S. Diano, T. L. Horvath, R. D. Cone and M. J. Low (2001). "Leptin activates anorexigenic POMC neurons through a neural network in the arcuate nucleus." Nature **411**(6836): 480-484.
Cox, J. E. and T. L. Powley (1981). "Prior vagotomy blocks VMH obesity in pair-fed rats." American Journal of Physiology **240**(5): E573-583.
Cox, K. H., D. V. DeLeon, L. M. Angerer and R. C. Angerer (1984). "Detection of mrnas in sea urchin embryos by in situ hybridization using asymmetric RNA probes." Developmental Biology **101**(2): 485-502.
De Vos, A., H. Heimberg, E. Quartier, P. Huypens, L. Bouwens, D. Pipeleers and F. Schuit (1995). "Human and rat beta cells differ in glucose transporter but not in glucokinase gene expression." Journal of Clinical Investigation **96**(5): 2489-2495.
de Vries, M. G., L. M. Arseneau, M. E. Lawson and J. L. Beverly (2003). "Extracellular Glucose in Rat Ventromedial Hypothalamus During Acute and Recurrent Hypoglycemia." Diabetes **52**(11): 2767-2773.
Della-Zuana, O., F. Presse, C. Ortola, J. Duhault, J. L. Nahon and N. Levens (2002). "Acute and chronic administration of melanin-concentrating hormone enhances food intake and body weight in Wistar and Sprague-Dawley rats." International Journal of Obesity **26**(10): 1289-1295.
Dhillo, W. S., C. J. Small, S. A. Stanley, P. H. Jethwa, L. J. Seal, K. G. Murphy, M. A. Ghatei and S. R. Bloom (2002). "Hypothalamic Interactions Between Neuropeptide Y, Agouti-Related Protein, Cocaine- and Amphetamine-Regulated Transcript and Alpha-Melanocyte-Stimulating Hormone In Vitro in Male Rats." Journal of Neuroendocrinology **14**(9): 725-730.
Diabetes, U. (2014). "Blood Sugar Level Ranges." from http://www.diabetes.co.uk/diabetes_care/blood-sugar-level-ranges.html.
Diggs-Andrews, K., J. Silverstein and S. Fisher (2009). "Glucose Sensing in the Central Nervous System " from http://www.cyberounds.com/cmecontent/art453.htm?pf=yes.

Domingos, A. I., A. Sordillo, M. O. Dietrich, Z.-W. Liu, L. A. Tellez, J. Vaynshteyn, J. G. Ferreira, M. I. Ekstrand, T. L. Horvath, I. E. de Araujo, J. M. Friedman and J. Nathans (2013). "Hypothalamic melanin concentrating hormone neurons communicate the nutrient value of sugar." eLife **2** e01462.doi:10.7554/elife.01462.
Domingos, A. I., J. Vaynshteyn, H. U. Voss, X. Ren, V. Gradinaru, F. Zang, K. Deisseroth, I. E. de Araujo and J. Friedman (2011). "Leptin regulates the reward value of nutrient." Nature Neuroscience **14**(12): 1562-1568.
Dumont, Y., D. Jacques, P. Bouchard and R. Quirion (1998). "Species differences in the expression and distribution of the neuropeptide Y Y1, Y2, Y4, and Y5 receptors in rodents, guinea pig, and primates brains." Journal of Comparative Neurology **402**(3): 372-384.
Dunlap, K., J. I. Luebke and T. J. Turner (1995). "Exocytotic Ca2+ channels in mammalian central neurons." Trends in Neurosciences **18**(2): 89-98.
Dunn-Meynell, A. A., V. H. Routh, L. Kang, L. Gaspers and B. E. Levin (2002). "Glucokinase Is the Likely Mediator of Glucosensing in Both Glucose-Excited and Glucose-Inhibited Central Neurons." Diabetes **51**(7): 2056-2065.
Dunn-Meynell, A. A., N. M. Sanders, D. Compton, T. C. Becker, J.-I. Eiki, B. B. Zhang and B. E. Levin (2009). "Relationship among Brain and Blood Glucose Levels and Spontaneous and Glucoprivic Feeding." The Journal of Neuroscience **29**(21): 8.
Dus, M., M. Ai and G. S. Suh (2013). "Taste-independent nutrient selection is mediated by a brain-specific Na+ /solute co-transporter in Drosophila." Nature Neuroscience **16**(5): 526-528.
Edwards, C., S. Abusnana, D. Sunter, K. Murphy, M. Ghatei and S. Bloom (1999). "The effect of the orexins on food intake: comparison with neuropeptide Y, melanin-concentrating hormone and galanin." Journal of Endocrinology **160**(3): R7-12.
Erickson, J. C., K. E. Clegg and R. D. Palmiter (1996). "Sensitivity to leptin and susceptibility to seizures of mice lacking neuropeptide Y." Nature **381**(6581): 415-418.
Evans, M. L., R. J. McCrimmon, D. E. Flanagan, T. Keshavarz, X. Fan, E. C. McNay, R. J. Jacob and R. S. Sherwin (2004). "Hypothalamic ATP-sensitive K + Channels Play a Key Role in Sensing Hypoglycemia and Triggering Counterregulatory Epinephrine and Glucagon Responses." Diabetes **53**(10): 2542-2551.
Fioramonti, X., A. Lorsignol, A. Taupignon and L. Pénicaud (2004). "A New ATP-Sensitive K+ Channel–Independent Mechanism Is Involved in Glucose-Excited Neurons of Mouse Arcuate Nucleus." Diabetes **53**(11): 2767-2775.
Fioramonti, X., N. Marsollier, Z. Song, K. A. Fakira, R. M. Patel, S. Brown, T. Duparc, A. Pica-Mendez, N. M. Sanders, C. Knauf, P. Valet, R. J. McCrimmon, A. Beuve, C. Magnan and V. H. Routh (2010). "Ventromedial Hypothalamic Nitric Oxide Production Is Necessary for Hypoglycemia Detection and Counterregulation." Diabetes **59**(2): 519-528.
Frese, T., I. Bazwinsky, E. Muhlbauer and E. Peschke (2007). "Circadian and age-dependent expression patterns of GLUT2 and glucokinase in the pancreatic beta-cell of diabetic and nondiabetic rats." Hormone and Metabolic Research **39**(8): 567-574.
Fu, L.-Y., C. Acuna-Goycolea and A. N. van den Pol (2004). "Neuropeptide Y Inhibits Hypocretin/Orexin Neurons by Multiple Presynaptic and Postsynaptic Mechanisms: Tonic Depression of the Hypothalamic Arousal System." The Journal of Neuroscience **24**(40): 8741-8751.
Gadsby, D. C., P. Vergani and L. Csanady (2006). "The ABC protein turned chloride channel whose failure causes cystic fibrosis." Nature **440**(7083): 477-483.
Galas, L., M. C. Tonon, D. Beaujean, R. Fredriksson, D. Larhammar, I. Lihrmann, S. Jegou, A. Fournier, N. Chartrel and H. Vaudry (2002). "Neuropeptide Y inhibits spontaneous α-melanocyte-stimulating hormone (α-MSH) release via a Y5 receptor and suppresses thyrotropin-releasing hormone-induced α-MSH secretion via a Y1 receptor in frog melanotrope cells." Endocrinology **143**(5): 1686-1694.
Garcia, M., C. Millan, C. Balmaceda-Aguilera, T. Castro, P. Pastor, H. Montecinos, K. Reinicke, F. Zuniga, J. C. Vera, S. A. Onate and F. Nualart (2003). "Hypothalamic ependymal-glial cells express the

glucose transporter GLUT2, a protein involved in glucose sensing." Journal of Neurochemistry **86**(3): 709-724.
Gardiner, J. V., W. M. Kong, H. Ward, K. G. Murphy, W. S. Dhillo and S. R. Bloom (2005). "AAV mediated expression of anti-sense neuropeptide Y cRNA in the arcuate nucleus of rats results in decreased weight gain and food intake." Biochem Biophys Res, Commun **327**(4): 1088-1093.
Gardlik, R., R. Palffy, J. Hodosy, J. Lukacs, J. Turna and P. Celec (2005). "Vectors and delivery systems in gene therapy." Medical Science Monitor **11**(4): Ra110-121.
Gerald, C., M. W. Walker, L. Criscione, E. L. Gustafson, C. Batzl-Hartmann, K. E. Smith, P. Vaysse, M. M. Durkin, T. M. Laz, D. L. Linemeyer, A. O. Schaffhauser, S. Whitebread, K. G. Hofbauer, R. I. Taber, T. A. Branchek and R. L. Weinshank (1996). "A receptor subtype involved in neuropeptide-Y-induced food intake." Nature **382**(6587): 168-171.
Ghamari-Langroudi, M., D. Srisai and R. D. Cone (2011). "Multinodal regulation of the arcuate/paraventricular nucleus circuit by leptin." Proceedings of the National Academy of Sciences **108**(1): 355-360.
Goward, C. R., R. Hartwell, T. Atkinson and M. D. Scawen (1986). "The purification and characterization of glucokinase from the thermophile Bacillus stearothermophilus." Biochem J **237**(2): 415-420.
Gribble, F. M., S. J. Tucker and F. M. Ashcroft (1997). "The essential role of the Walker A motifs of SUR1 in K-ATP channel activation by Mg-ADP and diazoxide." The EMBO Journal **16**(6): 1145-1152.
Grill, H. J. (2006). "Distributed Neural Control of Energy Balance: Contributions from Hindbrain and Hypothalamus." Obesity **14**(S8): 216S-221S.
Grimm, D., A. Kern, K. Rittner and J. A. Kleinschmidt (1999). "Novel tools for production and purification of recombinant adenoassociated virus vectors." Human Gene Therapy **9**(18):2745-2760.
Gropp, E., M. Shanabrough, E. Borok, A. W. Xu, R. Janoschek, T. Buch, L. Plum, N. Balthasar, B. Hampel, A. Waisman, G. S. Barsh, T. L. Horvath and J. C. Bruning (2005). "Agouti-related peptide-expressing neurons are mandatory for feeding." Nature Neuroscience **8**(10): 1289-1291.
Grossbard, L. and R. T. Schimke (1966). "Multiple Hexokinases of Rat Tissues: purification and comparison of soluble forms." Journal of Biological Chemistry **241**(15): 3546-3560.
Grupe, A., B. Hultgren, A. Ryan, Y. H. Ma, M. Bauer and T. A. Stewart (1995). "Transgenic knockouts reveal a critical requirement for pancreatic β cell glucokinase in maintaining glucose homeostasis." Cell **83**(1): 69-78.
Guan, X. M., H. Yu, M. Trumbauer, E. Frazier, L. H. Van der Ploeg and H. Chen (1998). "Induction of neuropeptide Y expression in dorsomedial hypothalamus of diet-induced obese mice." Neuroreport **9**(15): 3415-3419.
Halaas, J. L., K. S. Gajiwala, M. Maffei, S. L. Cohen, B. T. Chait, D. Rabinowitz, R. L. Lallone, S. K. Burley and J. M. Friedman (1995). "Weight-reducing effects of the plasma protein encoded by the obese gene." Science **269**(5223): 543-546.
Hambrock, A., C. Löffler-Walz and U. Quast (2002). "Glibenclamide binding to sulphonylurea receptor subtypes: dependence on adenine nucleotides." British Journal of Pharmacology **136**(7): 995-1004.
Harris, G. C., M. Wimmer and G. Aston-Jones (2005). "A role for lateral hypothalamic orexin neurons in reward seeking." Nature **437**(7058): 556-559.
Hawrylycz, M., L. Ng, D. Feng, S. Sunkin, A. Szafer and C. Dang (2014). The Allen Brain Atlas. Springer Handbook of Bio-/Neuroinformatics. N. Kasabov, Springer Berlin Heidelberg**:** 1111-1126.
Hayes, M. R., K. P. Skibicka, T. M. Leichner, D. J. Guarnieri, R. J. DiLeone, K. K. Bence and H. J. Grill (2010). "Endogenous Leptin Signaling in the Caudal Nucleus Tractus Solitarius and Area Postrema Is Required for Energy Balance Regulation." Cell Metabolism **11**(1): 77-83.
Hetherington, A. W. and S. W. Ranson (1940). "Hypothalamic lesions and adiposity in the rat." The Anatomical Record **78**(2): 149-172.

Horvath, T. L., S. Diano and A. N. van den Pol (1999). "Synaptic Interaction between Hypocretin (Orexin) and Neuropeptide Y Cells in the Rodent and Primate Hypothalamus: A Novel Circuit Implicated in Metabolic and Endocrine Regulations." The Journal of Neuroscience **19**(3): 1072-1087.
Howard, D. B., K. Powers, Y. Wang and B. K. Harvey (2008). "Tropism and toxicity of adeno-associated viral vector serotypes 1, 2, 5, 6, 7, 8, and 9 in rat neurons and glia in vitro." Virology **372**(1): 24-34.
Hussain, S., E. Richardson, Y. Ma, C. Holton, I. De Backer, N. Buckley, W. Dhillo, G. Bewick, S. Zhang, D. Carling, S. Bloom and J. Gardiner (2014). "Glucokinase activity in the arcuate nucleus regulates glucose intake." Journal of Clinical Investigation **125**(1): 337-349.
Ibrahim, N., M. A. Bosch, J. L. Smart, J. Qiu, M. Rubinstein, O. K. Rønnekleiv, M. J. Low and M. J. Kelly (2003). "Hypothalamic Proopiomelanocortin Neurons Are Glucose Responsive and Express KATP Channels." Endocrinology **144**(4): 1331-1340.
Inagaki, N., T. Gonoi and S. Seino (1997). "Subunit stoichiometry of the pancreatic β-cell ATP-sensitive K+ channel." FEBS Letters **409**(2): 232-236.
Iynedjian, P. B., P. R. Pilot, T. Nouspikel, J. L. Milburn, C. Quaade, S. Hughes, C. Ucla and C. B. Newgard (1989). "Differential expression and regulation of the glucokinase gene in liver and islets of Langerhans." Proc Natl Acad Sci U S A **86**(20): 7838-7842.
Jetton, T. L., Y. Liang, C. C. Pettepher, E. C. Zimmerman, F. G. Cox, K. Horvath, F. M. Matschinsky and M. A. Magnuson (1994). "Analysis of upstream glucokinase promoter activity in transgenic mice and identification of glucokinase in rare neuroendocrine cells in the brain and gut." J Biol Chem **269**(5): 3641-3654.
Jo, Y.-H., Y. Su, R. Gutierrez-Juarez and S. Chua (2009). "Oleic Acid Directly Regulates POMC Neuron Excitability in the Hypothalamus." American Physiological Society **101**(5): 2305-2316.
Johnson, P. M. and P. J. Kenny (2010). "Dopamine D2 receptors in addiction-like reward dysfunction and compulsive eating in obese rats." Nature Neuroscience **13**(5): 635-641.
Kaga, T., A. Inui, M. Okita, A. Asakawa, N. Ueno, M. Kasuga, M. Fujimiya, N. Nishimura, R. Dobashi, Y. Morimoto, I. M. Liu and J. T. Cheng (2001). "Modest overexpression of neuropeptide Y in the brain leads to obesity after high-sucrose feeding." Diabetes **50**(5): 1206-1210.
Kamata, K., M. Mitsuya, T. Nishimura, J.-i. Eiki and Y. Nagata (2004). "Structural Basis for Allosteric Regulation of the Monomeric Allosteric Enzyme Human Glucokinase." Structure **12**(3): 429-438.
Kang, L., A. A. Dunn-Meynell, V. H. Routh, L. D. Gaspers, Y. Nagata, T. Nishimura, J. Eiki, B. B. Zhang and B. E. Levin (2006). "Glucokinase Is a Critical Regulator of Ventromedial Hypothalamic Neuronal Glucosensing." Diabetes **55**(2): 412-420.
Kang, L., V. H. Routh, E. V. Kuzhikandathil, L. D. Gaspers and B. E. Levin (2004). "Physiological and Molecular Characteristics of Rat Hypothalamic Ventromedial Nucleus Glucosensing Neurons." Diabetes **53**(3): 549-559.
Kang, L., N. M. Sanders, A. A. Dunn-Meynell, L. D. Gaspers, V. H. Routh, A. P. Thomas and B. E. Levin (2008). "Prior hypoglycemia enhances glucose responsiveness in some ventromedial hypothalamic glucosensing neurons." American Journal of Physiology - Regulatory, Integrative and Comparative Physiology **294**(3): R784-R792.
Karschin, C., C. Ecke, F. M. Ashcroft and A. Karschin (1997). "Overlapping distribution of KATP channel-forming Kir6.2 subunit and the sulfonylurea receptor SUR1 in rodent brain." FEBS Letters **401**(1): 59-64.
Kay, M. A. (2011). "State-of-the-art gene-based therapies: the road ahead." Nature Reviews Genetics **12**(5): 316-328.
Kim, M. S., M. Rossi, S. Abusnana, D. Sunter, D. G. Morgan, C. J. Small, C. M. Edwards, M. M. Heath, S. A. Stanley, L. J. Seal, J. R. Bhatti, D. M. Smith, M. A. Ghatei and S. R. Bloom (2000). "Hypothalamic localization of the feeding effect of agouti-related peptide and alpha-melanocyte-stimulating hormone." Diabetes **49**(2): 177-182.
King, B. M. (2006). "The rise, fall, and resurrection of the ventromedial hypothalamus in the regulation of feeding behavior and body weight." Physiology & Behavior **87**(2): 221-244.

Kozlowski, R. Z., C. N. Hales and M. L. J. Ashford (1989). "Dual effects of diazoxide on ATP-K+ currents recorded from an insulin-secreting cell line." British Journal of Pharmacology **97**(4): 1039-1050.
Kumar, M. and G. G. Carmichael (1997). "Nuclear antisense RNA induces extensive adenosine modifications and nuclear retention of target transcripts." Proceedings of the National Academy of Sciences **94**(8): 3542-3547.
Kumar, M. and G. G. Carmichael (1998). "Antisense RNA: function and fate of duplex RNA in cells of higher eukaryotes." Microbiol Mol Biol Rev **62**(4): 1415-1434.
Kumar, M., B. Keller, N. Makalou and R. E. Sutton (2001). "Systematic determination of the packaging limit of lentiviral vectors." Human Gene Therapy **12**(15): 1893-1905.
Kurata, K., K. Fujimoto, T. Sakata, H. Etou and K. Fukagawa (1986). "D-glucose suppression of eating after intra-third ventricle infusion in rat." Physiology & Behavior **37**(4): 615-620.
Lam, A. P. and D. A. Dean (2010). "Progress and prospects: nuclear import of nonviral vectors." Gene Therapy **17**(4): 439-447.
Lam, T. K., A. Pocai, R. Gutierrez-Juarez, S. Obici, J. Bryan, L. Aguilar-Bryan, G. J. Schwartz and L. Rossetti (2005). "Hypothalamic sensing of circulating fatty acids is required for glucose homeostasis." Nature Medicine **11**(3): 320-327.
Lam, T. K., G. J. Schwartz and L. Rossetti (2005). "Hypothalamic sensing of fatty acids." Nature Neuroscience **8**(5): 579-584.
Langlet, F., Barry E. Levin, S. Luquet, M. Mazzone, A. Messina, Ambrose A. Dunn-Meynell, E. Balland, A. Lacombe, D. Mazur, P. Carmeliet, Sebastien G. Bouret, V. Prevot and B. Dehouck (2013). "Tanycytic VEGF-A Boosts Blood-Hypothalamus Barrier Plasticity and Access of Metabolic Signals to the Arcuate Nucleus in Response to Fasting." Cell Metabolism **17**(4): 607-617.
Langlet, F., A. Mullier, S. G. Bouret, V. Prevot and B. Dehouck (2013). "Tanycyte-like cells form a blood–cerebrospinal fluid barrier in the circumventricular organs of the mouse brain." Journal of Comparative Neurology **521**(15): spc1-spc1.
Lee, K., B. Li, X. Xi, Y. Suh and R. J. Martin (2005). "Role of neuronal energy status in the regulation of adenosine 5'-monophosphate-activated protein kinase, orexigenic neuropeptides expression, and feeding behavior." Endocrinology **146**(1): 3-10.
Lee, S. J., S. Verma, S. E. Simonds, M. A. Kirigiti, P. Kievit, S. R. Lindsley, A. Loche, M. S. Smith, M. A. Cowley and K. L. Grove (2013). "Leptin Stimulates Neuropeptide Y and Cocaine Amphetamine-Regulated Transcript Coexpressing Neuronal Activity in the Dorsomedial Hypothalamus in Diet-Induced Obese Mice." The Journal of Neuroscience **33**(38): 15306-15317.
Leino, R. L., D. Z. Gerhart, A. M. van Bueren, A. L. McCall and L. R. Drewes (1997). "Ultrastructural localization of GLUT 1 and GLUT 3 glucose transporters in rat brain." Journal of Neuroscience Research **49**(5): 617-626.
Leloup, C., M. Orosco, P. Serradas, S. Nicolaïdis and L. Pénicaud (1998). "Specific inhibition of GLUT2 in arcuate nucleus by antisense oligonucleotides suppresses nervous control of insulin secretion." Molecular Brain Research **57**(2): 275-280.
Levin, B. E., T. C. Becker, J.-i. Eiki, B. B. Zhang and A. A. Dunn-Meynell (2008). "Ventromedial Hypothalamic Glucokinase Is an Important Mediator of the Counterregulatory Response to Insulin-Induced Hypoglycemia." Diabetes **57**(5): 1371-1379.
Levin, B. E., C. Magnan, A. Dunn-Meynell and C. Le Foll (2011). "Metabolic Sensing and the Brain: Who, What, Where, and How?" Endocrinology **152**(7): 2552-2557.
Levin, B. E., V. H. Routh, L. Kang, N. M. Sanders and A. A. Dunn-Meynell (2004). "Neuronal glucosensing: what do we know after 50 years?" Diabetes **53**(10): 2521-2528.
Li, B., X. Xi, D. S. Roane, D. H. Ryan and R. J. Martin (2003). "Distribution of glucokinase, glucose transporter GLUT2, sulfonylurea receptor-1, glucagon-like peptide-1 receptor and neuropeptide Y messenger RNAs in rat brain by quantitative real time RT-PCR." Molecular Brain Research **113**(1–2): 139-142.
Liang, Y., H. Najafi and F. M. Matschinsky (1990). "Glucose regulates glucokinase activity in cultured islets from rat pancreas." Journal of Biological Chemistry **265**(28): 16863-16866.

Llinas, R., M. Sugimori, J. W. Lin and B. Cherksey (1989). "Blocking and isolation of a calcium channel from neurons in mammals and cephalopods utilizing a toxin fraction (FTX) from funnel-web spider poison." Proceedings of the National Academy of Sciences **86**(5): 1689-1693.
Longo, M., V. Jain, Y. P. Vedernikov, G. D. Hankins, R. E. Garfield and G. R. Saade (2003). "Effects of L-type Ca(2+)-channel blockade, K(+)(ATP)-channel opening and nitric oxide on human uterine contractility in relation to gestational age and labour." Molecular Human Reproduction **9**(3): 159-164.
Luquet, S., F. A. Perez, T. S. Hnasko and R. D. Palmiter (2005). "NPY/AgRP Neurons Are Essential for Feeding in Adult Mice but Can Be Ablated in Neonates." Science **310**(5748): 683-685.
Lynch, R. M., L. S. Tompkins, H. L. Brooks, A. A. Dunn-Meynell and B. E. Levin (2000). "Localization of glucokinase gene expression in the rat brain." Diabetes **49**(5): 693-700.
Maekawa, F., Y. Toyoda, N. Torii, I. Miwa, R. C. Thompson, D. L. Foster, S. Tsukahara, H. Tsukamura and K.-i. Maeda (2000). "Localization of Glucokinase-Like Immunoreactivity in the Rat Lower Brain Stem: For Possible Location of Brain Glucose-Sensing Mechanisms." Endocrinology **141**(1): 375-384.
Magnuson, M. A. and K. D. Shelton (1989). "An alternate promoter in the glucokinase gene is active in the pancreatic beta cell." Journal of Biological Chemistry **264**(27): 15936-15942.
Martin, G. M., P. C. Chen, P. Devaraneni and S. L. Shyng (2013). "Pharmacological rescue of trafficking-impaired ATP-sensitive potassium channels." Frontiers in Physiology **4**: 386.
Mashiko, S., R. Moriya, A. Ishihara, A. Gomori, H. Matsushita, S. Egashira, H. Iwaasa, T. Takahashi, Y. Haga, T. Fukami and A. Kanatani (2009). "Synergistic interaction between neuropeptide Y1 and Y5 receptor pathways in regulation of energy homeostasis." European Journal of Pharmacology **615**(1-3): 113-117.
Massa, M. L., J. J. Gagliardino and F. Francini (2011). "Liver glucokinase: An overview on the regulatorymechanisms of its activity." IUBMB Life **63**(1): 1-6.
Matschinsky, F. M. (2009). "Assessing the potential of glucokinase activators in diabetes therapy." Nat Rev Drug Discov **8**(5): 399-416.
Matschinsky, F. M. and J. E. Ellerman (1968). "Metabolism of Glucose in the Islets of Langerhans." Journal of Biological Chemistry **243**(10): 2730-2736.
Mayer, J. (1953). "Glucostatic Mechanism of Regulation of Food Intake." New England Journal of Medicine **249**(1): 13-16.
Mayer, J. (1955). "Regulation of energy intake and the body weight: the glucostatic theory and the lipostatic hypothesis." Annals of the New York Academy of Sciences **63**(1): 15-43.
McCrimmon, R. J., M. L. Evans, X. Fan, E. C. McNay, O. Chan, Y. Ding, W. Zhu, D. X. Gram and R. S. Sherwin (2005). "Activation of ATP-Sensitive K+ Channels in the Ventromedial Hypothalamus Amplifies Counterregulatory Hormone Responses to Hypoglycemia in Normal and Recurrently Hypoglycemic Rats." Diabetes **54**(11): 3169-3174.
Mercer, R. E., M. J. S. Chee and W. F. Colmers (2011). "The role of NPY in hypothalamic mediated food intake." Frontiers in Neuroendocrinology **32**(4): 398-415.
Migrenne, S., C. Cruciani-Guglielmacci, L. Kang, R. Wang, C. Rouch, A.-L. Lefèvre, A. Ktorza, V. H. Routh, B. E. Levin and C. Magnan (2006). "Fatty Acid Signaling in the Hypothalamus and the Neural Control of Insulin Secretion." Diabetes **55**(Supplement 2): S139-S144.
Miki, T., B. Liss, K. Minami, T. Shiuchi, A. Saraya, Y. Kashima, M. Horiuchi, F. Ashcroft, Y. Minokoshi, J. Roeper and S. Seino (2001). "ATP-sensitive K+ channels in the hypothalamus are essential for the maintenance of glucose homeostasis." Nature Neuroscience **4**(5): 507-512.
Miller, C. C., R. J. Martin, M. L. Whitney and G. L. Edwards (2002). "Intracerebroventricular injection of fructose stimulates feeding in rats." Nutr Neurosci **5**(5): 359-362.
Mitrakou, A., C. Ryan, T. Veneman, M. Mokan, T. Jenssen, I. Kiss, J. Durrant, P. Cryer and J. Gerich (1991). "Hierarchy of glycemic thresholds for counterregulatory hormone secretion, symptoms, and cerebral dysfunction." American Journal of Physiology - Endocrinology and Metabolism **260**(1): E67-E74.

Miwa, I., Y. Mita, T. Murata, J. Okuda, M. Sugiura, Y. Hamada and T. Chiba (1994). "Utility of 3-O-methyl-N-acetyl-D-glucosamine, an N-acetylglucosamine kinase inhibitor, for accurate assay of glucokinase in pancreatic islets and liver." Enzyme Protein **48**(3): 135-142.
Morin, S. M. and D. Gehlert (2006). "Distribution of NPY Y5-like immunoreactivity in the rat brain." Journal of Molecular Neuroscience **29**(2): 109-114.
Morris, J. F. and D. V. Pow (1991). "Widespread release of peptides in the central nervous system: Quantitation of tannic acid-captured exocytoses." The Anatomical Record **231**(4): 437-445.
Mountjoy, P. D., S. J. Bailey and G. A. Rutter (2007). "Inhibition by glucose or leptin of hypothalamic neurons expressing neuropeptide Y requires changes in AMP-activated protein kinase activity." Diabetologia **50**(1): 168-177.
Mountjoy, P. D. and G. A. Rutter (2007). "Glucose sensing by hypothalamic neurones and pancreatic islet cells: AMPle evidence for common mechanisms?" Experimental Physiology **92**(2): 311-319.
Mueckler, M. and B. Thorens (2013). "The SLC2 (GLUT) family of membrane transporters." Molecular Aspects of Medicine **34**(2–3): 121-138.
Mullier, A., S. G. Bouret, V. Prevot and B. Dehouck (2010). "Differential distribution of tight junction proteins suggests a role for tanycytes in blood-hypothalamus barrier regulation in the adult mouse brain." The Journal of Comparative Neurology **518**(7): 943-962.
Muroya, S., T. Yada, S. Shioda and M. Takigawa (1999). "Glucose-sensitive neurons in the rat arcuate nucleus contain neuropeptide Y." Neuroscience Letters **264**(1-3): 113-116.
Murphy, B. A., K. A. Fakira, Z. Song, A. Beuve and V. H. Routh (2009). "AMP-activated protein kinase and nitric oxide regulate the glucose sensitivity of ventromedial hypothalamic glucose-inhibited neurons." American Journal of Physiology - Cell Physiology **297**(3): C750-C758.
Nagashima, K., A. Takahashi, H. Ikeda, A. Hamasaki, N. Kuwamura, Y. Yamada and Y. Seino (2004). "Sulfonylurea and non-sulfonylurea hypoglycemic agents: pharmachological properties and tissue selectivity." Diabetes Research and Clinical Practice **66, Supplement**(0): S75-S78.
Navarro, M., F. R. De Fonseca, E. Alvarez, J. A. Chowen, J. A. Zueco, R. Gomez, J. Eng and E. Blázquez (1996). "Colocalization of Glucagon-Like Peptide-1 (GLP-1) Receptors, Glucose Transporter GLUT-2, and Glucokinase mRNAs in Rat Hypothalamic Cells: Evidence for a Role of GLP-1 Receptor Agonists as an Inhibitory Signal for Food and Water Intake." Journal of Neurochemistry **67**(5): 1982-1991.
O'Keefe, E. P. (2013). "siRNAs and shRNAs: Tools for Protein Knockdown by Gene Silencing." MATER METHODS **3**(197).
O'Malley, D., F. Reimann, A. K. Simpson and F. M. Gribble (2006). "Sodium-Coupled Glucose Cotransporters Contribute to Hypothalamic Glucose Sensing." Diabetes **55**(12): 3381-3386.
Oh, S. W., J. A. Harris, L. Ng, B. Winslow, N. Cain, S. Mihalas, Q. Wang, C. Lau, L. Kuan, A. M. Henry, M. T. Mortrud, B. Ouellette, T. N. Nguyen, S. A. Sorensen, C. R. Slaughterbeck, W. Wakeman, Y. Li, D. Feng, A. Ho, E. Nicholas, K. E. Hirokawa, P. Bohn, K. M. Joines, H. Peng, M. J. Hawrylycz, J. W. Phillips, J. G. Hohmann, P. Wohnoutka, C. R. Gerfen, C. Koch, A. Bernard, C. Dang, A. R. Jones and H. Zeng (2014). "A mesoscale connectome of the mouse brain." Nature **508**(7495): 207-214.
Osundiji, M. A., D. D. Lam, J. Shaw, C.-Y. Yueh, S. P. Markkula, P. Hurst, C. Colliva, A. Roda, L. K. Heisler and M. L. Evans (2012). "Brain Glucose Sensors Play a Significant Role in the Regulation of Pancreatic Glucose-Stimulated Insulin Secretion." Diabetes **61**(2): 321-328.
Page, K. A., O. Chan, J. Arora and et al. (2013). "EFfects of fructose vs glucose on regional cerebral blood flow in brain regions involved with appetite and reward pathways." Journal of the American Medical Association **309**(1): 63-70.
Palomeque, J., E. R. Chemaly, P. Colosi, J. A. Wellman, S. Zhou, F. Del Monte and R. J. Hajjar (2007). "Efficiency of eight different AAV serotypes in transducing rat myocardium in vivo." Gene Therapy **14**(13): 989-997.
Panksepp, J. and J. Rossi (1981). "d-Glucose infusions into the basal ventromedial hypothalamus and feeding." Behavioural Brain Research **3**(3): 381-392.

Park, Y. B., Y. J. Choi, S. Y. Park, J. Y. Kim, S. H. Kim, D. K. Song, K. C. Won and Y. W. Kim (2011). "ATP-Sensitive Potassium Channel-Deficient Mice Show Hyperphagia but Are Resistant to Obesity." Diabetes & Metabolism Journal **35**(3): 219-225.
Parker, J. A. and S. R. Bloom (2012). "Hypothalamic neuropeptides and the regulation of appetite." Neuropharmacology **63**(1): 18-30.
Parkinson, J. R., O. B. Chaudhri, Y. T. Kuo, B. C. Field, A. H. Herlihy, W. S. Dhillo, M. A. Ghatei, S. R. Bloom and J. D. Bell (2009). "Differential patterns of neuronal activation in the brainstem and hypothalamus following peripheral injection of GLP-1, oxyntomodulin and lithium chloride in mice detected by manganese-enhanced magnetic resonance imaging (MEMRI)." Neuroimage **44**(3): 1022-1031.
Parsons, M. P. and M. Hirasawa (2010). "ATP-Sensitive Potassium Channel-Mediated Lactate Effect on Orexin Neurons: Implications for Brain Energetics during Arousal." The Journal of Neuroscience **30**(24): 8061-8070.
Parton, L. E., C. P. Ye, R. Coppari, P. J. Enriori, B. Choi, C.-Y. Zhang, C. Xu, C. R. Vianna, N. Balthasar, C. E. Lee, J. K. Elmquist, M. A. Cowley and B. B. Lowell (2007). "Glucose sensing by POMC neurons regulates glucose homeostasis and is impaired in obesity." Nature **449**(7159): 228-232.
Paxinos, G. and C. Watson (2007). The rat brain in stereotaxic coordinates. 6th Edition San Diego, Elsevier Academic Press
Pellerin, L., A. K. Bouzier-Sore, A. Aubert, S. Serres, M. Merle, R. Costalat and P. J. Magistretti (2007). "Activity-dependent regulation of energy metabolism by astrocytes: an update." Glia **55**(12): 1251-1262.
Pellerin, L. and P. J. Magistretti (1994). "Glutamate uptake into astrocytes stimulates aerobic glycolysis: a mechanism coupling neuronal activity to glucose utilization." Proceedings of the National Academy of Sciences **91**(22): 10625-10629.
Pelletier, G., J. Guy, Y. S. Allen and J. M. Polak (1984). "Electron microscope immunocytochemical localization of neuropeptide Y (NPY) in the rat brain." Neuropeptides **4**(4): 319-324.
Peruzzo, B., F. E. Pastor, J. L. Blázquez, K. Schöbitz, B. Peláez, P. Amat and E. M. Rodríguez (2000). "A second look at the barriers of the medial basal hypothalamus." Experimental Brain Research **132**(1): 10-26.
Picciotto, M. R. W. K. (1998). "Using Knockout and Transgenic Mice to Study Neurophysiology and Behavior." Physiological Reviews **78**(4): 1131-1163.
Plum, L., X. Ma, B. Hampel, N. Balthasar, R. Coppari, xFc, H. nzberg, M. Shanabrough, D. Burdakov, E. Rother, R. Janoschek, J. Alber, B. F. Belgardt, L. Koch, J. Seibler, F. Schwenk, C. Fekete, A. Suzuki, T. W. Mak, W. Krone, T. L. Horvath, F. M. Ashcroft, Br, xFc and J. C. ning (2006). "Enhanced PIP3 signaling in POMC neurons causes KATP channel activation and leads to diet-sensitive obesity." The Journal of Clinical Investigation **116**(7): 1886-1901.
Ponnazhagan, S., P. Mukherjee, M. C. Yoder, X. S. Wang, S. Z. Zhou, J. Kaplan, S. Wadsworth and A. Srivastava (1997). "Adeno-associated virus 2-mediated gene transfer in vivo: organ-tropism and expression of transduced sequences in mice." Gene **190**(1): 203-210.
Printz, R. L., M. A. Magnuson and D. K. Granner (1993). "Mammalian glucokinase." Annual Review of Nutrition **13**: 463-496.
Pronchuk, N., A. G. Beck-Sickinger and W. F. Colmers (2002). "Multiple NPY Receptors Inhibit GABAA Synaptic Responses of Rat Medial Parvocellular Effector Neurons in the Hypothalamic Paraventricular Nucleus." Endocrinology **143**(2): 535-543.
Quevedo, J., M. Vianna, D. Daroit, A. G. Born, C. R. Kuyven, R. Roesler and J. A. Quillfeldt (1998). "L-Type Voltage-Dependent Calcium Channel Blocker Nifedipine Enhances Memory Retention When Infused into the Hippocampus." Neurobiology of Learning and Memory **69**(3): 320-325.
Quinonez, R. and R. E. Sutton (2002). "Lentiviral vectors for gene delivery into cells." DNA Cell Biology **21**(12): 937-951.
Randall, A. and R. W. Tsien (1995). "Pharmacological dissection of multiple types of Ca2+ channel currents in rat cerebellar granule neurons." Journal of Neuroscience **15**(4): 2995-3012.

Remedi, M. S., J. C. Koster, B. L. Patton and C. G. Nichols (2005). "ATP-sensitive K+ channel signaling in glucokinase-deficient diabetes." Diabetes(0012-1797 (Print)).
Richardson, E. (2011). Investigating the role of central nutrient-sensing neurones using adeno-associated viral manipulation of glucokinase. Department of Medicine, Imperial College London. Thesis. **PhD**.
Rinaman, L. (2010). "Ascending projections from the caudal visceral nucleus of the solitary tract to brain regions involved in food intake and energy expenditure." Brain Research **1350**: 18-34.
Roncero, I., E. Alvarez, P. Vazquez and E. Blazquez (2000). "Functional glucokinase isoforms are expressed in rat brain." Journal of neurochemistry **74**(5): 1848-1857.
Roseberry, A. G., H. Liu, A. C. Jackson, X. Cai and J. M. Friedman (2004). "Neuropeptide Y-Mediated Inhibition of Proopiomelanocortin Neurons in the Arcuate Nucleus Shows Enhanced Desensitization in ob/ob Mice." Neuron **41**(5): 711-722.
Rossi, M., M. S. Kim, D. G. A. Morgan, C. J. Small, C. M. B. Edwards, D. Sunter, S. Abusnana, A. P. Goldstone, S. H. Russell, S. A. Stanley, D. M. Smith, K. Yagaloff, M. A. Ghatei and S. R. Bloom (1998). "A C-Terminal Fragment of Agouti-Related Protein Increases Feeding and Antagonizes the Effect of Alpha-Melanocyte Stimulating Hormone in Vivo." Endocrinology **139**(10): 4428-4431.
Sahu, A., W. R. Crowley, S. P. Kalra and P. S. Kalra (1993). "Role of Multiple Voltage-Sensitive Calcium Channels in Depolarization-Induced Release of Neuropeptide Y and Luteinizing Hormone-Releasing Hormone from Rat Median Eminence-Arcuate Nucleus." Molecular and Cellular Neuroscience **4**(6): 492-498.
Šalković-Petrišić, M. and Z. Lacković (2003). "Intracerebroventricular administration of betacytotoxics alters expression of brain monoamine transporter genes." Journal of Neural Transmission **110**(1): 15-29.
Sambrook, J., E. F. Fritsch and T. Maniatis (1989). Molecular cloning - A Laboratory Manual. Cold Spring Harbor Press, Cold spring harbor laboratory press New York.
Sanz, C., I. Roncero, P. Vázquez, M. A. Navas and E. Blázquez (2007). "Effects of glucose and insulin on glucokinase activity in rat hypothalamus." Journal of Endocrinology **193**(2): 259-267.
Schuit, F. C., P. Huypens, H. Heimberg and D. G. Pipeleers (2001). "Glucose Sensing in Pancreatic β-Cells." Diabetes **50**(1): 1-11.
Schwartz, M. W., S. C. Woods, D. Porte, Jr., R. J. Seeley and D. G. Baskin (2000). "Central nervous system control of food intake." Nature **404**(6778): 661-671.
Sclafani, A. (2004). "Oral and postoral determinants of food reward." Physiology & Behavior **81**(5): 773-779.
Seal, L. J., C. J. Small, W. S. Dhillo, S. A. Stanley, C. R. Abbott, M. A. Ghatei and S. R. Bloom (2001). "PRL-Releasing Peptide Inhibits Food Intake in Male Rats via the Dorsomedial Hypothalamic Nucleus and not the Paraventricular Hypothalamic Nucleus." Endocrinology **142**(10): 4236-4243.
Seino, S. and T. Miki (2003). "Physiological and pathophysiological roles of ATP-sensitive K+ channels." Progress in Biophysics and Molecular Biology **81**(2): 133-176.
Shapiro, R. E. and R. R. Miselis (1985). "The central organization of the vagus nerve innervating the stomach of the rat." The Journal of Comparative Neurology **238**(4): 473-488.
Sheppard, D. N. and K. A. Robinson (1997). "Mechanism of Glibenclamide Inhibition of Cystic Fibrosis Transmembrane Conductance Regulator Cl− Channels Expressed in a Murine Cell Line." The Journal of Physiology **503**(2): 333-346.
Silver, I. and M. Erecinska (1994). "Extracellular glucose concentration in mammalian brain: continuous monitoring of changes during increased neuronal activity and upon limitation in oxygen supply in normo-, hypo-, and hyperglycemic animals." The Journal of Neuroscience **14**(8): 5068-5076.
Simms, B. A. and G. W. Zamponi (2014). "Neuronal voltage-gated calcium channels: structure, function, and dysfunction." Neuron **82**(1): 24-45.
Simpson, I. A., S. J. Vannucci, M. R. DeJoseph and R. A. Hawkins (2001). "Glucose Transporter Asymmetries in the Bovine Blood-Brain Barrier." Journal of Biological Chemistry **276**(16): 12725-12729.

Smith, P. A., P. Rorsman and F. M. Ashcroft (1989). "Modulation of dihydropyridine-sensitive Ca2+ channels by glucose metabolism in mouse pancreatic [beta] -cells." Nature **342**(6249): 550-553.
Song, Z., B. E. Levin, J. J. McArdle, N. Bakhos and V. H. Routh (2001). "Convergence of pre- and postsynaptic influences on glucosensing neurons in the ventromedial hypothalamic nucleus." Diabetes **50**(12): 2673-2681.
Song, Z. and V. H. Routh (2005). "Differential Effects of Glucose and Lactate on Glucosensing Neurons in the Ventromedial Hypothalamic Nucleus." Diabetes **54**(1): 15-22.
Spanswick, D., M. A. Smith, V. E. Groppi, S. D. Logan and M. L. Ashford (1997). "Leptin inhibits hypothalamic neurons by activation of ATP-sensitive potassium channels." Nature **390**(6659): 521-525.
Spanswick, D., M. A. Smith, S. Mirshamsi, V. H. Routh and M. L. Ashford (2000). "Insulin activates ATP-sensitive K+ channels in hypothalamic neurons of lean, but not obese rats." Nature Neuroscience **3**(8): 757-758.
Stachniak, T. J., A. Ghosh and S. M. Sternson (2014). "Chemogenetic synaptic silencing of neural circuits localizes a hypothalamus-->midbrain pathway for feeding behavior." Neuron **82**(4): 797-808.
Stanley, B. G., K. C. Anderson, M. H. Grayson and S. F. Leibowitz (1989). "Repeated hypothalamic stimulation with neuropeptide Y increases daily carbohydrate and fat intake and body weight gain in female rats." Physiology & Behavior **46**(2): 173-177.
Stanley, B. G., A. S. Chin and S. F. Leibowitz (1985). "Feeding and drinking elicited by central injection of neuropeptide Y: Evidence for a hypothalamic site(s) of action." Brain Research Bulletin **14**(6): 521-524.
Stevens, G., G. Singh, Y. Lu, G. Danaei, J. Lin, M. Finucane, A. Bahalim, R. McIntire, H. Gutierrez, M. Cowan, C. Paciorek, F. Farzadfar, L. Riley, M. Ezzati and t. G. B. o. M. R. F. o. C. D. C. Group (2012). "National, regional, and global trends in adult overweight and obesity prevalences." Population Health Metrics **10**(1): 22.
Tasker, J. G. and F. E. Dudek (1991). "Electrophysiological properties of neurones in the region of the paraventricular nucleus in slices of rat hypothalamus." J Physiol **434**: 271-293.
Terauchi, Y., H. Sakura, K. Yasuda, K. Iwamoto, N. Takahashi, K. Ito, H. Kasai, H. Suzuki, O. Ueda, N. Kamada, K. Jishage, K. Komeda, M. Noda, Y. Kanazawa, S. Taniguchi, I. Miwa, Y. Akanuma, T. Kodama, Y. Yazaki and T. Kadowaki (1995). "Pancreatic β-Cell-specific Targeted Disruption of Glucokinase Gene: Diabetes Mellitus Due To Defective Insulin Secretion To Glucose." Journal of Biological Chemistry **270**(51): 30253-30256.
Thorens, B. (2011). "Brain glucose sensing and neural regulation of insulin and glucagon secretion." Diabetes, Obesity and Metabolism **13**: 82-88.
Thorens, B. (2012). "Sensing of glucose in the brain." Handbook of Experimental Pharmacology (209): 277-294.
Tiesjema, B., R. A. H. Adan, M. C. M. Luijendijk, A. Kalsbeek and S. E. la Fleur (2007). "Differential Effects of Recombinant Adeno-Associated Virus-Mediated Neuropeptide Y Overexpression in the Hypothalamic Paraventricular Nucleus and Lateral Hypothalamus on Feeding Behavior." The Journal of Neuroscience **27**(51): 14139-14146.
Tong, Q., C.-P. Ye, J. E. Jones, J. K. Elmquist and B. B. Lowell (2008). "Synaptic release of GABA by AgRP neurons is required for normal regulation of energy balance." Nature Neuroscience **11**(9): 998-1000.
Tsujii, S. and G. A. Bray (1990). Effects of glucose, 2-deoxyglucose, phlorizin, and insulin on food intake of lean and fatty rats.
Tucker, S. J., F. M. Gribble, P. Proks, S. Trapp, T. J. Ryder, T. Haug, F. Reimann and F. M. Ashcroft (1998). "Molecular determinants of KATP channel inhibition by ATP." The EMBO Journal **17**(12): 3290-3296.
Turner, R. C., C. A. Cull, V. Frighi, R. R. Holman and U. K. P. D. S. G. for the (1999). "Glycemic control with diet, sulfonylurea, metformin, or insulin in patients with type 2 diabetes mellitus: Progressive

requirement for multiple therapies (ukpds 49)." Journal of the American Medical Association **281**(21): 2005-2012.
U. K. Prospective Diabetes Study Group (1998). "Intensive blood-glucose control with sulfonylurea or insulin compared with conventional treatment and risk of complications in patients with type 2 diabetes(UKPDS 33)." Lancet **352**: 837-853.
Uldry, M., M. Ibberson, M. Hosokawa and B. Thorens (2002). "GLUT2 is a high affinity glucosamine transporter." FEBS Letters **524**(1-3): 199-203.
van den Top, M., D. J. Lyons, K. Lee, E. Coderre, L. P. Renaud and D. Spanswick (2007). "Pharmacological and molecular characterization of ATP-sensitive K+ conductances in CART and NPY/AgRP expressing neurons of the hypothalamic arcuate nucleus." Neuroscience **144**(3): 815-824.
Vannucci, S. J., F. Maher and I. A. Simpson (1997). "Glucose transporter proteins in brain: Delivery of glucose to neurons and glia." Glia **21**(1): 2-21.
Viktoria, L. G., B. Matthias, L. B. Deepak, R. K. Sangeeta, R. S. Philip, M. Geltrude, C. B. Heiner and J. N. Alain (2013). "Bariatric surgery versus non-surgical treatment for obesity: a systematic review and meta-analysis of randomised controlled trials." BRITISH MEDICAL JOURNAL **347**.
Wang, R., X. Liu, S. T. Hentges, A. A. Dunn-Meynell, B. E. Levin, W. Wang and V. H. Routh (2004). "The regulation of glucose-excited neurons in the hypothalamic arcuate nucleus by glucose and feeding-relevant peptides." Diabetes **53**(8): 1959-1965.
Wang, Z., H. I. Ma, J. Li, L. Sun, J. Zhang and X. Xiao (2003). "Rapid and highly efficient transduction by double-stranded adeno-associated virus vectors in vitro and in vivo." Gene Therapy **10**(26): 2105-2111.
Weber, A. M., F. K. Wong, A. R. Tufford, L. C. Schlichter, V. Matveev and E. F. Stanley (2010). "N-type Ca2+ channels carry the largest current: implications for nanodomains and transmitter release." Nature Neuroscience **13**(11): 1348-1350.
Weiss, N. and G. W. Zamponi (2012). "Regulation of voltage-gated calcium channels by synaptic proteins." Advances in Experimental and Medical Biology **740**: 759-775.
Wilcox, J. N. (1993). "Fundamental principles of in situ hybridization." Journal of Histochemistry & Cytochemistry **41**(12): 1725-1733.
Wilson, J. E. and V. Chung (1989). "Rat brain hexokinase: further studies on the specificity of the hexose and hexose 6-phosphate binding sites." Archives of Biochemistry and Biophysics **269**(2): 517-525.
Wood, S. M., J. R. Wood, M. A. Ghatei, Y. C. Lee, D. O'Shaughnessy and S. R. Bloom (1981). "Bombesin, somatostatin and neurotensin-like immunoreactivity in bronchial carcinoma." J Clin Endocrinol Metab **53**(6): 1310-1312.
Woods, S. C., E. C. Lotter, L. D. McKay and D. Porte, Jr. (1979). "Chronic intracerebroventricular infusion of insulin reduces food intake and body weight of baboons." Nature **282**(5738): 503-505.
Woods, S. C., L. J. Stein, L. D. McKay and D. Porte (1984). "Suppression of food intake by intravenous nutrients and insulin in the baboon." American Physiological Society **247**(2): R393-R401.
Wu, W. N., P. F. Wu, J. Zhou, X. L. Guan, Z. Zhang, Y. J. Yang, L. H. Long, N. Xie, J. G. Chen and F. Wang (2013). "Orexin-A activates hypothalamic AMP-activated protein kinase signaling through a Ca(2)(+)-dependent mechanism involving voltage-gated L-type calcium channel." Molecular Pharmacology **84**(6): 876-887.
Wu, X., J. Gao, J. Yan, C. Owyang and Y. Li (2004). "Hypothalamus–Brain Stem Circuitry Responsible for Vagal Efferent Signaling to the Pancreas Evoked By Hypoglycemia in Rat." Journal of Neurophysiology **91**(4): 1734-1747.
Wynne, K., S. Stanley, B. McGowan and S. Bloom (2005). "Appetite control." Journal of Endocrinology **184**(2): 291-318.
Xu, W. and D. Lipscombe (2001). "Neuronal Ca(V)1.3alpha(1) L-type channels activate at relatively hyperpolarized membrane potentials and are incompletely inhibited by dihydropyridines." Journal of Neuroscience **21**(16): 5944-5951.

Yan, Z., Y. Zhang, D. Duan and J. F. Engelhardt (2000). "Trans-splicing vectors expand the utility of adeno-associated virus for Gene Therapyapy." Proceedings of the National Academy of Sciences **97**(12): 6716-6721.
Zarjevski, N., I. Cusin, R. Vettor, F. Rohner-Jeanrenaud and B. Jeanrenaud (1993). "Chronic intracerebroventricular neuropeptide-Y administration to normal rats mimics hormonal and metabolic changes of obesity." Endocrinology **133**(4): 1753-1758.
Zelent, B., A. Raimondo, A. Barrett, C. W. Buettger, P. Chen, A. L. Gloyn and F. M. Matschinsky (2014). "Analysis of the co-operative interaction between the allosterically regulated proteins GK and GKRP using tryptophan fluorescence." Biochemistry Journal **459**(3): 551-564.
Zhang, G., V. Gurtu and S. R. Kain (1996). "An enhanced green fluorescent protein allows sensitive detection of gene transfer in mammalian cells." Biochemical and Biophysical Research Communications **227**(3): 707-711.
Zhou, J., D. S. Roane, X. Xi, I. Bogacka, B. Li, D. H. Ryan and R. J. Martin (2003). "Short-Term Food Restriction and Refeeding Alter Expression of Genes Likely Involved in Brain Glucosensing." Experimental Biology and Medicine **228**(8): 943-950.
Zhou, L., N. Podolsky, Z. Sang, Y. Ding, X. Fan, Q. Tong, B. E. Levin and R. J. McCrimmon (2010). "The Medial Amygdalar Nucleus: A Novel Glucose-Sensing Region That Modulates the Counterregulatory Response to Hypoglycemia." Diabetes **59**(10): 2646-2652.
Zhou, L., C.-Y. Yueh, D. D. Lam, J. Shaw, M. Osundiji, A. S. Garfield, M. Evans and L. K. Heisler (2011). "Glucokinase inhibitor glucosamine stimulates feeding and activates hypothalamic neuropeptide Y and orexin neurons." Behavioural Brain Research **222**(1): 274-278.

7. Appendix

7.1 Appendix I – Solutions

ABC Buffer
Combine solutions A, B and C in the following proportions: 100:250:150 and store at -20°C.

Solution A
Add 1ml of 125mM $MgCl_2$ and 1.25M Tris-HCl (pH 8.0) to 18µl mercaptoethanol, 5µl 100mM dATP, 5µl 100mM dTTP and 5µl dGTP.
Solution B
2M Hepes (pH6.6) titrated with 4M NaOH.
Solution C
Random oligonucleotides (112µg/ml).

ω-agatoxin IVA was dissolved to a working concentration of 1µg/µl in 1% ethanol in GDW, aliquoted and stored at -80°C until required.

Amasino wash
Mix 250ml 1M Na phosphate buffer (pH 7.2), 2ml 500mM EDTA and 100ml 20% SDS with 650ml GDW.

5M Ammonium acetate
Dissolve 385g CH_3COONH_4 in 600ml autoclaved GDW then make up to 1L.

Ampicillin (100mg/ml)
Dissolve 1g ampicillin in 10ml GDW, sterilise by passage through a 0.2µm filter and distribute in 1ml aliquots.

aCSF:
Make aCSF immediately before use. To make 500ml aCSF mix 100ml 0.1M $NaHCO_3$, 100ml 0.63M NaCl, 5ml 0.09M $Na_2HPO_4.2H_2O$, 5ml 0.59M KCl, 5ml 0.09M $MgSO_4.7H_2O$, 450mg glucose, 88mg ascorbic acid, 5ml aprotinin (BDH) and 270ml GDW. Saturate with 95% O_2 and 5% CO_2 for at least 10 minutes, then add 10ml 0.07M $CaCl_2.2H_2O$.

56mM KCl aCSF:
Make aCSF immediately before use. To make 100ml 56mM KCl aCSF, mix 20ml 0.1M $NaHCO_3$, 11.6ml 0.63M NaCl, 1ml 0.09M $Na_2HPO_4.2H_2O$, 10ml 0.59M KCl, 1ml 0.09M $MgSO_4.7H_2O$, 90mg

glucose, 17.6mg ascorbic acid, 1ml aprotinin (BDH) and 53.4ml GDW. Saturate with 95% O_2 and 5% CO_2 for at least 10 minutes, then add 10ml 0.07M $CaCl_2.2H_2O$.

aCSF stock solutions:

0.09M disodium hydrogen orthophosphate dehydrate:
Dissolve 1.56g $Na_2HPO_4.2H_2O$ in 100ml GDW
0.07M calcium chloride dehydrate:
Dissolve 1.04g $CaCl_2.2\ H_2O$ in 100ml GDW
0.09M magnesium sulphate heptahydrate:
Dissolve 2.2g $MgSO_4.7H_2O$ in 100ml GDW
0.59M potassium chloride:
Dissolve 4.42g KCl in 100ml GDW
0.1M sodium bicarbonate:
Dissolve 4.62g $NaHCO_3$ in 500ml GDW
0.63M sodium chloride:
Dissolve 18.43g NaCl in 500ml GDW

2.5mM Aurintricarboxylic acid (ATA)
Dissolve 0.1183g ATA in 100ml GDW.

Baker's yeast tRNA (10mg/ml)
Make up with GDW, aliquot and store at -20°C.

BMS 193885 was dissolved in 100% DMSO, aliquoted and stored at -80°C. Immediately before use, aliquots were dissolved to a working concentration of 10mg/kg in 40%DMSO.

Caesium chloride-saturated propan-2-ol:
Mix 100g $CsCl_2$, 100ml GDW and 100ml propan-2-ol and leave to settle.

CGP 71683 was dissolved in 100% DMSO, aliquoted and stored at -80°C. Immediately before use, aliquots were dissolved to a working concentration of 10mg/kg in 40%DMSO.

Compound A (CpdA) was dissolved in 100% DMSO, aliquoted and stored at -80°C. Immediately before use, aliquots were dissolved to a working concentration of 0.5 nmol in 1% DMSO (cannulation studies) or 30 µM in 0.1%DMSO in aCSF (explant studies).

1% Cresyl violet solution
Add 1ml cresyl Violet to 99ml GDW, then pass through a Whatman GF/C filter.

Diazoxide was aliquoted and dissolved to a working concentration of 0.05M NaOH and 1% DMSO in GDW (cannulation studies) or 200 µM in 5mM NaOH and 0.1%DMSO in aCSF (explant studies).

100x Denhart's solution
Dissolve 10g ficoll, 10g polyvinylpyrrolidone (PVP) and 10g BSA (Pentax fraction V) and make up to 500ml with GDW.

Denaturing solution (DNA)
Dissolve 43.5g NaCl in 430 ml GDW. Add 25ml 10M NaOH and make up to 500ml with GDW.

1M Dithiothreitol (DTT)
Dissolve 154g $C_4H_{10}O_2S_2$ in 1L GDW. Aliquot and store at -20°C.

0.5M Ethylenediaminetetra-acetic acid (EDTA) (pH 8.0)
Dissolve 181.6g $C_{10}H_{14}H_2O_8Na.2H2O$ in 800ml GDW under pH 8.0 with NaOH. Make up to 1L with GDW.

4% Formaldehyde in 0.01M PBS
Add 8ml 40% formaldehyde solution to 400ml 0.01M PBS.

Formamide (de-ionised)
Add 2.7g duolite MB to 100ml formamide and stir until the duolite turns brown (~1 hour). Remove the duolite by passing through Whatman GF/C filters, aliquot and store at -20°C.

Glucose Tris EDTA
Final concentrations of 50mM glucose, 25mM Tris and 10mM EDTA.

Glibenclamide was aliquoted and dissolved to a working concentration of 0.05M NaOH and 1% DMSO in GDW (cannulation studies) or 100 µM in 5mM NaOH and 0.1%DMSO in aCSF (explant studies).

1x Hepes buffered saline (HeBS) (pH 7.05)
Dissolve 0.8g NaCl, 37.5mg KCl, 10.5mg, Na_2HPO_4, 0.11g dextrose and 0.5g Hepes in a total volume of 90mls GDW. Adjust to pH 7.05 with 0.5M NaOH and add GDW to a final volume of 100ml. Sterilise by passing through a 0.2µm filter and store in 5 ml aliquots at -20°C.

Hybridisation buffer for northern blot analysis and for dot-blot analysis
Add 0.5g dried milk powder and 0.5ml 500mM EDTA to 48ml GDW and leave at 37°C to dissolve. Allow to cool then add 25ml 1M Na phosphate buffer, 25ml 20% SDS and 1ml 2.5M ATA.

Hybridisation buffer for *in situ* hybridisation:
Prepare dextran sulphate solution by the addition of 1.5ml GDW to 1g dextran sulphate and incubate in a water bath at 60°C for two hours. Ensure minimum bubbles present. In a total volume of 4ml add together 1.25ml formamide, 300µl 5M NaCl, 200µl tRNA (10mg/ml), 50µl 100x Denhart's, 50µl 1M Tris (pH 8.0), 40µl 1M dithiothreitol (DTT), 10µl 0.5M EDTA (pH 8.0), 1.1ml GDW and 1ml (50%) dextran sulphate.

LB culture medium (pH 7.5)
Dissolve 10g NaCl, 10g tryptone and 5g yeast extract in 800ml GDW. Adjust to pH 7.5 with 10M NaOH. Sterilise by autoclaving and make up to 1L.

LB(amp) agar plates
Add 7g agar to 500ml LB and melt by autoclaving. Add 1000µL 100mg/mL ampicillin once gently re-melted and set in plates at 4°C.

Loading Buffer for DNA/RNA
Mix 3.125ml 80% glycerol, 50µl 0.5M $C_{10}H_{14}H_2O_8Na_2.H_2O$ and 6.075ml autoclaved GDW, then add 10mg orange G.

2M Magnesium chloride (MgCl2)
Dissolve 406.6g $MgCl_2.6H{=}O$ in 1L GDW.

Neutralising solution (pH 7.5)
Dissolve 43.5g NaCl and 60.2g $NH_2C(CH_2OH)_3$ in 430 ml GDW and adjust to pH 7.5 with ~35ml HCl.

Nifedipine was aliquoted under low light conditions and dissolved to a working concentration of 5µg/µl in 1% ethanol in GDW.

Phosphate buffered saline (PBS):
0.1M PBS (10x)
Dissolve 80g NaCl, 2g KCl, 14.4g Na_2HPO_4 (18.05g $Na_2HPO_4.2H_2O$ or 27.18g $Na_2HPO_4.7H_2O$) and 2.4g KH_2PO_4 in 800ml GDW.
0.01M PBS (1x)
Add 100ml 0.1M PBS to 900ml GDW.

Phosphate buffer (RIA buffer)
Dissolve 48g of $Na_2HPO_4.2H_2O$, 4.13g KH_2PO_4, 18.61g $C_{10}H_{14}H_2O_8Na_2.2H_2O$, 2.5g NaN_3 in 5L boiled and cooled GDW. Adjust pH to 7.4 ± 0.1.

5M Potassium acetate (KAc)
Dissolve 294.4g CH_3COOK in 500ml GDW. Add 115ml glacial acetic acid and make up to 1L with GDW.

3M Potassium hydroxide
Dissolve 198g KOH in 1L GDW.

Proteinase K (20mg/ml)
Dissolve 20mg in 1ml GDW, distribute into 100µl aliquots and store at -20°C.

RNase A (10mg/ml)
Dissolve 100mg RNase A in 10ml GDW. (Previously used 10mM Tris-HCl (pH 7.5) and 15mM NaCl but not needed) and boil for up to fifteen minutes to denature DNAses. Allow to cool, distribute into 800µl aliquots and store at -20°C. (Usually comes in 250mg vials)

20x Saline sodium citrate (SSC) buffer (pH 7.0)
Dissolve 1.735g NaCl and 882g $Na_3C_6H_5O_7.2H_2O$ in 8L GDW. Adjust to pH 7.0 and make up to 10L.

Sephadex G50
Add 8g fine grade Sephadex G50 beads (diameter: 20-80µm), 2ml 100x TE and 0.1ml 20% SDS to 200ml GDW and autoclave to expand the beads.

2M Sodium acetate (pH 5.2)
Dissolve 164.1g CH_3COONa in 800ml GDW, adjust to pH 5.2 with glacial acetic acid and make up to 1L with GDW.

3M Sodium chloride
Dissolve 175.3g NaCl in 1L GDW.

5M Sodium chloride
Dissolve 292.2g NaCl in 1L GDW.

20% (w/v) Sodium dodecyl sulphate (SDS)
Add 200g SDS to 800ml GDW and heat to 60°C while stirring. Allow to cool and make up to 1L with GDW.

0.2M Sodium hydroxide/1%SDS
Add 3ml 10M NaOH to 140ml GDW, mix and add 7.5ml 20% SDS.

10M Sodium hydroxide
Dissolve 400g NaOH in 500ml GDW. Make up to 1Lwith GDW.

1M Sodium phosphate buffer (pH 6.8)
Dissolve 26g NaH_2PO_4 and 44.6g Na_2HPO_4 in 1L GDW.

20x Sodium chloride, sodium hydrogen phosphate, EDTA (SSPE) buffer (pH 7.7)
Dissolve 1.753g NaCl, 14.2g Na_2HPO_4 and 7.4g $C_{10}H_{14}H_2O_8Na_2.2H_2O$ in 700ml GDW, adjust to pH 7.7 with 10M NaOH and make up to 1L with GDW.

0.1M Triethanolamine (TEA) buffer (pH 8.0)
Dissolve 18.6g $C_6H_{15}NO_3.HCl$ in 800ml GDW. Add NaOH to pH 8.0 and make up to 1L with GDW.

50x Tris-acetate-EDTA (TAE) buffer
Dissolve 242g $NH_2C(CH_2OH)_3$ in 843ml GDW then add 57ml glacial acetic acid and 100ml 0.5M $C_{10}H_{14}H_2O_8Na_2.2H_2O$.

100x Tris-EDTA (TE) buffer (pH 7.5)
Dissolve 121.1g $NH_2C(CH_2OH)_3$ and 3.7g $C_{10}H_{14}H_2O_8Na_2.2H_2O$ in 800ml GDW. Adjust to pH 7.5 with hydrochloric acid and make up to 1L with GDW.

Tris-EDTA-Sodium chloride (TES) buffer
Mix 25ml 1M Tris-HCl (pH 8.0), 5ml 5M NaCl and 5ml C10 $H_{14}H_2O_8Na_2.2H_2O$. Make up to 500ml with GDW.

Versene
Dissolve 16g NaCl, 0.4g KCl, 2.88g $Na_2HPO_4.2H_2O$, 1.2g $C_{10}H_{14}H_2O_8Na_2.2H_2O$ and 0.4g KH_2PO_4 in 1L GDW, add 3ml phenol red and make up to 2L with GDW. Sterilise by autoclaving.

7.2 Coronal section of the rat brain

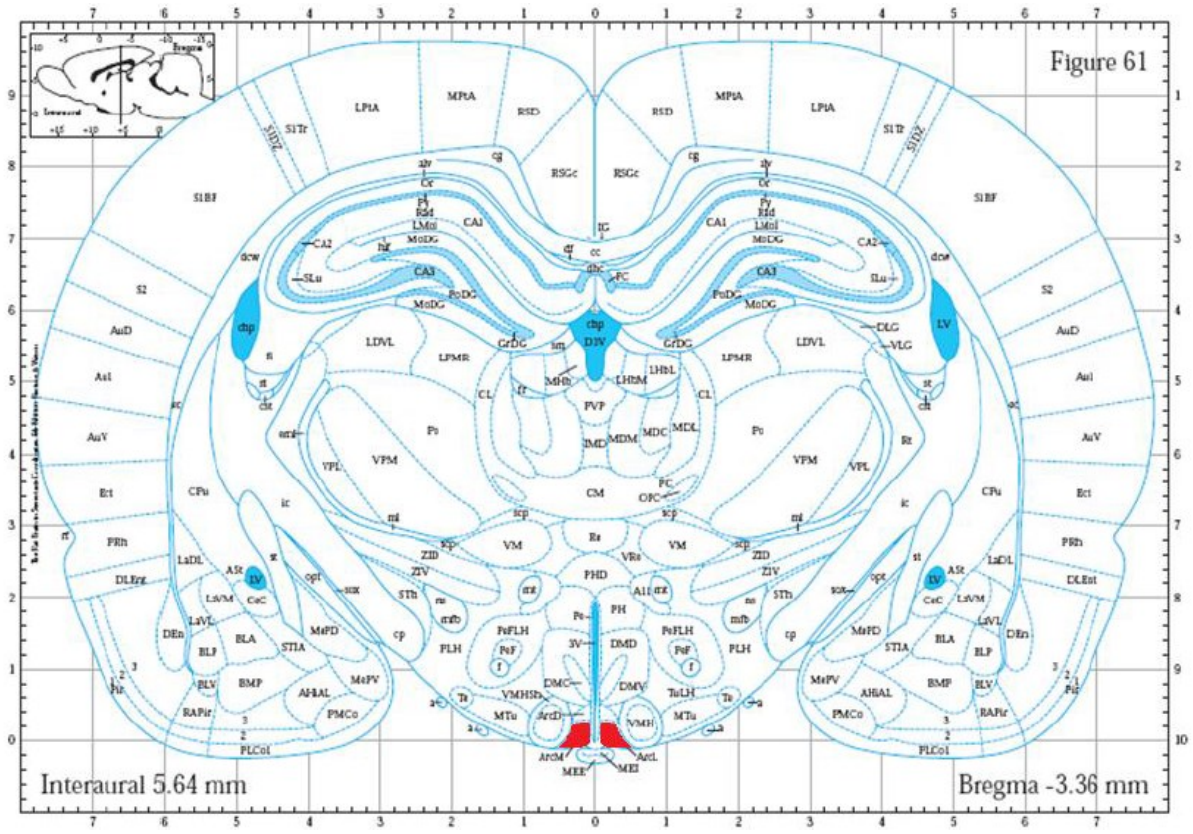


Figure 7.1 Schematic of a coronal section of the rat brain: Schematic showing 3.36mm posterior to bregma, which approximately corresponds to the co-ordinates used to target the ARC in this work (-3.4 from bregma). The ARC is highlighted in red. Reproduced from "The Rat Brain in Stereotaxic Co-ordinates" (Paxinos and Watson 2007).

7.3 Appendix II – Nutritional Information for RM1 standard chow diet

NUTRIENTS		Total	Supp (9)
Proximate Analysis			
Moisture (1)	%	10.00	
Crude Oil	%	2.71	
Crude Protein	%	14.37	
Crude Fibre	%	4.65	
Ash	%	6.00	
Nitrogen Free Extract	%	61.65	
Digestibility Co-Efficients (7)			
Digestible Crude Oil	%	2.46	
Digestible Crude Protein	%	12.91	
Carbohydrates, Fibre and Non Starch Polysaccharides (NSP)			
Total Dietary Fibre	%	17.04	
Pectin	%	1.52	
Hemicellulose	%	10.16	
Cellulose	%	4.32	
Lignin	%	1.68	
Starch	%	44.91	
Sugar	%	4.05	
Energy (5)			
Gross Energy	MJ/kg	14.72	
Digestible Energy (15)	MJ/kg	11.89	
Metabolisable Energy (15)	MJ/kg	10.75	
Atwater Fuel Energy (AFE) (8)	MJ/kg	13.73	
AFE from Oil	%	7.43	
AFE from Protein	%	17.50	
AFE from Carbohydrate	%	75.08	
Fatty Acids			
Saturated Fatty Acids			
C12:0 Lauric	%	0.02	
C14:0 Myristic	%	0.14	
C16:0 Palmitic	%	0.31	
C18:0 Stearic	%	0.04	
Monounsaturated Fatty Acids			
C14:1 Myristoleic	%	0.02	
C16:1 Palmitoleic	%	0.09	
C18:1 Oleic	%	0.77	
Polyunsaturated Fatty Acids			
C18:2(ω6) Linoleic	%	0.69	
C18:3(ω3) Linolenic	%	0.06	
C20:4(ω6) Arachidonic	%	0.13	
C22:5(ω3) Clupanodonic	%		
Amino Acids			
Arginine	%	0.91	
Lysine (6)	%	0.66	0.07
Methionine	%	0.22	0.04
Cystine	%	0.24	
Tryptophan	%	0.18	
Histidine	%	0.35	
Threonine	%	0.49	
Isoleucine	%	0.54	
Leucine	%	0.98	
Phenylalanine	%	0.66	
Valine	%	0.69	
Tyrosine	%	0.49	
Taurine	%		
Glycine	%	1.11	
Aspartic Acid	%	0.67	

NUTRIENTS		Total	Supp (9)
Glutamic Acid	%	3.17	
Proline	%	1.19	
Serine	%	0.55	
Hydroxyproline	%		
Hydroxylysine	%		
Alanine	%	0.16	
Macro Minerals			
Calcium	%	0.73	0.63
Total Phosphorus	%	0.52	0.05
Phytate Phosphorus	%	0.24	
Available Phosphorus	%	0.28	0.05
Sodium	%	0.25	0.19
Chloride	%	0.38	0.32
Potassium	%	0.67	
Magnesium	%	0.23	
Micro Minerals			
Iron	mg/kg	159.23	82.95
Copper	mg/kg	11.49	1.98
Manganese	mg/kg	72.40	19.58
Zinc	mg/kg	35.73	
Cobalt	µg/kg	633.94	550.63
Iodine	µg/kg	1202.49	1085.36
Selenium	µg/kg	298.87	100.73
Fluorine	mg/kg	10.48	
Vitamins			
β-Carotene (2)	mg/kg	0.16	
Retinol (2)	µg/kg	14996.23	14400.82
Vitamin A (2)	iu/kg	49987.07	48002.69
Cholecalciferol (3)	µg/kg	88.05	85.00
Vitamin D (3)	iu/kg	3522.02	3400.00
α-Tocopherol (4)	mg/kg	189.43	166.09
Vitamin E (4)	iu/kg	208.37	182.70
Vitamin B_1 (Thiamine)	mg/kg	54.26	46.11
Vitamin B_2 (Riboflavin)	mg/kg	61.17	57.83
Vitamin B_6 (Pyridoxine)	mg/kg	55.56	50.03
Vitamin B_{12} (Cyanocobalamine)	µg/kg	69.63	66.01
Vitamin C (Ascorbic Acid)	mg/kg	2.68	
Vitamin K (Menadione)	mg/kg	84.75	81.36
Folic Acid (Vitamin B_9)	mg/kg	19.06	17.64
Nicotinic Acid (Vitamin PP) (6)	mg/kg	183.08	120.50
Pantothenic Acid (Vitamin B_{5})	mg/kg	56.20	40.74
Choline (Vitamin B_{97})	mg/kg	1079.89	367.51
Inositol	mg/kg	2366.38	27.21
Biotin (Vitamin H) (6)	µg/kg	753.39	461.81

Notes

1. All values are calculated using a moisture basis of 10%.
   Typical moisture levels will range between 9.5 - 11.5%.
2. a. Vitamin A includes Retinol and the Retinol equivalents of β-carotene
   b. Retinol includes the Retinol equivalents of β-Carotene.
   c. 0.48 µg Retinol = 1 µg β-carotene = 1.6 iu Vitamin A activity
   d. 1 µg Retinol = 3.33* iu Vitamin A activity
   e. 1 iu Vitamin A = 0.3 µg Retinol = 0.6 µg β-carotene
   f. The standard analysis for Vitamin A does not detect β-carotene
3. 1µg Cholecalciferol (D_3) = 40.0 iu Vitamin D
4. 1 mg all-*rac*-α-tocopherol = 1.1 iu Vitamin E activity
   1 mg all-*rac*-α-tocopherol acetate = 1.0 iu Vitamin E activity
5. 1 MJ = 239.23 Kcalories = 239.23 Calories = 239,230 calories
6. These nutrients coming from natural raw materials such as cereals may have low availabilities due to the interactions with other compounds.
7. Based on in-vitro digestibility analysis.
8. AF Energy = Atwater Fuel Energy = (((CO%/100)*9000)+((CP%/100)*4000)+((NFE%/100)*4000)/239.23
9. Supplemented nutrients from manufactured and mined sources.
15. Calculated.

Figure 7.2 Nutritional information for RM1 standard chow diet.

7.4 Appendix III – DNA sequencing of plasmid for in situ hybrisidation

BLAST analysis of the GK-pTR-CGW sequence revealed that the plasmid contained a 69bp sequence with 100% homology to the rat pancreatic GK sequence (GenBank: M25807.1) as shown in figure 4.5.

ACCGCGGTGGCGGCCGCTCTAGAACTAGTGGATCCGGTACTCGAGCTACCGGTATTCAGA

TCTGGTACCTGGGCTGGTGGCTGCGCAGATGCTGGATGACAGAGCCAGGATGGAGGCCAC

CAAGAAGGAAAAGGTCGAGCAGATCCTGGCAGAGTTCCAGCTGCAGGAATTCGATATCAA

GCTTATCGATACCGTCGACCTCGAGGGGGGGCCCGGTACCCAGCTTTTGTTCCCTTTAGT

GAGGGTTAATTGCGCGCTTGGCGTAATCATGGTCATAGCTGTTTCCTGTGTGAAATTGTT

ATCCGCTCACAATTCCACACAACATACGAGCCGGAAGCATAAAGTGTAAAGCCTGGGGTG

CCTAATGAGTGAGCTAACTCACATTAATTGCGTTGCGCTCACTGCCCGCTTTCCAGTCGG

GAAACCTGTCGTGCCAGCTGCATTAATGAATCGGCCAACGCGCGGGGAGAGGCGGTTTGC

GTATTGGGCGCTCTTCCGCTTCCTCGCTCACTGACTCGCTGCGCTCGGTCGTTCGGCTGC

GGCGAGCGG

Figure 7.3 Sequence of GK-pTR-CGW-plasmid: containing GK insert (underlined) and cloning sites for BamH1 (highlighted green) and PstI (highlighted blue).

7.5 Appendix IV – List of suppliers

Abbott Laboratories Ltd, Maidenhead, UK

Advanced Biotechnology Centre, Imperial College, London, UK

Animalcare Limited, Dunnington, York, UK

Applied Biosystems, Warrington, UK

ATCC, Middlesex, UK

Bachem, San Carlos, USA

Bachem, UK

Bayer UK Ltd, Bury St Edmunds, UK

Beckman Coulter, Buckinghamshire, UK

Bilaney, Sevenoaks, UK

Braun Medical Ltd., Sheffield, UK

Bright Instrument Company, Huntingdon, Cambridgeshire, UK

Boehringer Ingelheim, Berkshire, UK

Charles River, Bicester, UK

Chemicon International Inc., USA

Clintech, Dublin, Ireland

CP Pharmaceuticals, Wrexham, UK

David Kofp Instruments, Tujunga, CA, USA

Du Pont, Bristol, UK

Eli Lilly & Co.Ltd, Basingstoke, UK

Enzo Life Science, Exeter, UK

Eppendorf, Hamburg, Germany

Ethicon, Gargrave, Yorkshire, UK

Fine Science Tools, Linton, UK

Fisher Scientific UK, Loughborough, Leicestershire, UK

GE Healthcare, Buckinghamshire, UK

Genomics Core Laboratory, Imperial College London, UK

Graphpad Prism, Graphpad Sorfware, San Diego, CA, USA

Helena biosciences, Sunderland, UK

Invitrogen Life Technologies, Paisley, UK

Jet X-Ray, London, UK

Kemdent, Swindon, UK

Kodak, Hemel Hempstead, Hertfordshire, UK

Kopf Instruments, Tujunga, California, USA

LEO Pharma, Buckinghamshire, UK

L.E West, Barking, UK

Life Sciences Technology, Eggenstein, Germany

Linco Research, Missouri, USA

Merck Pharmaceuticals, Whitehouse Station, NJ, USA

Microfield Scientific Ltd, Dartmouth, UK

Microvette, Sarstedt, Numbrecht, Germany

Millipore, Watford, Hertfordshire, UK

Millpledge Veterinary, Nottinghamshire, UK

Montrose fasteners, Bucks, UK

Nikon, Kingston Upon Thames, Surrey, UK

NE Technology, UK

New England Biolabs (UK) Ltd, Hitchin, Hertfordshire, UK

Novagen, Nottingham, UK

Oswell DNA Services, Southampton, UK

Parke-Davis, Pontypool, UK

Pharmacia & Upjohn, Sweden

Pierce, Rockford, IL, USA

Plastics-One, Roanoke, Virginia, USA (via Bilaney)

Promega, Madison, WI, USA

Randox Laboratories Ltd, County Antrim, UK

Research Diets Inc, New Brunswick, NJ, USA

Seton Scholl Healthcare Ltd., Gloucester, UK

Shandon Southern Products Ltd, Runcorn, UK

Schering-Plough Ltd., Hertfordshire, UK

Sigma Ltd, Poole, Dorset, UK

Special Diet Services, Witham, Essex, UK

Stata, Stata Corp LP, USA

ThermoFisher Scientific Leicestershire, UK

Tyco Healthcare, Hampshire, UK

Ultracrimp, Du Pont, Wilmington, DE, USA

Vet Tech Solutions Ltd, Cheshire, UK

VWR International Ltd, Poole, UK

Wallace, Waltham, MA, USA

WPA, Cambridgeshire, UK